MOLECULAR STRUCTURE AND
INTERFACIAL BEHAVIOUR OF POLYMERS

4951

Boudewijn van Lent

MOLECULAR STRUCTURE AND
INTERFACIAL BEHAVIOUR OF POLYMERS

Proefschrift
ter verkrijging van de graad van
doctor in de landbouwwetenschappen,
op gezag van de rector magnificus,
dr. H.C. van der Plas,
in het openbaar te verdedigen
op dinsdag 7 november 1989
des namiddags te vier uur in de aula
van de Landbouwuniversiteit te Wageningen

Stellingen

I

De vlokking van harige deeltjes in aanwezigheid van niet-adsorberend polymeer wordt behalve door depletie van dit polymeer (zoals bij kale deeltjes) ook veroorzaakt door een verhoging van de entropie van de harige lagen ten opzichte van de toestand dat de deeltjes zich op oneindige afstand van elkaar bevinden.

Dit proefschrift, hoofdstuk 4

II

Een homodispers AB-statistisch copolymeer met een bepaalde AB-verhouding adsorbeert nooit sterker dan een homodispers diblok-copolymeer met een even groot moleculgewicht en een identieke AB-verhouding onder dezelfde omstandigheden.

Dit proefschrift, hoofdstuk 3

III

Het toepassen van het Rotational-Isomeric-State (RIS) model van Leermakers en Scheutjens op de systemen die in dit proefschrift beschreven worden zal geen veranderingen in de kwalitatieve trends te zien geven.

Leermakers F.A.M. and Scheutjens J.M.H.M., J. Chem. Phys. (1988), 89, 3264

IV

Bij de berekening van het volumefractieprofiel van eindstandig verankerde ketens op bolvormige deeltjes vergeten Baskir, Hatton en Suter de eindjes aan elkaar te knopen.

Baskir J.N., Hatton T.A., and Suter U.W. J. Phys. Chem. (1989), 93, 969

V

Een heterogeen oppervlak, een oppervlak met verschillende soorten adsorptieplaatsen, kan de vorm van de adsorptie-isothermen van co-polymeren zeer sterk beïnvloeden.

Katinka van der Linden, Doctoraalverslag, Landbouwuniversiteit Wageningen (1989)

VI

De nationalistische houding van vele Nederlanders zal er toe leiden dat het openstellen van de grenzen in 1992 nauwelijks invloed zal hebben op het gaan werken van Nederlanders in andere EEG landen.

VII

Niet de juist afgestudeerden maar de net gepromoveerden zijn momenteel de verloren generatie aan de universiteiten in Nederland.

VIII

In tegenstelling tot een erkend garagebedrijf moet Beun de Haas het alleen hebben van zijn goede naam.

IX

Tijdens 1 dag op de boerderij kan men meer over het boerenbedrijf leren dan in 9 jaar Landbouwuniversiteit

IJzendijke, augustus 1989

proefschrift *Boudewijn van Lent*
Molecular Structure and Interfacial Behaviour of Polymers
Wageningen, 7 november 1989

Chapter 1

Introduction

General

In this thesis new models for several systems containing polymers at interfaces will be developed. Especially the influence of the molecular structure of the polymer (e.g., copolymers, grafted polymers) on its interfacial behaviour will be studied. The models are based on the self-consistent field theory of Scheutjens and Fleer[1,2] for the adsorption of homopolymers.

Polymers near interfaces play an important role in many industrial processes and in biological systems. For instance, polymers are used in coatings for magnetic tapes and disks, as stabilizing agents for paint pigments, in food, in adhesives, and in pharmaceutical products. A long list of applications in which polymers are used is compiled in an article by Eirich.[3]

The structure of the molecules is very important in obtaining the desired effects in these applications. Therefore, one should have a good insight in the influence of the molecular structure on the interfacial behaviour of polymers. Ergo, theoretical models must be able to account for specific molecular properties. The theories used in this thesis are based on a statistical thermodynamic method in which it is possible to account for the structure of these molecules as well as for specific interactions between them. So far, no other theories have been able to do this for the investigated systems without introducing (more) severe simplifications.

Polymer Adsorption and Depletion

A polymer is defined as a macromolecule, which is composed of a large number of repeating units. These units, or segments, can be identical (homopolymer), chemically different (copolymer) and/or

charged (polyelectrolyte). Two phenomena of polymers near a solid-liquid interface can be distinguished: adsorption and depletion.

In the case of adsorption, the polymer segments in contact with the surface have gained energy upon adsorption from the bulk solution. This causes segments to accumulate on the surface. The remainder of the chains, connected to these segments, is pulled towards the surface. In this way, a concentration gradient develops: a high concentration of segments is present on the surface, decaying with distance from the surface towards a constant concentration in the bulk solution (Figure 1a).
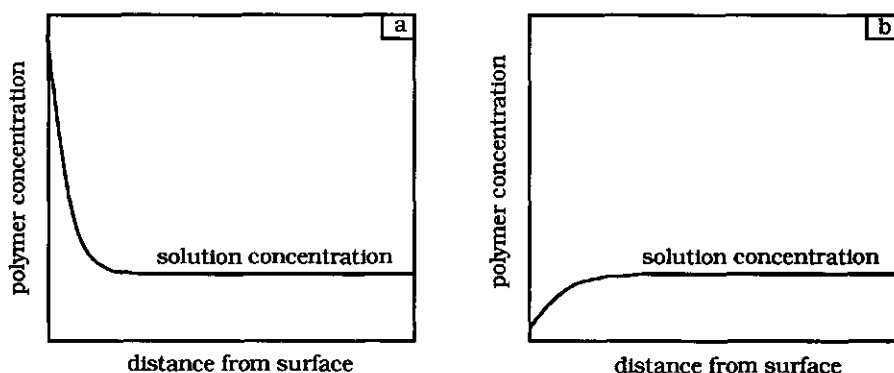
Figure 1. *Schematic concentration profiles of (a) adsorbed polymer and (b) depleted polymer.*

In the last decade, the understanding of the adsorption behaviour of polymers (in particular homopolymers) has increased considerably. Within an adsorbed chain one can distinguish trains, loops and tails. A train is a number of consecutive segments (≥1) which are in contact with the surface. Loops and tails protrude into the solution. Loops have both ends attached to train ends, whereas tails have one end free. If a small number of chains is adsorbed, homopolymers assume a very flat conformation with many segments in trains and only few in loops and tails. On the other hand, when the adsorbed amount is high, homopolymers have a large fraction of segments in loops and tails and relatively less in trains. The adsorption energy per segment is not necessarily high in order to find large adsorbed amounts. A

substantial fraction of segments of the same chain are in contact with the surface, and hence the gain in adsorption energy per molecule can be considerable, even if the contribution per segment is small.

Adsorption takes only place if the adsorption energy is higher than a certain critical value. In the vicinity of the surface the possible number of arrangements of a macromolecule, and hence its conformational entropy, is smaller than in the bulk solution. If the adsorption energy is not large enough to overcome the loss in conformational entropy, the polymers are depleted from the surface so that the concentration near the surface is lower than in the bulk solution (see Figure 1b). Depletion is a special case of the general phenomenon known as negative adsorption.

Polymers and Colloidal Stability

Due to London-v.d Waals forces, colloidal particles attract each other. Therefore, if no repulsive force is present, they will flocculate, i.e., form large aggregates which precipitate from the solution. A thick adsorbed polymer layer can form a steric barrier which opposes flocculation (Figure 2a). However, if only a small number of molecules is in contact with the surface, the chains can form bridges, i.e., adsorb on both surfaces when two particles come close (Figure 2b). Consequently, colloids covered by polymer, but below saturation, show enhanced flocculation.
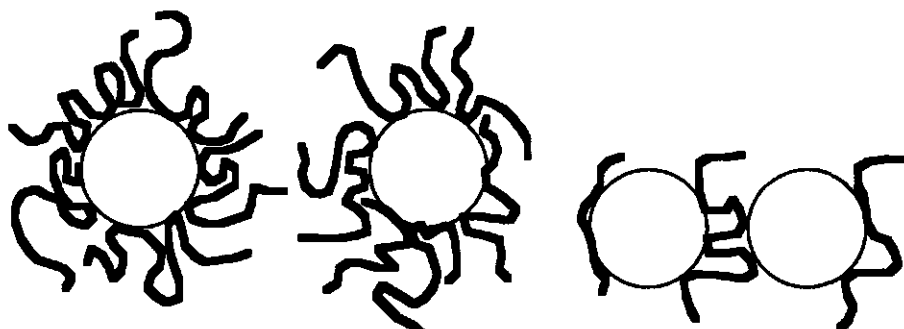
Figure 2.   (a) Sterically   (b) Bridging
                    stabilized particles   flocculation

Homopolymer solutions are known to phase separate under poor solvency conditions. In that case, one phase has a high concentration of polymer and the other a high solvent concentration. The solvent quality can decrease by changing the temperature, or by adding a nonsolvent for the polymer. In a similar way, instability of particles stabilized with homopolymers can be induced by decreasing the solvency for the adsorbed chains.

When two particles approach each other in a solution of nonadsorbing polymer, the polymer avoids the region between the two particles. At small separation, the polymer would be squeezed, causing a large reduction of the conformational entropy. The conformational entropy loss drives the polymer out of the gap, so that only pure solvent remains between the particles. Hence a concentration difference and, consequently, an osmotic pressure between the bulk solution and this interparticle zone arises which can force the particles to flocculate.

Specific Polymers and their Properties

The structure, composition and molecular weight of a polymer determines strongly its adsorption and solution properties. In the second section of this chapter a distinction was made between homopolymers, copolymers and polyelectrolytes. A homopolymer can be linear, branched or ring shaped. In copolymers the distribution of the different segments along the chain can be arranged in different ways:

1) Block copolymers: the segment types are grouped in sequential blocks. For example, AB diblock copolymers have two different blocks in the chain: an A block and a B block.

2) Random copolymers: the segment types are randomly distributed along the chain. In this case the various molecules in the system do, as a rule, not have the same fraction of the different segment types. The composition per molecule shows a certain distribution around its average.

3) Copolymers with a given sequence: the segment types are distributed in the same order in all chains, like in proteins. Hence, all molecules are identical.

4) Alternating copolymers: there are only bonds between two different segment types.

Block copolymers can show unusual solution behaviour. Above a certain critical concentration, block copolymers can form (soluble) aggregates if one of the blocks is insoluble in the solvent. The core of such an aggregate consists of insoluble blocks which are shielded from the (selective) solvent by the soluble blocks. The aggregate can assume different shapes, e.g., they may have a spherical (micelle), cylindrical, or lamellar (membrane) geometry. For random and alternating copolymers this behaviour is not so often observed, because they cannot separate their different segments so easily.

The adsorption behaviour of block copolymers can be quite different from that of homopolymers. The adsorbing blocks form a dense layer near the surface, whereas the nonadsorbing blocks give rise to long dangling tails which protrude into the solution. In this way a thick adsorbed layer is formed. Because the tails are not attracted by the surface, bridging flocculation is less conceivable. Hence a very effective barrier against flocculation is obtained. The stabilization of colloidal suspensions by block copolymers is less sensitive to variations in the dispersion medium than in the case of homopolymers.

Grafted polymers are a special category of molecules, because they are chemically bonded to a solid surface with one or more of their segments. By grafting the polymer, extremely high surface densities of the molecules can be obtained, much higher than with only physically adsorbing polymer. Therefore, grafted layers can be very effective in stabilizing colloidal particles.

Self-Consistent Field Theory

In 1979, Scheutjens and Fleer[1] introduced a self-consistent field theory, which was able to describe the adsorption properties of homopolymers rather well. The theory is based on relatively simple Boltzmann-statistics. The space is divided into discrete layers parallel to the surface. In the first layer, the polymer segments gain adsorption energy with respect to the segments in the other layers. In every layer, a Boltzmann factor can be defined, which depends on the po-

tential in this layer. This potential is a function of the adsorption energy, the concentration of other segments and solvent molecules in the same layer, and the interaction energies between the different components in the system. (This is to some extent comparable to the gravitational field, where the Boltzmann factor is determined by the mass of the particles, the height, and the gravitational constant. A difference is that the Boltzmann factor is independent of the local concentration.) To find the Boltzmann factor of a certain conformation of a polymer chain, it is assumed that the potential of the chain is the sum of the potentials of its segments. In this lattice theory, a conformation is defined as the sequence of layers in which the successive segments of a chain are situated. Assume we have a trimer with segment 1 in layer 1, and segments 2 and 3 in layer 2. The potential of this conformation is equal to the segment potential in layer 1 plus twice the segment potential in layer 2. With the Boltzmann factors of all the different conformations, the concentration profile can be calculated. For a polymer, the number of possible conformations becomes very large. Using a clever matrix method developed by DiMarzio and Rubin,[4] the computing time for the potentials of the different conformations is relatively short. The computer is not only needed to enumerate these potentials. The concentrations are determined by the potentials in the layers (the field) which on their turn depend on the local concentrations. Using a numerical iteration method, it is possible to find this self-consistent field and corresponding concentration profile.

This theory has turned out to be very useful to describe the behaviour of various systems containing polymers or surfactant-like molecules near interfaces. In a second paper Scheutjens and Fleer[2] showed how it is possible to calculate the size distribution and the fraction of segments in trains, loops, and tails. A detailed picture of the adsorbed layer was obtained. The interaction between two surfaces coated with adsorbed polymer was calculated in a third paper.[5] Depletion interaction between two surfaces has also been worked out.[6] Cosgrove et al.[7] showed how the configuration of terminally attached chains can be modelled. Employing conformation statistics in three dimensions, Van Lent et al.[8] enumerated the adsorption of ring polymers. Leermakers et al.[9] adapted the theory to describe the

formation of lamellar membranes of lipid molecules. This work was extended to take into account the difference in energy between trans and gauche bonds[10] (using the Rotational Isomeric State (RIS) scheme), and to incorporate the so called anisotropic molecular field in a membrane.[11] In two other papers,[12,13] it was shown how micelle and vesicle formation can be calculated. Theodorou[14] used the basis of the theory to calculate surface tensions of polymer liquids. The adsorption of block copolymers and the interaction between two surfaces coated with block copolymers has recently been worked out by Evers et al.[15] Using a multi sternlayer model Böhmer et al.[16] have extended the theory to describe polyelectrolyte adsorption.

Outline of this Study

In this study the self-consistent field theory will be extended to several systems which are known to be of importance in practical applications. Much attention will be paid to systems in which the structure of the polymer molecules largely affects the adsorption and/or has specific contributions to the interaction between two surfaces.

In chapter 2, the adsorption of block copolymers, which can form micelles in the bulk solution, will be considered. Adsorption as well as micelle formation are calculated. Obviously, this theory can also be used for the adsorption of surfactants (being small block copolymers).

In chapter 3, the adsorption of random copolymers is treated, taking properly into account all possible sequences of the segments in the chains. The difference in adsorption properties between random copolymers, block copolymers, and homopolymers is evaluated.

The destabilization of particles coated with terminally attached chains (so called hairy particles) in solutions of free polymer is not fully understood, see for example ref. (17). In chapter 4, the depletion interaction between hairy surfaces in the presence of nonadsorbing polymer is calculated. A detailed picture of the changes in the conformations of the grafted and free polymer is given. The explanation of the interaction in these systems turns out to be much more complex than that for the interaction between hard (uncovered) surfaces in a solution of nonadsorbing polymer.

Computational Aspects.

All programs were written in Simula. One of the main problems is to find a set of sufficiently linear equations so that the segment potentials converge iteratively to the equilibrium self-consistent field. A detailed description of the numerical analysis can be found in the PhD thesis of O.A. Evers.[15] A numerical routine, called NEWTON, written by J.M.H.M. Scheutjens, was used to solve the equations.

References

1) Scheutjens J.M.H.M., and Fleer G.J., J. Phys. Chem. (1979), 83, 1619

2) Scheutjens J.M.H.M., and Fleer G.J., J. Phys. Chem. (1980), 84, 178

3) Eirich F.J., J. Colloid Interface Sci. (1977), 58, 423

4) DiMarzio E.A., and Rubin R.J., J. Chem. Phys.(1971), 55, 4318

5) Scheutjens J.M.H.M., and Fleer G.J., Macromolecules(1985), 18, 1882

6) Scheutjens J.M.H.M., and Fleer G.J., Adv. Colloid Interface Sci. (1982), 16, 361; Erratum: ibid. (1983), 18, 309

7) Cosgrove T., Heath T., Van Lent B., Leermakers F., and Scheutjens J., Macromolecules(1987), 20, 1692

8) Van Lent B., Scheutjens J., and Cosgrove T., Macromolecules(1987), 20, 366

9) Leermakers F.A.M., Scheutjens J.M.H.M., and Lyklema J., Biophysical Chem.(1983), 18, 353

10) Leermakers F.A.M., and Scheutjens J.M.H.M., J. Chem. Phys.(1988), 89, 3264

11) Leermakers F.A.M., and Scheutjens J.M.H.M., J. Chem. Phys.(1988), 89, 6912

12) Leermakers F.A.M., Van der Schoot P.P.A.M., Scheutjens J.M.H.M., and Lyklema J., In Surfactants in Solution, Modern Applications; Mittal K.L., Ed.; in press

13) Leermakers F.A.M., and Scheutjens J.M.H.M., J. Phys. Chem. submitted

14) Theodorou D.N., Macromolecules(1988), <u>21</u>, 1391, ibid. 1400, ibid. 1411, ibid. 1422

15) Evers O.A., PhD thesis, Wageningen, Agricultural University(1989); Macromolecules, submitted

16) Böhmer M.R., Evers O.A., and Scheutjens J.M.H.M., submitted to Macromolecules

17) Vincent B., Edwards J., Emmet S., and Jones A., Colloids and Surfaces(1986), <u>18</u>, 261

Chapter 2

Influence of Association on Adsorption
Properties of Block Copolymers

Abstract

The self-consistent field theory of Scheutjens and Fleer for the adsorption of homopolymers has been modified to study the adsorption of block copolymers from a selective solvent. With this extension it is possible to calculate the critical micelle concentration (cmc; for spherical or planar associates) and to show the influence of the self-aggregation of block copolymers on their adsorption behaviour. The statistical weight of all possible conformations in the lattice is taken into account. Lateral interactions are calculated with a mean field approximation within each layer. For planar structures parallel lattice layers are used; for modelling micelles a spherical lattice is introduced. The cmc is determined from a small system thermodynamics argument of Hall and Pethica. For molecules with a long lyophobic block extremely low cmc values are found. The adsorption of these block copolymers on lyophobic surfaces increases sharply just below the cmc and is essentially constant at higher concentrations of polymer. Thick adsorption layers are formed. The effect of the interaction parameters is shown.

I Introduction

Recently, the self consistent-field theory (SCF) of Scheutjens and Fleer[1,2] for homopolymer adsorption at the solid-liquid interface has been extended to the case of block copolymers.[3] This theory assumes equilibrium between adsorbed polymers and a homogeneous bulk solution. For homopolymers this assumption is reasonable for quite a large concentration range. Block copolymers, however, can form association structures like micelles and lamellar membranes. In that case the critical micelle (or membrane) concentration, the cmc,

will limit the chemical potential of the polymer and, hence, the adsorption. When the cmc has been reached, polymer added to the solution will mainly aggregate and thus hardly affect the adsorption. For surfactants this has already been found experimentally, see for example ref (4 and 5).

Leermakers et al.[6] have derived equations to model chains in spherical and cylindrical lattices. Using these types of lattices, they have extended the SCF theory to calculate the equilibrium association structures for small surfactants. We will apply this method to investigate the association of block copolymers in solution and limit ourselves to spherical (micelle) and planar (membrane) lattices. The association structure with the lowest concentration of free polymer in solution and thus the lowest chemical potential is chosen as the equilibrium state. This concentration of free polymer is the maximum concentration for which calculation of the adsorption is relevant.

In this article the theories for the adsorption of block copolymers[3] and the association of surfactants[6] are combined. In section II we describe the SCF theory for block copolymers in associates of planar geometry. We shortly review the model for spherical micelles in section III. In section IV the calculation of the cmc is explained. The influence of chain length and structure of the block copolymers on the cmc are shown in section V. We also examine the influence of the different interaction parameters. Finally, the adsorption behaviour of these associating block copolymers is analyzed in some detail. Adsorption isotherms on lyophilic and lyophobic surfaces are shown. (We use the generic terms lyophilic and lyophobic for solvent-liking and solvent-disliking, respectively, to avoid less general terms like polar, apolar, hydrophilic and hydrophobic.) The effects of chain length, block sizes, solvency, and adsorption energy on the adsorption are examined.

II Self-Consistent Field Theory

In this section we explain the theory for a lattice of planar geometry. In case of adsorption at the solid-liquid interface the first lattice layer is assumed to be adjacent to the surface. For membranes the

first layer is in the centre of the bilayer, where a reflecting boundary
is assumed. The layers are numbered $z = 1$ to M. Each layer has L
sites. A lattice site has Z neighbours of which a fraction λ_1 is in the
next, a fraction λ_0 in the same, and a fraction λ_{-1} in the previous
layer. For a hexagonal lattice $\lambda_{-1} = \lambda_1 = 0.25$ and $\lambda_0 = 0.5$. A polymer
or a solvent molecule of type i (i = 1,2, ...) has a volume fraction $\phi_i(z)$
in layer z of which a volume fraction $\phi_{xi}(z)$ are segments of type x (x
= A, B, ...). Similarly, $\phi_x(z)$ is the total volume fraction of x segments
in layer z. So $\phi_x(z)$ is the summation of $\phi_{xi}(z)$ over all i, the total con-
tribution from all molecules having segments of type x.

We neglect inhomogeneities within each layer z. Only the density
profile perpendicular to the lattice layers will be considered. The SCF
theory calculates the most probable set of conformations, where the
system is at its minimum free energy. A conformation is defined as
the sequence of layers in which the successive segments of a chain
are situated.

For each segment s of molecule i we can write an end segment-
distribution function $G_i(z,s\,|\,1)$. It describes the average weight of
walks along molecule i, starting at segment 1 in an arbitrary layer in
the system and ending after s - 1 steps in layer z. $G_i(z,s\,|\,1)$ is related
to the end-segment distribution function of a walk of s - 2 steps (s - 1
segments):

$$G_i(z,s|1) = G_i(z,s)\{\lambda_{-1} G_i(z-1,s-1|1) + \lambda_0 G_i(z,s-1|1) + \lambda_1 G_i(z+1,s-1|1)\} \qquad (1)$$

$G_i(z,s)$ is the statistical weight of a free segment s in layer z. If seg-
ment s is of type x then $G_i(z,s)$ equals the segment weighting factor
$G_x(z)$. This is a Boltzmann factor, which gives the relative preference
of segment type x to be in layer z rather than in the homogeneous
bulk solution. In the bulk solution $G_x(z) = 1$. For every segment type
one can define such a factor. The expression for these factors will be
given later. Note that for copolymers each segment can be of a differ-
ent type. Equation (1) is a recurrence relation. Starting with segment
1 and ending at segment r_i, we calculate all end segment distribution
functions of chains of lengths between 1 and r_i segments. For exam-
ple, if segment 1 is of type A we have $G_i(z,1\,|\,1) = G_A(z)$. When we

consider adsorption, we set $G_x(z) = 0$ for $z \leq 0$. For membranes, however, we set $G_x(-z+1) = G_x(z)$. This has the effect of placing a mirror between layers 0 and 1.

We want to know the distribution function $G_i(z,s\,|\,1;r)$ of segment s of a chain of r_i segments. We start a walk at segment 1 and another walk at segment r_i and stop both walks at segment s. $G_i(z,s\,|\,1;r)$ is a combination of end-segment distribution functions of the two walks:

$$G_i(z,s\,|\,1;r) = \frac{G_i(z,s\,|\,1)\,G_i(z,s\,|\,r)}{G_i(z,s)} \tag{2}$$

We divide by $G_i(z,s)$, because this factor is included in both walks. In this way we are able to calculate all the distribution functions of all segments. The sum of these functions gives the volume fraction $\phi_i(z)$ of molecules of given type i in layer z:

$$\phi_i(z) = C_i \sum_{s=1}^{r_i} \frac{G_i(z,s\,|\,1)G_i(z,s\,|\,r)}{G_i(z,s)} \tag{3}$$

One can find $\phi_{Ai}(z)$ by performing the summation in equation (3) only over those segments which are of type A. The quantity C_i is a normalization factor. We can derive this factor from the volume fraction ϕ_i^b in the bulk solution, where all the end-segment distribution functions are unity. If we substitute this into equation (3) we see that:

$$C_i = \frac{\phi_i^b}{r_i} \tag{4}$$

We can also express C_i in the total amount $\theta_i = \sum_{z=1}^{M} \phi_i(z)$ of polymer segments in the system (in equivalent monolayers). The average of the end segment distribution function of a chain of r_i segments is $\sum_{z=1}^{M} G_i(z,r\,|\,1)/M$. The average volume fraction equals θ_i/M. Hence

$$C_i = \frac{\theta_i}{r_i \sum_{z=1}^{M} G_i(z,r\,|\,1)} \tag{5}$$

As said before, to use equation (1), we need an expression for $G_A(z)$, $G_B(z)$, etc. The molecules will distribute themselves according to the effective potential field they are feeling. The energy of a certain conformation is the sum of the potentials $u(z)$ of the different segments. A molecule of three segments with segment A in layer 1 and two B segments in layer 2 would have an energy level of $u_A(1) + 2u_B(2)$. The weighting factor for this conformation would be $\lambda_1\lambda_0 \mathrm{Exp}((-u_A(1) - 2u_B(2))/kT)$. This should be equal to $\lambda_1\lambda_0 G_A G_B^2$. The segmental weighting factor $G_x(z)$ is now defined as:

$$G_x(z) = e^{\dfrac{-u_x(z)}{kT}} \tag{6}$$

The expression for $u_x(z)$ has been derived from statistical thermodynamics.[3]

$$u_x(z) = u'(z) + kT\sum_y \chi_{xy}\left(<\phi_y(z)> - \phi_y^b \right) \tag{7}$$

The subscripts x and y can refer to any segment in the system (A, B, ...). The site volume fraction, $<\phi_x(z)>$, is defined as:

$$<\phi_x(z)> = \lambda_{-1}\phi_x(z-1) + \lambda_0\phi_x(z) + \lambda_1\phi_x(z+1) \tag{8}$$

In equation (7), the first term, $u'(z)$, is a potential that accounts for the hard core interaction in layer z relative to the bulk solution and is independent of the segment type. It is essentially a Lagrange multiplier, which arises in the free energy minimization[3] because of the boundary condition $\sum_i \phi_i(z) = 1$. Physically, with increasing segment density, the hard-core potential (with respect to the bulk solution) is assumed to switch from $-\infty$ to $+\infty$ at the moment that $\sum_i \phi_i(z)$ passes 1. The equilibrium values of $u'(z)$ depend strongly on the system under consideration and are of the order of 1 kT or less. Unfortunately, no explicit expression for $u'(z)$ is available. The values are obtained by numerically adjusting $u'(z)$ so that $\sum_i \phi_i(z)$ (obtained from eq. (3)) is unity for each layer z.

The second part of equation (7) expresses the specific interaction term, in which χ_{xy} is the familiar Flory-Huggins parameter for the interaction between monomers of types x and y.[7] For z large $\phi_x(z) = \phi_x^b$, $u_x(z) \approx 0$, and $G_x(z) = 1$. In the summation over y, we have also included the interaction energy between a segment and the surface (x = S). The volume fraction of the solid is 1 in layer 0 and 0 for z > 0. As we can see from equation (7) the interaction between segments A and the surface S equals $kT\chi_{AS}\lambda_1$.

With equations (3), (6) and (7) and the condition that $\sum_i \phi_i(z) = 1$ for each layer z, we are in principle able to calculate numerically the adsorption profile or the profile of a membrane for a given amount of polymer or a given bulk concentration.[1,3]

III Spherical Lattices

By comparing calculated free energies of membranes and micelles, we can analyze which structure is preferred. For the modeling of micelles we have to modify the structure of the lattice. Figure (1) shows a cross section through the centre of a spherical lattice. The layers are numbered sequentially, starting at the centre of the lattice. For the spherical lattice the following conditions must hold:
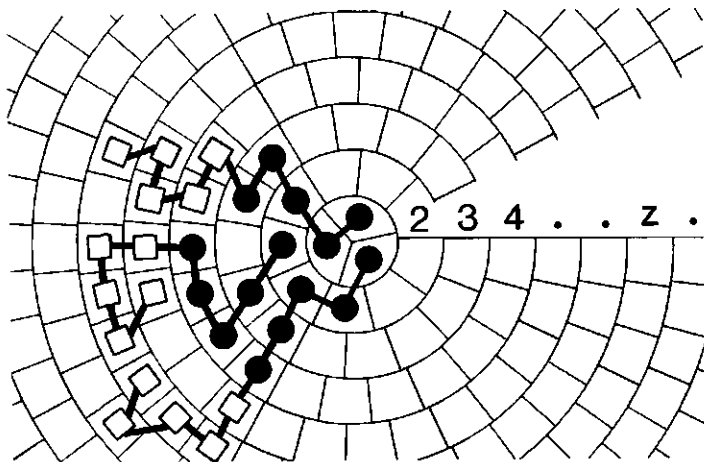
Figure 1.   *Block copolymers in a spherical lattice.*

1. All lattice sites have equal volume.
2. All lattice layers are equidistant.
3. The coordination number Z is constant for each lattice site.

These conditions have certain consequences. Sites in different layers have different shapes. The total number of lattice sites $L(z)$ in layer z is no longer an integer. The position of neighbouring sites is variable. The volume $V(z)$ in number of lattice sites of a spherical lattice equal:

$$V(z) = (4/3)\pi z^3 \tag{9}$$

Differentiating equation (9) with respect to z gives the surface area:

$$S(z) = 4\pi z^2 \tag{10}$$

The number of sites in layer z is the difference in volume between $V(z)$ and $V(z-1)$:

$$L(z) = V(z) - V(z-1) \tag{11}$$

In the spherical lattice λ_0, λ_1 and λ_{-1} are a function of z. The following relation must still hold:

$$\lambda_{-1}(z) + \lambda_0(z) + \lambda_1(z) = 1 \tag{12}$$

If we generate a particular conformation of a molecule and calculate its statistical weight, it should not make any difference at which end of the molecule we have started our walk. Therefore

$$Z\lambda_{-1}(z)L(z) = Z\lambda_1(z-1)L(z-1) \tag{13}$$

The transition factors λ_{-1} and λ_1 are proportional to the surface area per site in contact with the adjacent layer. Thus, the final equations are given by

$$\lambda_1(z) = \lambda_1^b S(z)/L(z) \qquad \lambda_{-1}(z) = \lambda_{-1}^b S(z-1)/L(z) \tag{14}$$

where λ_1^b and λ_{-1}^b are the values of the transition factors for the equivalent planar lattice, i.e., at $z \to \infty$. For micelles the λ's in equations (1) and (8) have to be substituted by those of equations (12) and (14). In equation (5), θ_i has to be replaced by $n_i r_i$, which equals $\sum_{z=1}^{M} L(z)\phi_i(z)$ and the denominator changes into $r_i \sum_{z=1}^{M} L(z)G_i(z,r\,|\,1)$.

IV The Cmc

The theory for association structures as outlined in sections II and III gives us the equilibrium structure of a single micelle or membrane in equilibrium with a homogeneous bulk solution. What we do want to know is the critical micelle or (membrane) concentration of a solution of block copolymers, where an unknown number of micelles is being formed. In this section the equilibrium condition for a micellar solution is explained and the implementation of this condition into our model is described.

We can apply small system thermodynamics to our micellar solution.[8] The solution is divided into subsystems of a volume V_s, which contain one micelle each and have a composition that is determined by the overall concentration $\bar{\phi}_i$. The excess free energy A_s^{exc} of a small system can be defined. It contains a part A_m^{σ}, which describes the free energy necessary to create a micelle with fixed centre of mass and an entropy term, which contains the translational entropy of the micelles.[8]

$$A_s^{exc} = A_m^{\sigma} + kT\ln(V_m\,/V_s) \tag{15}$$

V_m is the volume of a micelle. The expression for A_m^{σ} is equivalent with the expression for the surface free energy in ref. (3):

$$\frac{A_m^{\sigma}}{kT} = -\sum_z L(z)u'(z) - \sum_i n_i^{exc}$$

$$-\frac{1}{2}\sum_x\sum_y\sum_z L(z)\chi_{xy}\{\phi_x(z) < \phi_y(z) > -\phi_x^b\phi_y^b\} \tag{16}$$
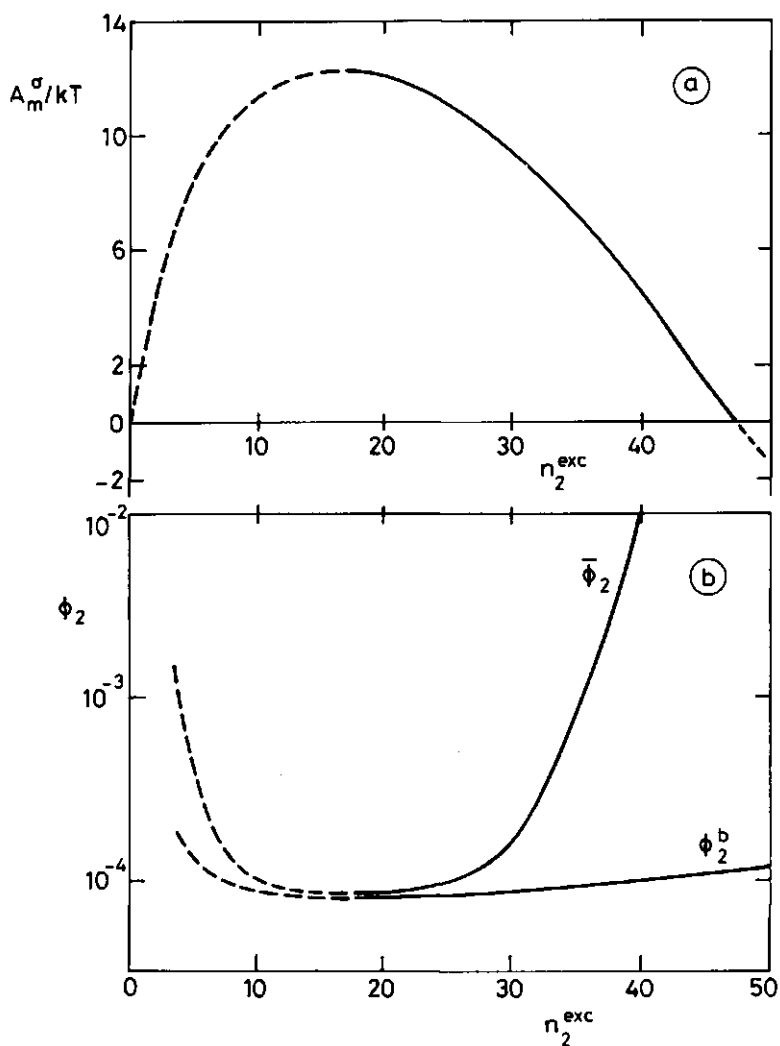
Figure 2. *(a) Excess free energy of aggregation A_m^σ, as a function of the excess number of $A_{70}B_{30}$ molecules per micelle, n_2^{exc}, in a B solvent. (b) Corresponding composition $\bar{\phi}_2$ and the equilibrium polymer concentration ϕ_2^b in the same system. The dashed part of the curves represent thermodynamically unstable regimes. $\chi_{AB} = 1$.*

A typical curve for A_m^σ as a function of n_2^{exc}, the excess number of molecules 2 aggregated in a spherical micelle with respect to their

equilibrium concentration, is shown in Figure (2a). This figure is calculated with the theory as outlined in the previous sections for a system consisting of $A_{70}B_{30}$ molecules (component 2) in a B solvent (component 1), with $\chi_{AB} = 1$. Throughout this paper, the A block is lyophobic. With increasing n_2^{exc}, the free energy A_m^{σ} initially rises, as it is unfavourable for the molecules to aggregate in such small numbers. The interaction energy gained is outweighted by the loss in entropy of the individual molecules. Above a certain aggregation number, in this case 18, it becomes energetically more and more favourable to associate and A_m^{σ} decreases. In equilibrium[8]

$$dA = -SdT - PdV + \sum_i n_i \mu_i + A_s^{exc} dN_m = 0 \qquad (17)$$

where A is the free energy of the whole system of volume $V = N_m V_s$ and N_m is the total number of micelles (or subsystems). To fulfill the condition that $dA = 0$ at constant T, V, and $\{n_i\}$, A_s^{exc} has to be zero. If A_s^{exc} would be negative or positive, A would decrease by forming a higher or lower number of micelles, respectively. Applying this to equation (15) shows that the extra free energy due to aggregation must be balanced by the entropy of the micelles. Moreover, from equation (15) we see that A_m^{σ} should be positive, because obviously $V_m \leq V_s$.

We will now derive how the equilibrium concentration ϕ_2^b of polymer depends on the composition $\bar{\phi}_2$ of the system. The excess number of polymer molecules n_2^{exc} in micelles is related to the small system volume V_s expressed in number of lattice sites, and the overall composition $\bar{\phi}_2$ by $n_2^{exc} r_2 = V_s(\bar{\phi}_2 - \phi_2^b)$. Rewriting this relation gives

$$V_s = \frac{n_2^{exc} r_2}{\bar{\phi}_2 - \phi_2^b} \qquad (18)$$

As the volume fraction of polymer in the core of a micelle is virtually constant, the volume of a micelle expressed in number of lattice sites can be approximated by:
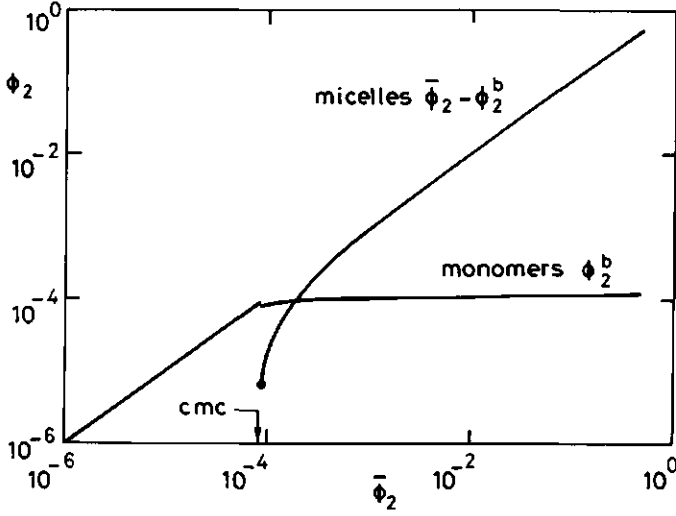
Figure 3. *Equilibrium concentration* ϕ_2^b *and volume fraction of micelles* $\bar{\phi}_2$ - ϕ_2^b *as a function of composition* $\bar{\phi}_2$ *for an* $A_{70}B_{30}$ *block copolymer in a B solvent.*

$$V_m \approx \frac{n_2^{exc} r_2}{\phi_2(1) - \phi_2^b} \tag{19}$$

Combination of equation (15), (18) and (19) gives:

$$\bar{\phi}_2 \approx (\phi_2(1) - \phi_2^b)e^{-A_m^\sigma/kT} + \phi_2^b \tag{20}$$

allowing $\bar{\phi}_2$ to be computed from the concentration profile. In Figure (2b), $\bar{\phi}_2$ and ϕ_2^b are plotted as a function of n_2^{exc}. It can be seen that a minimum concentration, the cmc, is necessary to create micelles. Note that, in correspondence with the Gibbs adsorption equation, ϕ_2^b is at its minimum when A_m^σ is at its maximum. Increasing the composition beyond the cmc will increase n_2^{exc}. For the same composition, ϕ_2^b at the right hand-side of the minimum, and therefore the chemical potential, μ_2, is lower than the corresponding value at the left hand side. Therefore, the dashed portion of the curves in Figure (2) represent thermodynamically unstable micelles. In Figure (3), the

overall composition $\bar{\phi}_2$ is subdivided into the equilibrium concentra-
tion, ϕ_2^b, and the excess volume fraction of aggregated molecules, $\bar{\phi}_2$
- ϕ_2^b. At the cmc, the equilibrium concentration ϕ_2^b drops because of
the formation of micelles. The concentration of micelles and hence
the reduction in equilibrium concentration equals the difference be-
tween the two curves at their minimum (around $n_2^{exc} = 18$) in Figure
(2a). It can be seen that beyond the cmc the equilibrium concentra-
tion hardly increases and all additional molecules aggregate, as ex-
pected.

The procedure for calculating the equilibrium concentration for a
given composition $\bar{\phi}_2$ is as follows. We start with a certain number n_i
of each molecule in a system of M layers. With the theory, as outlined
in sections II and III, n_i^{exc} and ϕ_i^b are calculated. Substitution of
these parameters and the chosen composition into equations (18)
and (19) gives the small system and micelle volumes. Substituting
these values and A_m^σ, obtained from equation (16), into equation (15)
gives A_s^{exc}. Now the amount of polymer in the system can be changed
and the whole procedure can be repeated until $A_s^{exc} = 0$. Obviously, a
numerical procedure is needed to solve this problem. Note that the
small system volume may be different from the volume of the M lay-
ers under consideration.

For membranes, L is very large and the entropy term per surface
site $L^{-1}\ln(V_m/V_s)$ is negligible. We only have to find the equilibrium
concentration ϕ_2^b for which A_m^σ/L equals zero.

V Results and Discussion

In the first part of this section some general trends for micelle and
membrane formation will be studied. In the second part the influence
of micellization on the adsorption of block copolymers will be shown.
For all the calculations λ_1^b and λ_{-1}^b have been taken equal to 0.25
(hexagonal lattice). The choice of lattice slightly affects the numerical
results but not the general trends, see for example ref (1, 9, and 10).

In Figure (4), typical segment density profiles are shown of a mi-
celle of $A_{70}B_{30}$ block copolymers in a B solvent. The interaction be-
tween A and B segments is repulsive: $\chi_{AB} = 1$. In the centre of the

micelle a high concentration of A segments is found. This concentration is essentially equal to that in the concentrated phase at the binodal, calculated with Flory's equation for phase separation between an A_{70} homopolymer and a B solvent.(7) The core of A segments is surrounded by a shell of B segments, where the solvent density is not much lower than in the bulk solution. The concentration of solvent in the core is far from zero. For higher values of χ_{AB} this concentration decreases strongly.
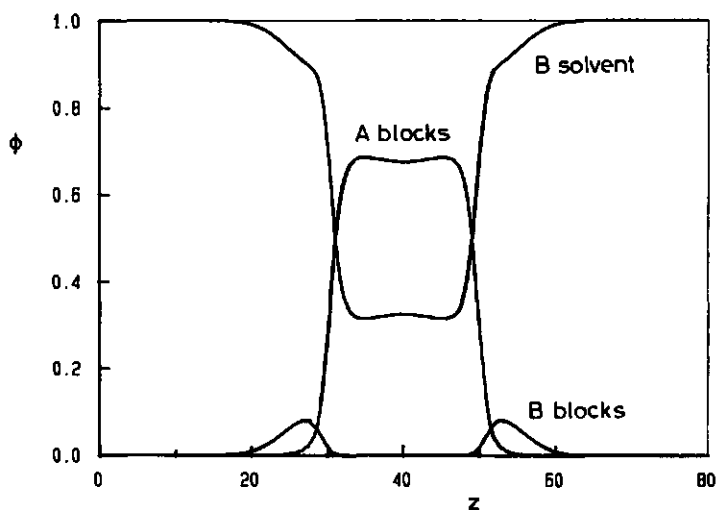
Figure 4. *Segment density profiles of a micelle of an $A_{70}B_{30}$ block copolymer in a B solvent. The layers are renumbered; z = 40 is the centre of the micelle. χ_{AB} = 1.*

In Figure (5), the effect of the number of lyophobic segments on the formation of micelles and membranes is shown for an AB block copolymer of 100 segments in a B solvent. In this figure χ_{AB} = 1.5. The concentration where global phase separation between solvent and polymer would occur has also been calculated, using the extended Flory-Huggins formulas for the chemical potential μ_i of (randomly mixed) copolymers[3]:

$$(\mu_i - \mu_i^*)/kT = \ln\phi_i + 1 - r_i \sum_j \phi_j /r_j$$

$$+ (1/2)r_i \sum_x \sum_y \chi_{xy}(\phi_{xi}^* - \phi_x)(\phi_y - \phi_{yi}^*) \qquad (21)$$
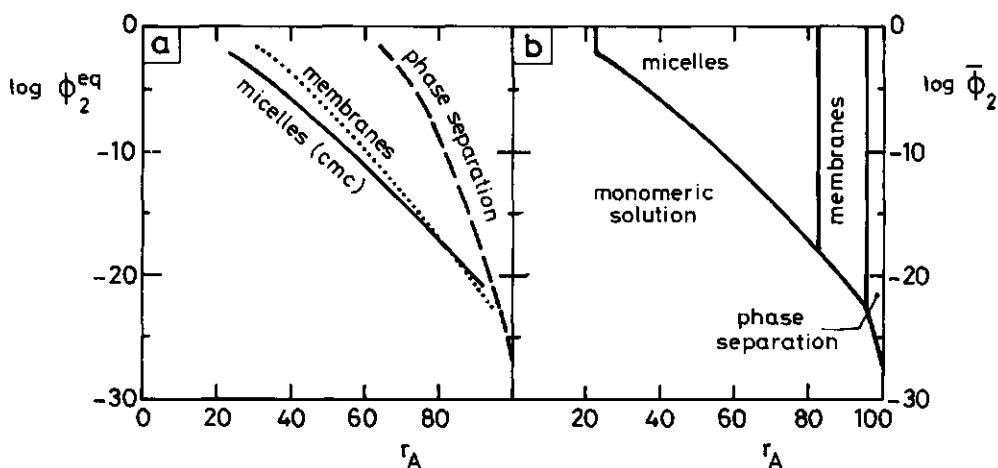
Figure 5. *Phase behaviour of AB block copolymers of chain length $r_2 = 100$ in a B solvent. $\chi_{AB} = 1.5$.*

(a) Equilibrium concentration of polymer in the presence of micelles (solid curve), membranes (dotted curve), and global phase separation (dashed curve) as a function of the number of A segments per molecule.

(b) Phase diagram, in which the regions are indicated where micelles, membranes, phase separation and a monomeric solution occur.

Here, μ_i^* is the chemical potential and $\phi_{xi}^* = r_{xi}/r_i$ is the volume fraction of segments of type x, in amorphous polymer of type i. A more detailed analysis of the phase behaviour of random copolymers has been made by Koningsveld and Kleintjes.[11] In Figure (5a), the equilibrium concentration for micelles, membranes, and global phase separation is shown as a function of r_A. As is known from Figure (2), for micelles this concentration varies only slightly with composition. For (noninteracting) membranes and phase separation this concentration is independent of $\bar{\phi}_2$. If the A blocks are very short, there is
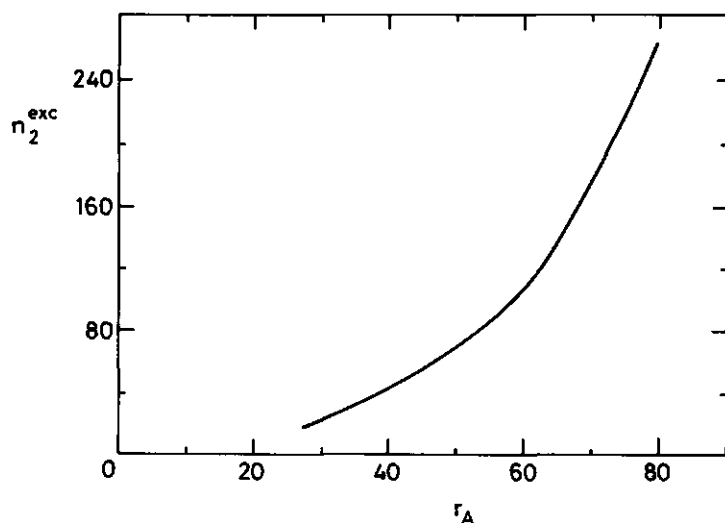
Figure 6. *Aggregation number n_2^{exc}, of a micelle as a function of the number of A segments in the polymer of Figure (5).*
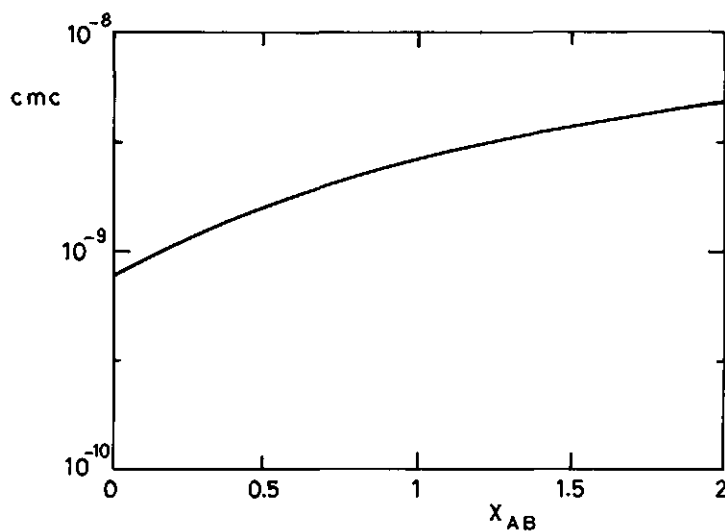

Figure 7. *Critical micelle concentration of an $A_{50}B_{50}$ di-block copolymer as a function of χ_{AB}. The χ parameters for the segment solvent interactions are: $\chi_{A0} = 1.5$, and $\chi_{B0} = 0$.*

no aggregation. Micelles are formed if the length of the A block is long enough. The critical micelle concentration is lower than the critical membrane concentration, except for high A/B ratios. When the B part becomes much smaller than the A part, a transition from micellar- to membrane-like structures (with a smaller surface area per molecule) is found. Finally, when the polymers consist mainly of A segments, the polymer and solvent will phase separate globally, because χ_{AB} is larger than the critical value for homopolymers of 100 A segments. The cmc for block copolymers with a large fraction of A is extremely low. This means that these molecules will usually be associated. Lowering χ_{AB} or decreasing the molecular weight will increase the cmc, which is mainly a function of $r_A\chi_{AB}$. In Figure (5b), a phase diagram is constructed by plotting $\bar{\phi}_2$ instead of ϕ_2^b. The areas where micelles, membranes, phase separation, and a monomeric solution occur are indicated. In this case, the lines form the boundaries between the different regions where the various structures exist. On the boundary between micelles and membranes both association structures coexist, i.e. they have the same equilibrium concentration for a certain composition. Here, this transition is rather sharp and virtually independent of $\bar{\phi}_2$, but in other systems there could be a wider range of coexistence. Of course, other structures than spherical or lamellar aggregates are possible, but these examples illustrate clearly a well known transition from more spherical to more lamellar structures as the A/B ratio increases.

In Figure (6), the aggregation number n_2^{exc}, of micelles of AB diblock copolymers from Figure (5), is plotted as a function of the length of the A block. As expected, the aggregation number increases strongly with increasing length of the A block.

The interaction between A and B segments is usually independent of the solvent quality. In Figure (5), the solvent molecules are of the same type as the B segments in the polymer. In Figure (7), the interaction χ_{AB} between the two segment types of an $A_{50}B_{50}$ block copolymer is varied, while the interactions between A and B segments and solvent (0) is kept constant ($\chi_{A0} = 1.5$ and $\chi_{B0} = 0$). A lower χ_{AB} appears to decrease the cmc. In the micelle are more contacts between A and B blocks than in the homogeneous bulk solution.
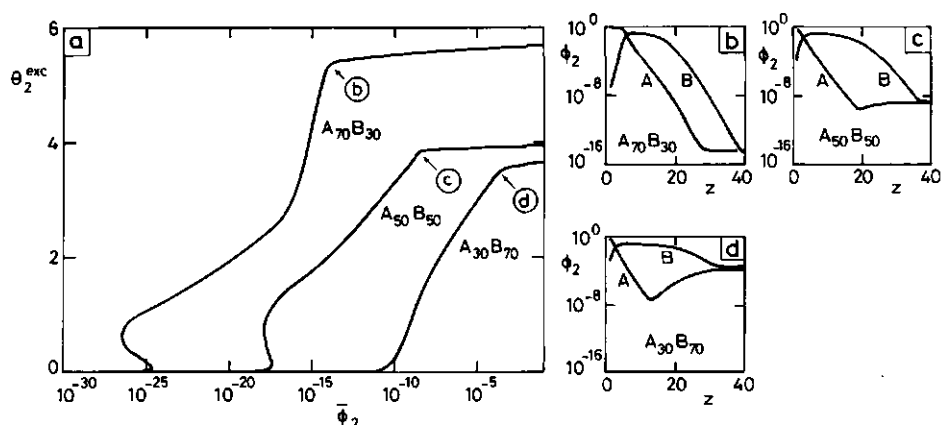
Figure 8. *(a) Adsorption isotherms for three different block copolymers: $A_{70}B_{30}$, $A_{50}B_{50}$ and $A_{30}B_{70}$ in a B solvent. Segment density profiles calculated in the plateau region of the adsorption isotherms.*

(b) $A_{70}B_{30}$, $\phi_2^b = 7*10^{-15}$, $\theta_2 = 5.4$;

(c) $A_{50}B_{50}$, $\phi_2^b = 26*10^{-10}$, $\theta_2 = 3.9$;

(b) $A_{30}B_{70}$, $\phi_2^b = 26*10^{-5}$, $\theta_2 = 3.6$;

Interaction parameters: $\chi_{AB} = 1.5$, $\chi_{AS} = -4$, $\chi_{BS} = \chi_{0S} = 0$.

Therefore, a higher χ_{AB} is unfavourable for aggregation. At $\chi_{AB} = 1.5$ the situation as in Figure (5) at $r_A = 50$ is recovered.

In Figure (8a), adsorption isotherms are shown for three different diblock copolymers, differing in A/B ratio: $A_{70}B_{30}$, $A_{50}B_{50}$, and $A_{30}B_{70}$. The A segments adsorb preferentially, $\chi_{AS} = -4$, while $\chi_{BS} = 0$. The interaction parameters between the different monomers are the same as in Figure (5). The adsorption isotherms are plotted as a function of the overall composition of the solution. For the $A_{30}B_{70}$ block copolymers the adsorbed amount increases steadily until the cmc at $\bar{\phi}_2 = 26*10^{-5}$ is reached. The adsorption hardly increases any further, because the concentration of free polymer in solution remains almost constant. The adsorption levels off near the point where A_m^{σ} is maximal (see Figure (2)). The $A_{70}B_{30}$ and $A_{50}B_{50}$ molecules show a slightly different behaviour. An S-shaped isotherm can be observed: as soon as a few chains adsorb, a cooperative aggre-

gation effect of A segments on the surface occurs. The adsorbed amount of the $A_{70}B_{30}$ increases until a semi-plateau is reached. Near the cmc, θ_2^{exc} rises again very sharply and levels off at the cmc. Adsorption isotherms with similar shape have been found for small surfactant molecules, see for example ref. (4) and (5). The surface acts as a condensation nucleus.

In parts b-d of Figure (8) the segment density profiles of the three different polymers at their maximum adsorbed amount are shown. The surface is occupied by A segments, whereas the B blocks form dangling tails. The longer the B block the further the polymer extends into the solution. Eventually, the densities of A and B segments decrease exponentially to their solution concentration. The dip in the profile of segments A in Figure (8d) occurs because these segments try to avoid the thick unfavourable layer of B segments.

Figure (9) illustrates the effect of chain length on the adsorbed amount and the difference in adsorption between molecules with adsorbing A blocks and molecules with adsorbing B blocks. In all the graphs of Figure (9), we have used $r_A/r_2 = 0.7$, $\chi_{AB} = \chi_{A0} = 1$ and $\chi_{B0} = 0$. In Figure (9a), adsorption isotherms are shown for $r_2 = 100$. The curve for adsorbing A blocks ($\chi_{AS} = -4$) can be compared with the $A_{70}B_{30}$ curve in Figure (8a), where $\chi_{AB} = 1.5$ instead of 1. Now the adsorption starts at about the same equilibrium concentration, but the cooperative effect has disappeared and the cmc is much higher for these molecules. The cooperative effect reappears when $\chi_{BS} = -4$ (adsorbing lyophilic blocks). This is more evident in the inset of Figure (9a). The volume fraction at which adsorption starts is much higher in this case, because the B blocks are much shorter than the A blocks. In Figure (9b), the excess adsorbed amount, θ_2^{exc}, at the cmc is shown as a function of chain length r_2. For the upper curve $\chi_{BS} = -4$, while $\chi_{AS} = \chi_{0S} = 0$, for the lower curve $\chi_{AS} = -4$ and $\chi_{BS} = \chi_{0S} = 0$. The concomitant cmc values are plotted in Figure (9c). The adsorbed amount is about twice as much when B rather than A segments adsorb preferentially. When $\chi_{BS} = -4$, a bilayer is formed at the surface. This is illustrated in Figure (9d), where a segment density profile for $r_2 = 100$ has been drawn. The B segments have a maximum in their profile in the layer adjacent to the surface and a second smaller maximum about 15 layers away from the surface. The
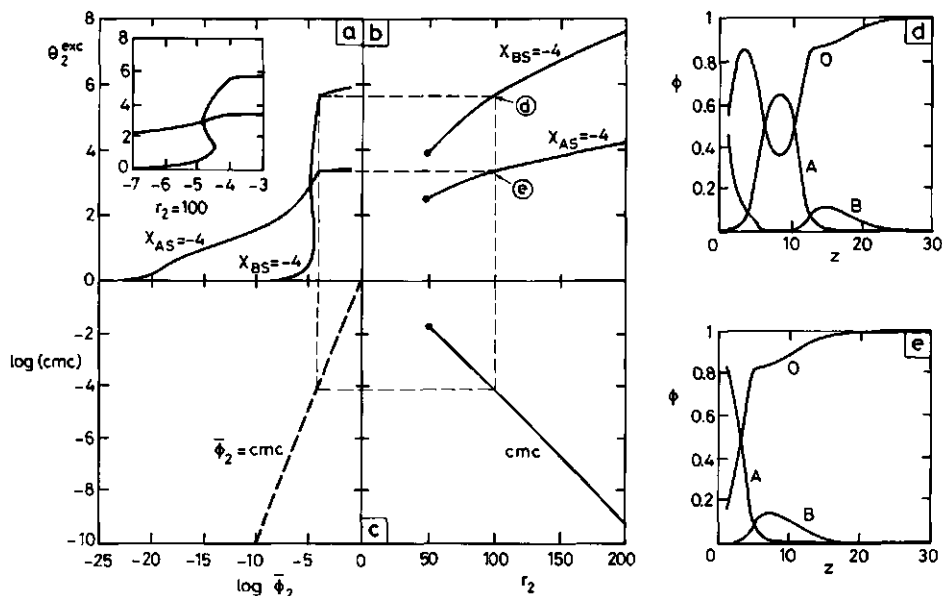
Figure 9. *Relation (dashed lines) between adsorption isotherms ((a) and inset), the adsorption at the cmc (b) and the cmc as a function of the chain length (c), both for adsorbing A segments (χ_{AS} = -4, χ_{BS} = 0) and for adsorbing B segments (χ_{AS} = 0, χ_{BS} = -4). Segment density profiles at the points indicated in (b) are given in (d) and (e). r_A/r_2 = 0.7, χ_{AB} = χ_{A0} = 1, χ_{B0} = 0.*

A segments have a maximum in their profile at z = 8, while the concentration of solvent is minimal at this distance. In Figure (9e) a profile is shown for the case that χ_{AS} = -4 and r_2 = 100. Here, only a monolayer is formed. Although the cmc reduces drastically when r_2 is increased (Figure (9c)), in both cases the adsorbed amount still rises with increasing chain length (Figure (9b)). The dashed lines in Figure (9) connect points for the same situation (at the cmc for r_2 = 100) and have been drawn to show the relation between partc a-c of Figure (9). The bottom left quadrant has no physical relevance.

In Figure (10), the excess adsorbed amount at the cmc is shown as a function of the adsorption energy of A blocks, χ_{AS}, for $A_{30}B_{70}$ and $A_{50}B_{50}$ molecules in a B solvent. As in Figure (8), χ_{AB} = 1.5 and χ_{BS} =

0. The adsorbed amount of $A_{30}B_{70}$ molecules increases strongly when χ_{AS} becomes more negative than a critical value. This is also well-known from adsorption of homopolymers.[12,13] The $A_{50}B_{50}$ molecules show an S-shaped curve. This arises from the cooperative adsorption of these molecules (see also Figure (8)). The S-shape in Figure (10) occurs only if the S-shape in the adsorption isotherm (such as in Figure 8a) is located around the cmc and χ_{AS} is near the critical value.
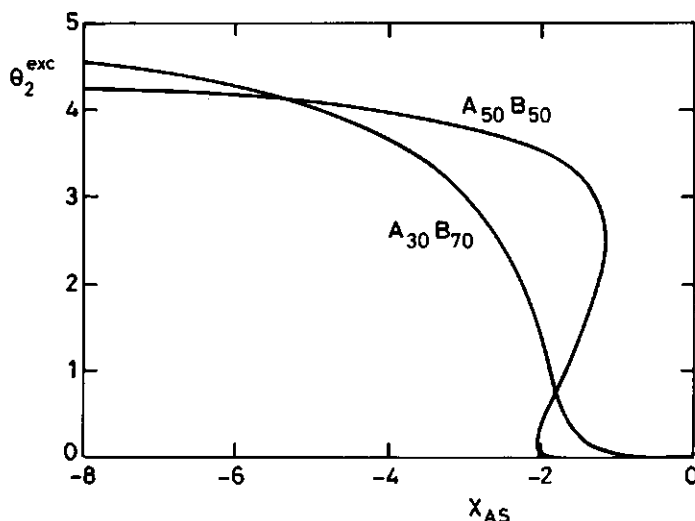
Figure 10. *Excess adsorbed amount calculated at the cmc as a function of χ_{AS} for $A_{30}B_{70}$ (cmc = $26*10^{-5}$) and $A_{50}B_{50}$ (cmc = $26*10^{-10}$) molecules in a B solvent. χ_{AB} = 1.5 and χ_{BS} = 0.*

VI Conclusions

The length of lyophobic (A) blocks in combination with the solvent quality ($r_A\chi_{AO}$) is the leading factor for the critical micelle concentration of diblock copolymers. A strong repulsion between A and B segments (high χ_{AB}) slightly opposes aggregation. Usually the aggregates are spherical, but when the lyophobic (A) blocks are much longer than the B blocks, a lamellar bilayer (membrane) is the preferred aggregation structure, because of its smaller surface area per

molecule. The concentration of solvent in the lyophobic centre of the aggregates can be high.

Aggregation of block copolymers influences the adsorption properties of these molecules strongly. Beyond the cmc the adsorption on a solid-liquid interface is almost constant. When the lyophobic block adsorbs preferentially and is much longer than the lyophilic block, a strong increase in the adsorbed amount occurs near the cmc. If the solvent quality is extremely poor (high χ_{AO}) , the cmc is very low, an S-shaped isotherm can be observed and the adsorbed amount in the plateau region is high. Clearly, the surface acts as a condensation nucleus. Reducing the length of the A block or increasing the solvent quality raises the cmc, and diminishes the S-shape of the isotherm. Competition between adsorption and micellization is observed only for weakly adsorbing A blocks in a very poor solvent. If the lyophilic block adsorbs on a lyophilic surface, a bilayer can be formed on the surface.

References

1)   Scheutjens J.M.H.M. and Fleer G.J., J. Phys. chem. (1979), 83, 1619.

2)   Scheutjens J.M.H.M. and Fleer G.J., J. Phys. chem. (1980), 84, 178.

3)   Evers O.A., PhD thesis, Wageningen Agricultural University (1989).

4)   Mathai K.G. and Ottewill R.H., Trans Faraday Soc. (1966), 62, 750, ibid., 759.

5)   Corkhill J.M., Goodman J.F., and Tate J.R., Trans Faraday Soc. (1966) 62, 979.

6)   Leermakers F.A.M.,Van der Schoot P.P.A.M., Scheutjens J.M.H.M., and Lyklema J. in: "Surfactants in Solution, Modern Applications", K.L. Mittal, Ed.; in press.

7)   Flory P.J., "Principles of Polymer Chemistry", Cornell University Press, Ithaca NY (1953).

8)   Hall D.G. and Pethica B.A., in "Nonionic Surfactants", M.J. Schick Ed., Marcel Dekker, NY (1976), chap. 16.

9) Roe R.J., J. Chem. Phys. (1974), <u>60</u>, 4192.

10) Cosgrove T., Heath T., Van Lent B., Leermakers F., and Scheutjens J., Macromolecules (1987), <u>20</u>, 1692.

11) Koningsveld R. and Kleintjes L., Macromolecules (1985), <u>18</u>, 243.

12) Scheutjens J.M.H.M., Fleer G.J., and Cohen Stuart M.A., Colloids Surfaces. (1986), <u>21</u>, 285.

13) Van der Beek G.P., and Cohen Stuart M.A., J. Physique (Les Ulis.,Fr.) (1988), <u>49</u>, 1449

Chapter 3

Adsorption of Random Copolymers from Solution

Abstract

In this paper a theory for the adsorption of random copolymers of uniform chain length is presented. The self-consistent field model of Evers for adsorption of copolymers with a given order of segments within the chains is extended so that polymer may consist of a statistically determined mixture of molecules which differ in primary structure. The sequence distribution of random copolymers is determined by the average fraction of each segment type in the polymer and by the sequence correlation factors (blockiness). For fully random copolymer, i.e., when the correlation in segment order is absent, the model reduces to a variation of the two state model of Björling et al. for adsorption of PEO, in which the segments assume two energetically different states. For this case, expressions for the average adsorption energy and solvent quality are obtained. Results are given for random copolymers with two different segment types. Chains with a higher than average content of adsorbing segments are preferentially adsorbed from the bulk solution. Only in the beginning of the segment density profile, the fraction of adsorbing segments is higher than average. In the remainder of the profile the segment composition is the same as in the bulk solution. The adsorption behaviour of random copolymers is remarkably different from that of diblock copolymers. Much higher adsorbed amounts are found for diblock copolymers than for random copolymers with the same average fraction of adsorbing segments. The adsorption of random copolymers is usually less than that of homopolymer of equal length and consisting of the same type of adsorbing segments. Only for very high adsorption energies the adsorbed amounts are essentially the same. The influence of blockiness and interaction parameters is studied.

Introduction

In many colloidal dispersions, copolymers are used as stabilizing agents. In recent years much attention has been paid to the adsorption behaviour of block copolymers, both experimentally[1-3] and theoretically.[3-7] In practice copolymers often have a random distribution of different segments along the chain. The primary structure of the chain depends on the way these random copolymers are synthesized. In general, random copolymers are very heterodisperse, both in chain length and in primary structure. Many theories have been developed to describe the sequence distribution and degree of polydispersity of random copolymers, see for example ref 8-10.

Two types of random copolymers can be distinguished. The first type are polymers synthesized by means of copolymerization in a mixture of two or more different monomer types. The rate constants for the reaction between the different monomers are usually unequal and these random copolymers will therefore be very polydisperse in length. The second type of random copolymers are randomly modified homopolymers. This type is made by randomly modifying a fraction of the segments of a homopolymer and thus can be rather monodisperse in length.

Not many studies have been carried out to analyse the adsorption properties of random copolymers. The reported results[11-15] concern randomly synthesized copolymers with high values of the polydispersity ratio M_w/M_n.

The heterodispersity of random copolymers makes it difficult to describe their adsorption properties theoretically. Marques and Joanny[16] use a blob model, in which the chains are monodisperse and the adsorbing segments are regularly distributed along the chain. However, for random copolymer all possible sequences with their appropriate statistical weight should be taken into account. In this paper we will present a model where the chains are monodisperse in length only. All possible sequences are taken into account. A simple model is used to calculate the sequence distribution from the fraction of each segment type present in the polymer and a blockiness parameter. This sequence distribution is incorporated into the model for adsorption of copolymers of a given sequence as described by E-

vers.[4] The theory of Evers is an extension of the homopolymer adsorption model of Scheutjens and Fleer.[17,18]

In the results section, we study the adsorption of random copolymers with different fractions of adsorbing segments. The blockiness of the chains is varied. The influence of solvency conditions for the different segments and the interaction between the segments and the surface is described. The adsorption of random copolymers is compared with the adsorption of diblock copolymers and homopolymers.

Theory

In the first part of this section it is explained how the adsorption of copolymer chains, all with the same given sequence, can be calculated using a lattice model. In the second part the extension to adsorption of random copolymers is described, taking into account all possible sequences.

The lattice consists of layers parallel to the surface, numbered $z = 1$ to M. Layer 1 is adjacent to the surface and layer M is in the bulk solution. Each layer has L sites. A lattice site has Z nearest neighbours, of which a fraction λ_0 in the same, λ_{-1} in the previous, and λ_1 in the next layer. For a hexagonal lattice $\lambda_1 = \lambda_{-1} = 0.25$ and $\lambda_0 = 0.5$. A polymer chain of type i consists of r_i segments. There are n_i chains of polymer i in the system. In layer z the polymer has a volume fraction $\phi_i(z)$, of which $\phi_{xi}(z)$ are due to segments of type x. The segment types are denoted by $x = $ A, B, ... The total volume fraction of segments x in layer z equals $\sum_i \phi_{xi}(z)$.

All possible conformations of the different chains in the lattice are taken into account. In equilibrium, the surface free energy is minimal. This means, that the grand canonical partition function has to be maximized. Evers[4] has formulated the grand canonical partition function for a system which contains block copolymers. From the maximization of this partition function, he derives the free segment weighting factor $G_x(z)$. This is a Boltzmann factor, giving the preference of a certain segment x to be in layer z rather than in the bulk solution:

$$G_x(z) = e^{\dfrac{-u_x(z)}{kT}}$$ (1)

$u_x(z)$ is the potential which segment x feels in layer z. For $u_x(z)$ the following equation holds:

$$u_x(z) = u'(z) + kT\sum_y \chi_{xy}\left(<\phi_y(z)> - \phi_y^b\right)$$ (2)

The first term, u'(z), in equation (2) is a hard core potential, independent of x, that reflects the constraint $\sum_i \phi_i(z) = 1$. The second term accounts for the interactions of segment x with neighbouring segments. It contains χ_{xy}, the Flory-Huggins parameter for the interaction between segments of type x and y, and ϕ_y^b the volume fraction of segments y in the bulk solution. The contact volume fraction $<\phi_y(z)>$ is a weighted average of the volume fractions in layer z-1, z and z+1:

$$<\phi_y(z)> = \lambda_{-1}\phi_y(z-1) + \lambda_0\phi_y(z) + \lambda_1\phi_y(z+1)$$ (3)

The interaction with the solid surface S is also taken into account through equation 2. The interaction parameter between the solid and segments x is equal to χ_{xS} and the volume fraction of surface sites is unity in layer z = 0 and zero for z > 0. Thus the interaction between the surface and a segments x in layer 1 is $kT\lambda_{-1}\chi_{xS}$. Note that $G_x(z)$ equals 1 in the bulk solution.

Copolymer adsorption

With the segment weighting factors, it is possible to obtain the statistical weight of all possible conformations. Consider an AB dimer. The end segment distribution function $G_B(z,2|1)$, giving the weight of all conformations with segment B in layer z and, in principle, the first segment anywhere in the system (but in this case segment A is in one of the layers z-1, z or z+1) equals:

$$G_B(z,2|1) = G_B(z) \{\lambda_{-1} G_A(z-1,1|1) + \lambda_0 G_A(z,1|1) + \lambda_1 G_A(z+1,1|1)\}$$

$$= G_B(z) < G_A(z,1|1) >$$

$$(4)$$

$G_A(z,1|1)$ is by definition equal to $G_A(z)$. The end segment distribution function for a trimer can be derived from that of a dimer in a similar way. Generally, for any type of molecule i, equation (4) can be transformed into the following recurrence relation:

$$G_i(z,s|1) = G_i(z,s) < G_i(z,s-1|1) > \tag{5}$$

For example, $G_i(z,s)$ equals $G_A(z)$ if segment number s is an A segment. It is also possible to enumerate a different end segment distribution function, starting at the other end of the chain. (For the dimer under consideration this means that we start at segment B.) Equation (5) changes into:

$$G_i(z,s|r) = G_i(z,s) < G_i(z,s+1|r) > \tag{6}$$

To find the volume fraction $\phi_i(z)$, the two types of end segment distribution functions (Equations 5 and 6) are combined. This means that the two walks, starting at segments 1 and r, respectively, somewhere in the system and ending at segment s in layer z, are connected and contribute to $\phi_i(z)$:

$$\phi_i(z) = C_i \sum_{s=1}^{r_i} \frac{G_i(z,s|1)G_i(z,s|r)}{G_i(z,s)} \tag{7a}$$

The volume fractions due to segment x are obtained by:

$$\phi_{xi}(z) = C_i \sum_{s=1}^{r_i} \frac{G_{xi}(z,s|1)G_{xi}(z,s|r)}{G_x(z)} \tag{7b}$$

For a copolymer with a given sequence distribution $G_{xi}(z,s \mid 1) = G_i(z,s \mid 1)$ if segment s is of type x and zero otherwise. The fact that $G_i(z,s)$ occurs in the denominator of equation (7) arises because in the product of the two end segment distribution functions $G_i(z,s)$ is counted twice. The factor C_i is a normalization constant, which is determined by the boundary condition that in the bulk solution $\phi_i(z)$ has to be equal to ϕ_i^b. Substituting $G = 1$ into equation (7) for every z and s gives:

$$C_i = \frac{\phi_i^b}{r_i} \qquad (8)$$

With equations (1, 2, 5-8) and the boundary condition $\sum_i \phi_i(z) = 1$ the adsorption profile is calculated numerically.[4]

From the profile, it is possible to obtain $\theta_i = \sum_z \phi_i(z)$, the total number of segments of component i per surface site. In order to find θ_i^a, the adsorbed amount due to chains with at least one segment on the surface, the number of free chains is to be subtracted from θ_i. The volume fractions of free chains (chains with none of their segments in the first layer) can be computed using equations (1, 5-8) under the condition that $G_x(1) = 0$. The excess adsorbed amount, θ_i^{exc}, is calculated as $\sum_z (\phi_i(z) - \phi_i^b)$.

Random copolymers

In this section we will present a model where the chains are monodisperse in length only. All possible sequences are taken into account. As mentioned in the introduction, such polymers may be synthesized by modifying a fraction of the monomers of a monodisperse homopolymer.

We assume that each segment in polymer i has a probability v_{xi} to be an x segment, independent of its ranking number. Then the average fraction of x segments in polymer i is v_{xi}. We define transition coefficients T_{xyi} that give the probability that in the molecules i the neighbouring segment of an x segment will be of type y, with $0 \leq T_{xyi} \leq 1$ and $\sum_y T_{xyi} = 1$. For a fully random copolymer i we have $T_{xxi} = T_{yxi} = v_{xi}$ and $T_{yyi} = T_{xyi} = v_{yi}$, for an alternating copolymer i consisting

of two types of segments A and B $T_{AAi} = T_{BBi} = 0$ and $T_{ABi} = T_{BAi} = 1$. Other combinations may be expressed in the so-called blocky constant B_i, see below.

The various transition coefficients must obey certain relations. The neighbouring segment of a randomly chosen segment in a chain has a probability of v_{yi} to be a y segment, so that the following relation must hold:

$$\sum_x v_{xi} T_{xyi} = v_{yi} \tag{9}$$

An xy sequence must have the same probability as a yx sequence, therefore

$$v_{xi} T_{xyi} = v_{yi} T_{yxi} \tag{10}$$

Note that for a copolymer consisting of two different types of segments, relation (10) can be obtained from relation (9) using $\sum_y T_{xyi} = 1$. Equation (10) can be rewritten as:

$$T_{xyi} = \frac{v_{yi}}{v_{xi}} T_{yxi} \tag{11}$$

In case of copolymers consisting of two types of segments, A and B, four transition factors can be defined: T_{AAi}, T_{ABi}, T_{BAi}, and T_{BBi}. For instance, the sequence ABBAB has a probability of $v_{Ai} T_{ABi} T_{BBi} T_{BAi} T_{ABi}$. The type of the first segment is not influenced by a previous segment, therefore only the factor v_{Ai} is present. The next segment is a B so we multiply with T_{ABi}. Continuing like this leads to the given probability. Because of the symmetry condition (equation 10) this sequence probability equals $T_{BAi} T_{BBi} T_{ABi} T_{BAi} v_{Bi}$. As shown in this example, it is possible to describe this sequence probability as a product of transition factors from segment 2 to 1, 3 to 2, ..., r to r - 1 and the occurrence probability v_{xi} of the last segment. Taking this product of transition factors into account for the calculation of the end segment distribution function, equation (5) becomes

$$G_{xi}(z,s|1) = G_x(z) \sum_y T_{xyi} < G_{yi}(z,s-1|1) > \tag{12}$$

The expression for $G_{xi}(z,s|r)$ can be written as

$$G_{xi}(z,s|r) = G_x(z) \sum_y T_{xyi} < G_{yi}(z,s+1|r) > \tag{13}$$

For these "symmetrical" random copolymers, equation (13) is redundant, because $G_{xi}(z,s|r) = G_{xi}(z,r-s+1|1)$. The volume fractions due to segment x can now be obtained by:

$$\phi_{xi}(z) = \frac{v_{xi}\phi_i^b}{r_i} \sum_{s=1}^{r_i} \frac{G_{xi}(z,s|1)G_{xi}(z,s|r)}{G_x(z)} \tag{14}$$

The numerical data can be calculated in a similar way as for copolymers with a given sequence, see previous section.

Blocky constant

For random copolymers consisting of two types of segments we define a blocky constant B_i as:

$$B_i = T_{AAi} - T_{BAi} \tag{15}$$

If B_i equals 1 ($T_{BAi} = T_{ABi} = 0$), we are dealing with a mixture of two homopolymers A and B with bulk solution concentrations $v_{Ai}\phi_i^b$ and $v_{Bi}\phi_i^b$, respectively. If $B_i = -1$ ($T_{AAi} = T_{BBi} = 0$) an alternating copolymer is considered, whereas for $B_i = 0$ the primary structure is fully random. The sequence distribution of a random copolymer with two different segments is completely determined by the parameters v_{Ai} and B_i. Only for $v_{Ai} = 0.5$, B_i can be any number between -1 and 1. In general, the limits for B_i (at a given v_{Ai}) are:

$$\max(\frac{-v_{Ai}}{v_{Bi}}, \frac{-v_{Bi}}{v_{Ai}}) \le B_i \le 1 \tag{16}$$

These limits are obtained from equations (9) and (15) and the condition $0 \leq T_{xyi} \leq 1$.

Fully random copolymer

In appendix A, it is shown that the adsorption of fully random copolymer consisting of two types of segments can be modeled by a two state model for homopolymers as proposed by Björling et al.[19] The weighting factor for this "homopolymer", $G_i(z)$, is equal to

$$G_1(z) = v_{A1} G_A(z) + v_{B1} G_B(z) \tag{17}$$

In combination with equation (1), the following relation for $u_i(z)$ is obtained:

$$u_1(z) = u_B(z) - kT\ln\left(v_{B1} + v_{A1} e^{(u_B(z) - u_A(z))/kT}\right) \tag{18}$$

Series expansions of equation (18) and neglecting all terms of an order higher than two leads to the following relation for $u_i(z)$:

$$u_1(z) \approx v_{A1} u_A(z) + v_{B1} u_B(z) - \frac{v_{A1} v_{B1}}{2kT}\left(u_A(z) - u_B(z)\right)^2 \tag{19}$$

From equation (2) and (18) it follows that the adsorption profile $\phi_i(z)$ of AB random copolymer in solvent 0, with $\chi_{AB} = 0$ and A and B segments differing in adsorption energy only, can be enumerated by calculating the adsorption of a homopolymer with interaction parameter $\chi_{i0} = \chi_{B0} = \chi_{A0}$ and χ_{iS} equal to :

$$\chi_{iS} = \chi_{BS} - \frac{1}{\lambda_1}\ln\left(v_{B1} + v_{A1} e^{\lambda_1(\chi_{BS} - \chi_{AS})}\right) \quad (\chi_{10} = \chi_{A0} = \chi_{B0}, \chi_{AB} = 0) \tag{20}$$

Results and Discussion

For all our calculations we have used a hexagonal lattice, i.e., $\lambda_0 =$ 0.5, and $\lambda_{-1} = \lambda_1 = 0.25$. We only show results for copolymers consisting of two different types of segments: A and B. In all cases A is the preferentially adsorbing segment. We denote solvent by $i = 1$ ($r_1 = 1$) and polymer by $i = 2$. In the first part of this section we only consider fully random copolymers ($B_2 = 0$), for which $v_{A2} = T_{AA2} = T_{BA2}$ (see equations 9 and 15). In the second part the influence of the blocky constant is considered.
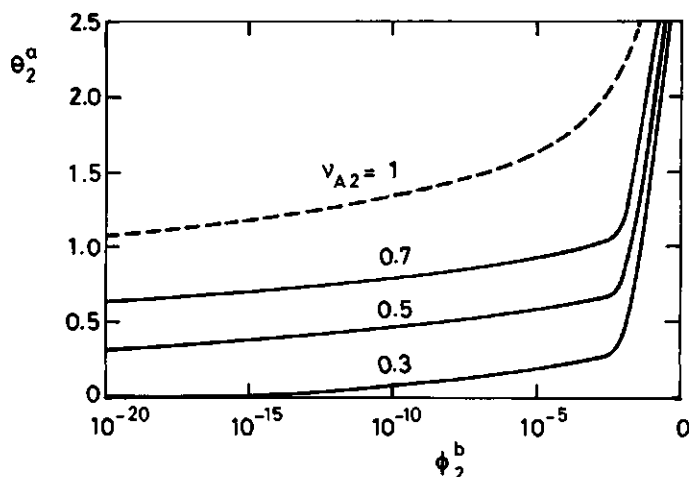
Figure 1. *Adsorption isotherms for a homopolymer of 500 segments (dashed curve) and for three AB random copolymers of 500 segments with different fractions of A segments: $v_{A2} = 0.3$, 0.5, and 0.7 (solid curves), in a B solvent. $B_2 = 0$, $\chi_{AB} = 0.5$, $\chi_{AS} = -4$, $\chi_{BS} = 0$.*

In Figure (1) three adsorption isotherms with different fractions of A segments are shown for an AB random copolymer of 500 segments in a B solvent. The isotherm of a homopolymer ($v_{A2} = 1$, dashed curve) is also given. The solvent is a theta solvent for the A segments, i.e., $\chi_{AB} = 0.5$, and the A segments have a preferential interaction with the surface S: $\chi_{AS} = -4$, whereas $\chi_{BS} = 0$. All isotherms are of the high affinity type and their shapes are equivalent. The strong increase
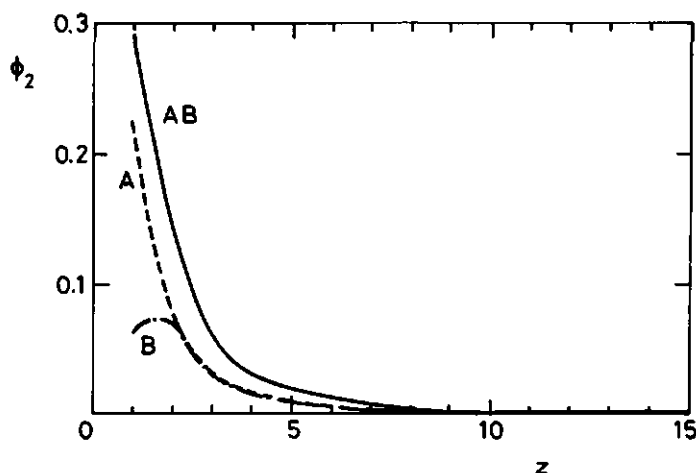
Figure 2. *Segment density profile for the AB random copolymer of Figure (1) with $v_{A2} = 0.5$ at $\phi_2^b = 10^{-4}$ (solid curve) and the contribution from A segments (dashed curve) and B segments (dashed-dotted curve).*

at high bulk volume fractions is due to the fact that at those concentrations the polymer is pushed towards the surface. The highest fraction of A segments leads obviously to the highest adsorbed amount. Cosgrove et al.[12] find a rounded shape for the adsorption isotherm of copolymer of vinyl acetate and ethylene on silica. We were not able to obtain a similar shape. Their result might be due to the high degree of polydispersity of their samples, which is known to cause a rounded adsorption isotherm.[20]

The volume fraction profiles of the A and the B segments of the polymer with $v_{A2} = 0.5$ at $\phi_2^b = 10^{-4}$ in Figure (1) are given in Figure (2). Only in the first few layers near the surface there is a preference for A segments. The adsorbed amount for A segments equals $\theta_{A2}^a = 0.386$, while $\theta_{B2}^a = 0.214$. On the surface, the preference for A segments is caused by the higher adsorption energy. At $z = 2$ the positive value of χ_{AB} favours A segments as neighbours of A segments on the surface.

This tendency to adsorb chains with a higher than average content of A segments is more clearly demonstrated in Figure (3). In Figure (3a) the total adsorbed amount, θ_2^a, that of the A segments, θ_{A2}^a, and

the quantity $v_{A2}\theta_2^a$, the adsorbed amount of A segments if the adsorbed molecules had the same average content of A segments as in the bulk solution, are plotted for an AB random copolymer of 100 segments with a volume fraction in the bulk solution of $\phi_2^b = 0.01$ in B solvent. The interaction parameters are the same as in Figure (1). The adsorbed amount becomes larger when the average fraction of A segments increases. Comparing the adsorbed amount θ_{A2}^a of A segments with $v_{A2}\theta_2^a$, we see that except for $v_{A2} = 0$ (B homopolymer) and $v_{A2} = 1$ (A homopolymer), θ_{A2}^a is always higher than $v_{A2}\theta_2^a$. This preference of chains with a higher A fraction near the surface is especially pronounced for a high solution volume to surface area ratio. In our model, the composition of the bulk solution does not change when the polymers adsorb, which corresponds to a volume to surface area ratio of infinity. However, for a low volume to surface area ratio chains with a high number of A segments in the solution would soon be exhausted and the preference would appear less pronounced. To quantify the preferential adsorption, we define an excess parameter v_{A1}^{exc} as follows

$$v_{A1}^{exc} = \frac{\theta_{A1}^a}{\theta_1^a} - v_{A1} \tag{21}$$

In Figure (3b) the parameter v_{A2}^{exc} is shown as a function of v_{A2}. For $v_{A2} = 0.52$ a maximum in v_{A2}^{exc} is found, whereas v_{A2}^{exc} is equal to zero for $v_{A2} = 0$ and $v_{A2} = 1$. The position of the maximum depends strongly on the adsorption energy parameter χ_{AS}. For higher adsorption energies the maximum occurs at lower values of v_{A2}.

In Figure (3c) the number distribution in the solution is given for $v_{A2} = 0.1$, 0.5 and 0.9. These distributions are binomial and can be calculated by:

$$v(r_{A1}) = \frac{r_1!}{r_{A1}!(r_1 - r_{A1})!} v_{A1}^{r_{A1}} v_{B1}^{r_{B1}} \tag{22}$$

This preferential adsorption is demonstrated by experiments of Pennings.[15] He has measured the adsorption of a random copolymer
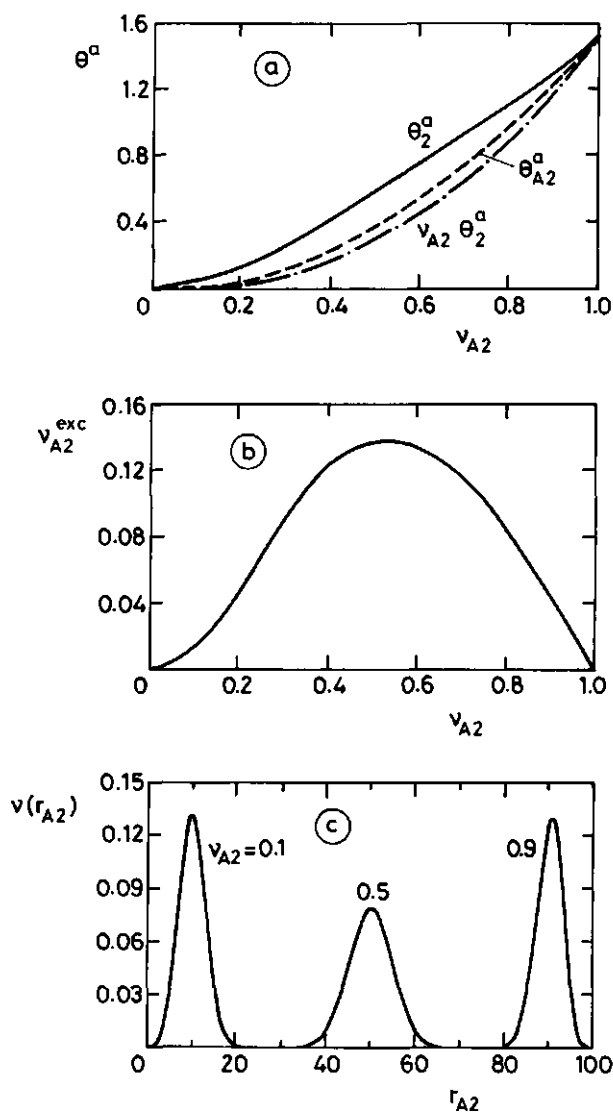
Figure 3. *(a) Adsorbed amount of an AB random copolymer (solid curve) and the contribution of A segments (dashed curve) in a B solvent as a function of the fraction of A segments. The contribution of A segments if the fraction of A segments would be the same as in the bulk solution, $v_{A2}\theta_2^a$, is also shown (dashed-dotted curve).*

(b)   Preferential adsorption v_{A2}^{exc} as a function of v_{A2}.

(c)   Distribution of A segments over the polymer chains, $v(r_{A2})$, for three different values of v_{A2} (indicated).

Parameters: $B_2 = 0$, $r_2 = 100$, $\chi_{AB} = 0.5$, $\chi_{AS} = -4$, $\chi_{BS} = 0$. $\phi_2^b = 10^{-2}$.

of vinyl chloride (87% by weight) and vinyl acetate (13% by weight) from different solvents on aluminium. A stronger adsorption energy or a decreased solubility of vinyl acetate leads to a higher volume fraction directly on the aluminium substrate. For a gold substrate no preference is observed. His explanation is that in this case all solvents used adsorb more strongly than the vinyl acetate groups.
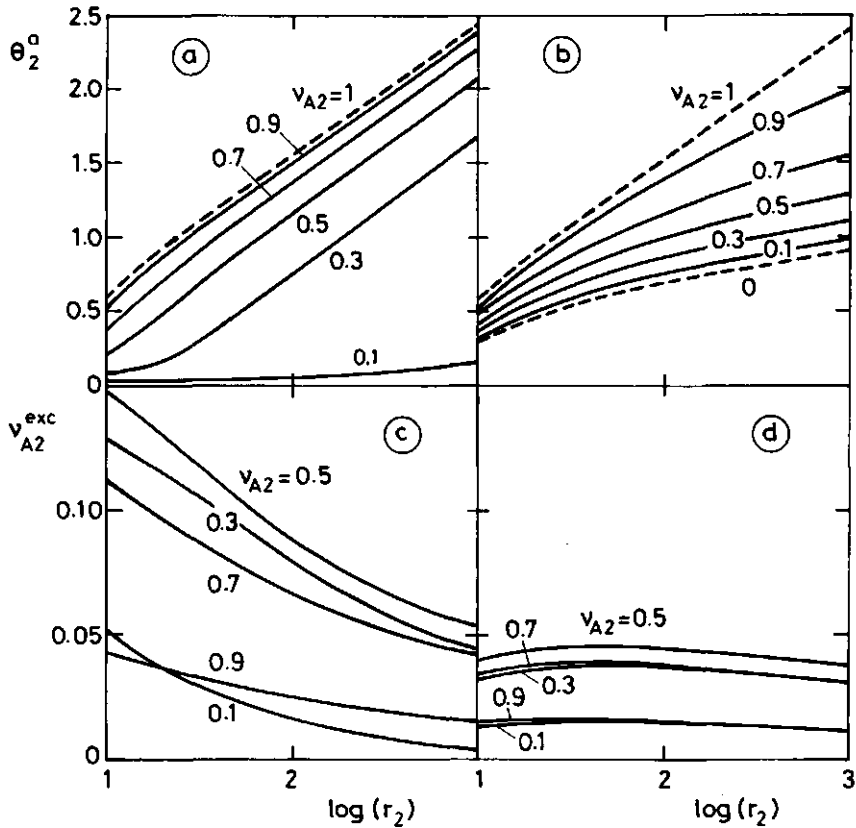
Figure 4. (a,b) Adsorbed amount θ_2^a of an AB random copolymer as a function of chain length r_2 for different values of v_{A2} (indicated). (c,d) Preferential adsorption, v_{A2}^{exc}, as a function of chain length for different values of v_{A2}. Parameters: $B_2 = 0$, $\chi_{A0} = 0.5$, $\chi_{AB} = 0$, $\chi_{AS} = -4$, $\phi_2^b = 10^{-2}$. Parameters for (a,c) $\chi_{B0} = 0.5$, $\chi_{BS} = 0$, for (b,d): $\chi_{B0} = 0$, $\chi_{BS} = -4$

The adsorbed amount as a function of the chain length of random AB copolymers with different fractions of A segments in solvent 0 is shown in Figure (4). The adsorption of a homopolymer is represented by a dashed line. In Figure (4a) the A and B segments have different adsorption energies: χ_{AS} = -4 and χ_{BS} = 0, but their solvency is the same: $\chi_{A0} = \chi_{B0}$ = 0.5 and χ_{AB} = 0 (Θ-solvent). According to equation (20), the adsorbed amount for these random copolymers where the A segments and B segments only differ in adsorption energy can also be obtained exactly by calculating the adsorbed amount for homopolymers with χ_{20} = 0.5 and χ_{2S} = - $(1/\lambda_1)$ ln(v_{B2} + $v_{A2}e$). Increasing the fraction of A segments increases the adsorbed amount. For all values of v_{A2} the adsorbed amount θ_2^a increases essentially linearly with log(r_2). This is known for homopolymers in a theta solvent[17], see the dashed line. The curve for a random copolymer shows the same slope. The curves are horizontally shifted to higher chain lengths, exactly as for a lower adsorption energy of homopolymers.

In Figure (4c), the preference for A segments (v_{A2}^{exc}) is shown as a function of log(r_2). The parameters are the same as in Figure (4a). For all values of v_{A2} the preference decreases as a function of log(r_2). The relative heterogeneity is for short chains much larger than for long chains. For the shown values of v_{A2}, the preference is largest for v_{A2} = 0.5 (see also Figure 3b). The initial slope of the curves decreases with increasing value of v_{A2}. The average fraction of chains with a high A content is reduced more strongly for small v_{A2} as compared to large v_{A2} values.

In Figure (4b) the effect of different solvency for the A and B segments is shown. Both types of segments have the same interaction with the surface: $\chi_{AS} = \chi_{BS}$ = -4. The interaction with the solvent is χ_{A0} = 0.5, whereas $\chi_{B0} = \chi_{AB}$ = 0. From equation (19), it can be seen that in first approximation the adsorbed amount for these systems is almost equal to that of an homopolymer with χ_{2S} is -4 and χ_{20} = $v_{A2}\chi_{A0}$ + $v_{B2}\chi_{B0}$. In contrast to Figure (4a), changing v_{A2} now gives a different shape of the curve. At v_{A2} = 0 (B homopolymer in an athermal solvent), the curve levels off as a function of log(r_2), see bottom dashed line. Increasing the fraction of A segments changes the shape

of the curve to that observed for a homopolymer ($v_{A2} = 1$) in a Θ solvent, see upper dashed line.

The preference for A segments as a function of $\log(r_2)$ for the cases of Figure (4b) is shown in Figure (4d). The preference v_{A2} is less pronounced than in Figure (4c), because both segments gain adsorption energy at the surface. For all values of v_{A2} a shallow maximum can be observed. Longer chains have larger A sequences, giving rise to a cooperative mutual attraction on the surface. This on itself would lead to a higher value of v_{A2}^{exc} with increasing chain length. On the other hand, the same argument as given for Figure (4c) holds: the relative heterogeneity is smaller for larger chains. These two opposing effects cause this maximum.
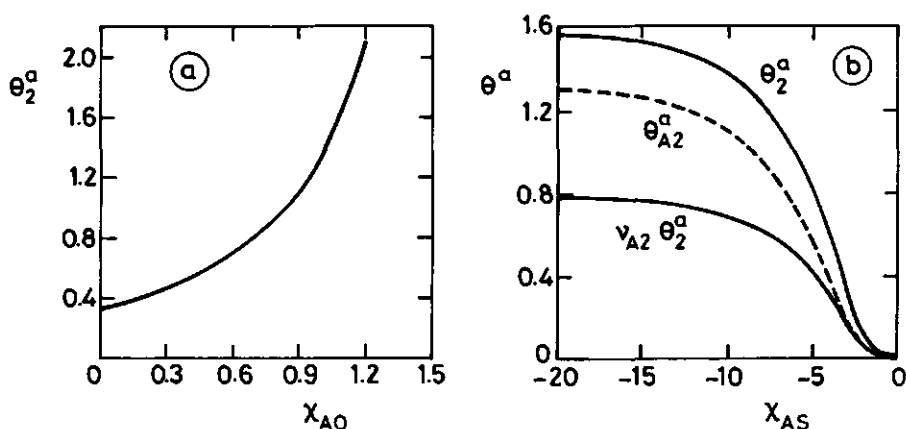
Figure 5. *Effect of the solvent quality for the A segments, χ_{AO}, (a, $\chi_{AS} = -4$) and the adsorption energy, χ_{AS}, (b, $\chi_{AO} = 0.5$) on the adsorbed amount of an AB random copolymer of 100 segments with $v_{A2} = 0.5$, $B_2 = 0$, $\chi_{AB} = 0.5$, $\chi_{BO} = 0$, $\chi_{OS} = 0$, $\phi_2^b = 10^{-2}$. In Figure (b) the adsorbed amount due to the A segments (dashed curve) and the quantity $v_{A2}\theta_2^a$ are shown as well.*

In Figure (5), for an AB random copolymer, the effect of the interaction parameters between A segments and the solvent and A segments and the surface is shown. The chains have a length of 100 segments, and $v_{A2} = 0.5$. The adsorbed amount is calculated for $\phi_2^b =$

0.01. The effect of varying the solvency conditions for the A segments is demonstrated in Figure (5a). The interactions between the A and B segments and B and solvent 0 are kept constant (χ_{AB} = 0.5 and χ_{B0} = 0), whereas χ_{A0} varies. The critical value for χ_{A0} where phase separation as predicted by the extended Flory-Huggins equations[4] is 1.47. As the solvency for the A segments becomes worse (higher χ_{A0}), the adsorbed amount increases. Near χ_{A0} = 1 the adsorbed amount rises sharply. For $\chi_{A0} \geq 1.47$ phase separation occurs.

In Figure (5b) the effect of the adsorption energy χ_{AS} on the adsorbed amount is illustrated. The solvent consists of B monomers. The interaction between segments A and B is equal to χ_{AB} = 0.5. A weak attraction between the A segments and the surface (small negative χ_{AS} value), is needed to compensate for the loss in conformational entropy when the polymers adsorb. As the attraction increases, θ_2^a first rises strongly and becomes constant for high negative χ_{AS} values. A similar shape is observed, both experimentally and theoretically, for the adsorbed amount of homopolymer as a function of χ_{AS}.[21,22] A more detailed comparison with the adsorption of homopolymers will be made below. The preference for A segments (the difference between the dashed and the dotted curves in Figure 5b) increases and becomes almost constant as the interaction between A segments and the surface becomes more attractive.

The adsorption of random copolymers and homopolymers is compared in Figure (6). The adsorbed amount, θ_2^a, is plotted as a function of χ_{AS} for an AB random copolymer with different values of v_{A2} in an athermal B solvent (χ_{AB} = 0). Analogous to Figure 4a, the adsorbed amount of these random copolymers is the same as for homopolymers with χ_{20} = 0 and χ_{2S} = - $(1/\lambda_1)$ ln(v_{B2} + v_{A2}e), see equation (20). Similarly, the critical adsorption energy for the A segments for a random copolymer with given v_{A2}, v_{B2}, solvencies, and $\chi_{BS} = \chi_{0S}$ = 0 can be obtained from $\lambda_1 \chi_{AS}^{cr}$ = ln(v_{A2}) - ln($-v_{B2}$ + exp($-\lambda_1 \chi_{2S}^{cr}$)). Here χ_{2S}^{cr} = $(1/\lambda_1)$ln$(1 - \lambda_1)$ is the critical adsorption energy parameter for homopolymers which for a hexagonal lattice is equal to -1.15. In the same figure the adsorption of an A homopolymer in this B solvent is given. It can be seen that for extremely high attractive forces between the A segments and the surface the adsorbed amount of the random copolymers is equal to that of the ho-
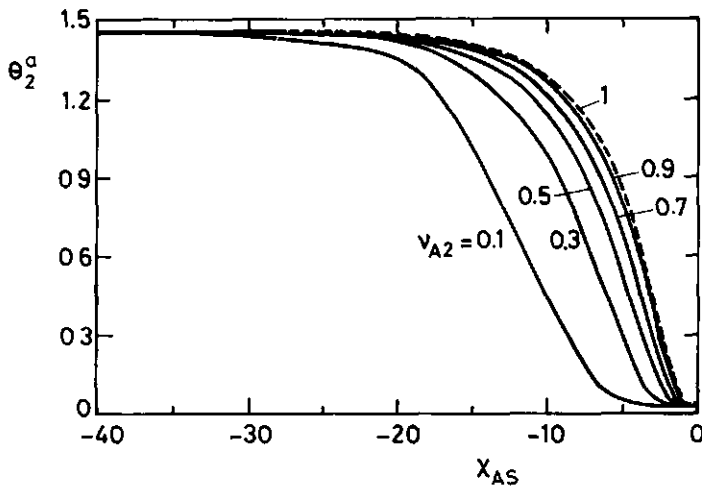
Figure 6. *Adsorbed amount, θ_2^a, as a function of χ_{AS} for AB random copolymers of 100 segments with six different values of v_{A2} (indicated) in a B solvent. The dashed line shows the adsorbed amount of an A homopolymer. $B_2 = 0$, $\chi_{AB} = 0$, $\chi_{BS} = 0$, $\phi_2^b = 10^{-2}$.*

mopolymer. This high adsorption energy causes the first layer to be fully occupied with A segments. The loss of conformational entropy of the B parts is completely overruled by this high tendency of the A segments to adsorb. As could be seen in Figure (5b), the preference becomes constant. Obviously, for random copolymers with a lower value of v_{A2}, a stronger attraction (larger negative χ_{AS}) is needed to find the same adsorbed amount as for A homopolymers.

In Figure (7) a comparison is made between the adsorption from a B solvent of an $A_{250}B_{250}$ diblock copolymer and an AB random copolymer with the same chain length and fraction of A segments (50%). The volume fraction of polymer in the bulk solution is $\phi_2^b = 10^{-4}$ (see the full curves at $z > 60$), and the interaction parameters are $\chi_{AB} = 0.5$, $\chi_{AS} = -4$, and $\chi_{BS} = 0$. The excess adsorbed amount of the block copolymer ($\theta_2^{exc} = 2.19$) is much higher than that of the random copolymer ($\theta_2^{exc} = 0.60$). The block copolymer adsorbs with the A blocks on the surface and forms long dangling tails of B blocks. The random copolymer cannot spatially separate the A and B seg-
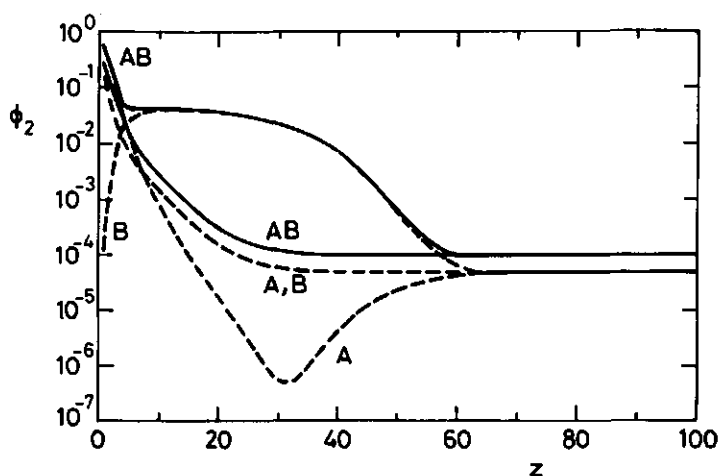
Figure 7. *Segment density profiles of adsorbed AB random and $A_{250}B_{250}$ diblock copolymer in a B solvent (solid lines). Dashed lines: contribution due to A segments (A) and B segments (B) of block copolymer and of random copolymer (A,B). Parameters: $\chi_{AB} = 0.5$, $\chi_{AS} = -4$, $\chi_{BS} = 0$, $\phi_2^b = 10^{-4}$, $r_2 = 500$. Random copolymer: $v_{A2} = 0.5$, $B_2 = 0$, $\theta_2^a = 0.60$. Block copolymer: $\theta_2^a = 2.19$*

ments and therefore many B segments occupy surface sites. This is partially compensated for by a preferential adsorption of chains with a higher number of A segments. As has been demonstrated in Figure (2), only in the first few layers there is a higher volume fraction of A segments of the random copolymer compared to B segments. However, on a log scale as in Figure 7 this is hardly noticeable. At larger z, the profiles of the A and B segments of the random copolymer coincide.

If the adsorption of A segments is not very strong, random copolymers need a higher fraction of A segments to adsorb than block copolymers (not shown). For a block copolymer, the critical adsorption energy is almost equal to that of a homopolymer consisting of the adsorbing segments, whereas for random copolymers the critical adsorption energy is higher than that value, see for example Figure (6). This is due to the effect that a block copolymer can form long dangling B tails, whereas the random copolymer cannot adsorb without

many B segments on the surface. The adsorption of random copolymer increases monotonically with v_{A2} under these conditions. The adsorption of block copolymers, however, has a maximum as a function of v_{A2}.[7] For very low values of v_{A2} the A block is too short to anchor the polymer. For very high values of v_{A2} almost all the segments in the chains are competing for surface sites. At the maximum, the A block can gain enough adsorption energy and the B blocks are long enough to contribute significantly to the adsorbed amount.

With the results given thus far we can speculate on the experimental results of Diaz-Barrios and coworkers[13,14] on randomly synthesized copolymers of styrene-vinylferrocene and methylmethacrylate-vinylferrocene. Diaz-Barrios and Howard[13] find a maximum in the adsorbed amount of a random copolymer of styrene and vinylferrocene in CCl_4 on silica and titanium dioxide. The samples were very heterodisperse, both in composition and in length. The reactivity ratios of the two monomers are highly different; for styrene 2.63 and for vinylferrocene 0.07. It is very likely that their sample contained many chains with a styrene block followed by a vinylferrocene block. This would lead to a block copolymer behaviour, i.e., a maximum in the adsorption as a function of the fraction of vinylferrocene. When they used chloroform as the solvent only a weak increase in the adsorbed amount as a function of the vinylferrocene content is observed, suggesting a similar kind of solubility and adsorption energy for the two types of monomers. Diaz-Barrios and Rengel[14] find a very peculiar behaviour for random copolymers of metylmethacrylate and vinylferrocene. A few percent of vinylferrocene decreases the adsorption. Further increase in the vinylferrocene content shows a second maximum in the adsorbed amount. This behaviour of the adsorbed amount as a function of the vinylferrocene content cannot be explained completely with the argument given above for the copolymers of styrene and vinylferrocene. The explanation given by Diaz-Barrios and Rengel is that methylmethacrylate adsorbs stronger than vinylferrocene, whereas vinylferrocene is less soluble in chloroform than methylmethacrylate. In our opinion this would lead to a minimum in the adsorbed amount instead of this second maximum. We expect that a few percent of vinylferrocene gives a behaviour of the adsorbed amount as in Figure (3a). Vinylferrocene adsorbs less strong

than methylmethacrylate and therefore the adsorbed amount decreases initially. The reactivity ratios are: 0.18 for vinylferrocene, and 0.67 for methylmethacrylate. This means that methylmethacrylate mainly reacts with itself. This would give a substantial amount of block copolymers in the mixture leading to this second maximum. The first decrease in the adsorbed amount is not observed for the styrene vinylferrocene copolymers, because the reactivity ratios differ much more than in the case of vinylferrocene methylmethacrylate copolymers. This would lead to the formation of a large number of styrene vinylferrocene block copolymers, even at low content of vinylferrocene. However, on the basis of the available information we can not verify this hypothesis for these two copolymers.
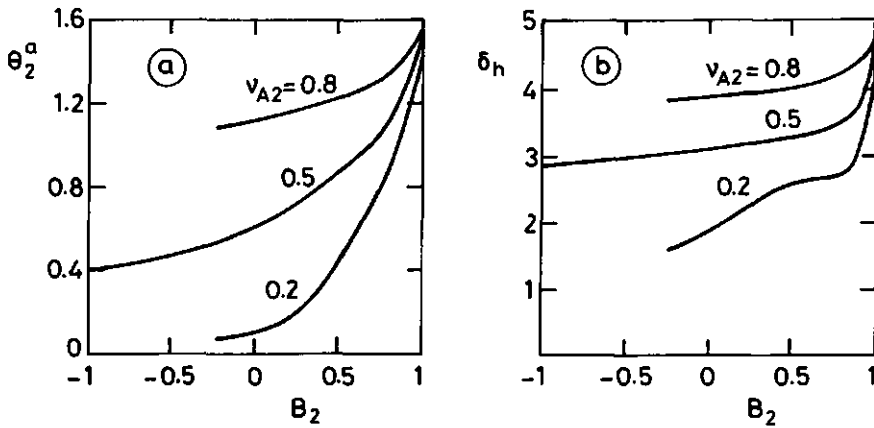
Figure 8. *Adsorbed amount (a) and the hydrodynamic thickness (b) as a function of the blockiness parameter B_2 for an AB random copolymer of 100 segments for three indicated values of v_{A2} in a B solvent. $\chi_{AB} = 0.5$, $\chi_{AS} = -4$, $\chi_{BS} = 0$, $\phi_2^b = 10^{-2}$.*

So far, only fully random copolymers (i.e. $B_2 = 0$) have been discussed. In Figure (8), the influence of the blockiness of the chains on the adsorbed amount θ_2^a (Figure 8a) and on the hydrodynamic layer thickness δ_h (Figure 8b) is shown for three different values of v_{A2}. The hydrodynamic layer thickness is calculated according to a method proposed by Scheutjens et al.[21] As can be obtained from
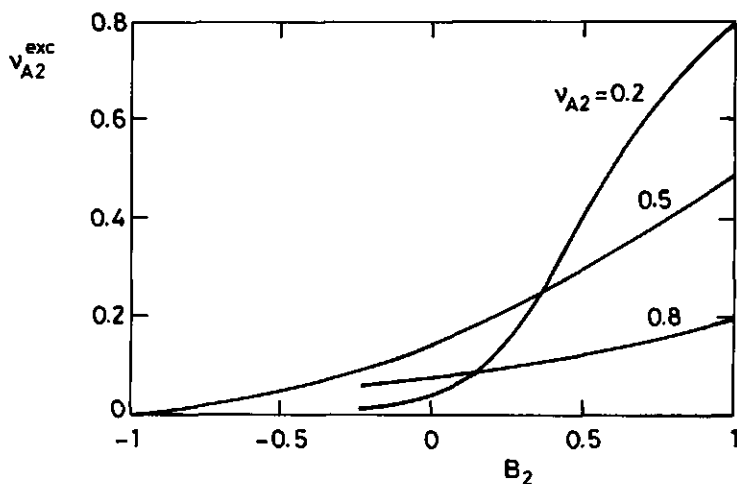
Figure 9.   *Effect of blockiness on the preference v_{A2}^{exc} for the systems of Figure (8).*
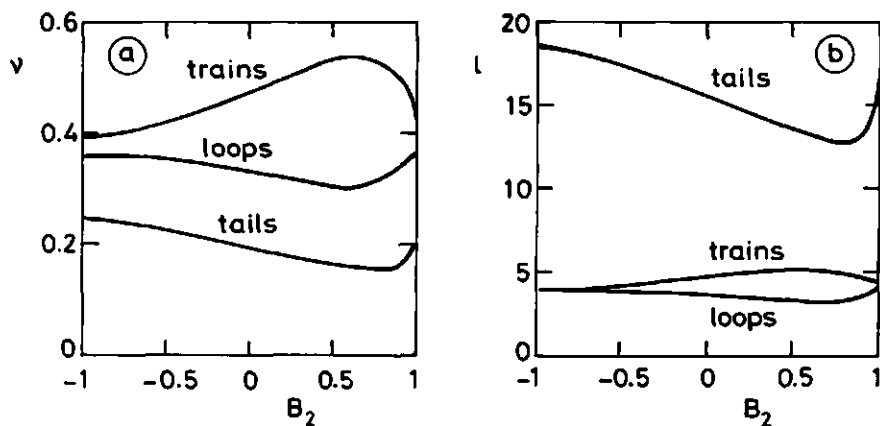
Figure 10.   *The fraction (a) and the average length (b) of trains, loops and tails as a function of B_2 for the system with $v_{A2} = 0.5$ in Figure (8)*

equation (16), for $v_{A2} = 0.2$ and 0.8 the value of the blockiness parameter B_2 is between -0.25 and 1, whereas for $v_{A2} = 0.5$ the limits for B_2 are -1 and 1. For all three values of v_{A2}, the adsorbed amount becomes larger when the random copolymers become more blocky. The chains can form longer A trains on the surface without the in-

terference of the B segments. At $B_2 = 1$, a solution with A homopolymers and B homopolymers is obtained. For all possible values of B_2, increasing v_{A2} will increase the adsorbed amount. The difference between two values of v_{A2} is most pronounced when B_2 is minimal. At $B_2 = 1$ the increase in adsorption with v_{A2} is due to the increase in the solution volume fraction of A homopolymer. As the adsorption is in the pseudo plateau region of the isotherm, there is only a minor effect on θ_2^a.

In Figure (8b), the corresponding hydrodynamic layer thickness δ_h is given. For $v_{A2} = 0.5$ and 0.8, δ_h increases slightly with increasing blockiness until $B_2 \approx 0.9$. From that point on δ_h rises sharply as a function of B_2. For $v_{A2} = 0.2$ the hydrodynamic layer thickness initially increases stronger than for the other two shown values of v_{A2}. The observed trends in Figure (8) will be explained with the help of Figures (9) and (10).

In Figure (9), the effect of the blockiness on the preferential adsorption (equation 21) is illustrated for the same systems as in Figure (8). At $B_2 = -1$ no preferential adsorption occurs, because all molecules in an alternating copolymer have the same primary structure. With increasing B_2 the length distribution of A blocks becomes wider, especially for $v_{A2} = 0.5$ (see Figure 3c), and hence the preferential adsorption increases. When $B_2 = 1$, only the A homopolymers adsorb, giving $v_{A2}^{exc} \approx 1 - v_{A2}$. Consequently, curves for $v_{A2} < 0.5$ cross each other, whereas curves for $v_{A2} > 0.5$ do not.

In Figure (10), the fraction of segments in trains, loops and tails (Figure 10a) and the average length of trains loops and tails (Figure 10b) are given as a function of B_2 for the case of $v_{A2} = 0.5$ in Figure (8). The calculation of these quantities is described in Appendix B. The fraction of segments in trains shows a maximum around $B_2 = 0.7$, whereas the fraction of segments in both loops and tails passes a minimum as a function of B_2. For loops this minimum is around $B_2 = 0.7$, whereas for tails it is situated near $B_2 = 0.9$. Similarly, the average length of trains as a function of B_2 shows a maximum around $B_2 = 0.6$, whereas in the curves for the average length of loops and tails a minimum can be observed. As B_2 increases the preferential adsorption of chains with many A segments increases (Figure 9) leading to shorter tails and loops and longer trains. The adsorbed amount in-

creases slightly (Figure 8a). Combination of these two effects gives an almost constant hydrodynamic layer thickness up to $B_2 \approx 0.9$ (Figure 8b). At very high values of B_2, the adsorbed amount becomes much larger leading to longer tails and loops and a higher value for δ_h.

Conclusions

A model for the adsorption of random copolymers has been developed. The blockiness as well as the average fractions of different segments in the polymer can be varied. The adsorbed amount for AB random copolymer with adsorbing A segments is usually less than that of the corresponding A homopolymer. Only for very high adsorption energies of the A segments the adsorbed amount is equal. In contrast, a block copolymer with the same fraction of A segments as in the random copolymer adsorbs stronger and the segment density profiles are remarkably different. The profile of the block copolymer shows a dense A layer on the surface and B tails dangling into the solution, whereas random copolymers show a homopolymer-like segment density profile.

There is a strong preferential adsorption of chains with a higher number of A segments. A higher fraction of A segments increases the total adsorbed amount, but decreases the heterogeneity of the A sequences. At a constant fraction of A segments the adsorbed amount increases with increasing blockiness, but the hydrodynamic layer thickness is almost independent of the blockiness.

Fully random copolymers, consisting of two types of segments, can be modeled by a two state model as developed by Björling et al.[22] If the only difference is the adsorption energy between the two segments, the adsorbed amount can be obtained from the adsorption of a homopolymer with an adsorption energy which is a weighted average of the adsorption energies of the two segment types.

Appendix A

In this appendix we show that fully random copolymers can be modeled as "homopolymers" with a segmental weighting factor $G_i(z)$ which is equal to $\sum_x v_{xi} G_x(z)$. This modeling of fully random copolymers as homopolymers of which each segment can be any of two or more possible types is analogous to the two state model of Björling et al.[19] for grafted polyethylene oxide chains, where each segment can be in a trans or a gauche state. Each of these states is accompanied by a different interaction with the solvent.

Let us define

$$G_i(z) = \sum_x v_{xi} G_x(z) \tag{A1}$$

$$G_i(z,s|\,1) = \sum_x v_{xi} G_{xi}(z,s|\,1) \tag{A2}$$

and

$$G_i(z,s|\,r) = \sum_x v_{xi} G_{xi}(z,s|\,r) \tag{A3}$$

For fully random copolymers $T_{xyi} = v_{yi}$. Combining this identity with equations (12) and (A2) we see that

$$G_{xi}(z,s|\,1) = G_x(z) < G_i(z,s-1|\,1) > \tag{A4}$$

Substituting equations (A4) and (A1) into (A2) we obtain

$$G_i(z,s|\,1) = G_i(z) < G_i(z,s-1|\,1) > \tag{A5}$$

Similarly, using equations (13) and (A3) instead of (12) and (A2), it is found that

$$G_{xi}(z,s|\,r) = G_x(z) < G_i(z,s+1|\,r) > \tag{A6}$$

and

$$G_1(z,s|r) = G_1(z) < G_1(z,s+1|r) >$$ (A7)

Substituting equations (A4) and (A6) into equation (14) gives:

$$\phi_1(z) = \sum_x \phi_{x1}(z) = \frac{\phi_1^b}{r_1} \sum_{s=1}^{r_1} \frac{G_1(z,s|1)G_1(z,s|r)}{G_1(z,s)}$$ (A8)

Finally, as $v_{x1}(z) = \phi_{x1}(z)/\phi_1(z)$, it can be derived from equations (14) and (A8) that

$$v_{x1}(z) = \frac{v_{x1}G_x(z)}{G_1(z)}$$ (A9)

Applying this multi-state model, the numerical analyses can be carried out as follows. For each segment type x and layer z there is one unknown parameter $u_x(z)$ and one equation:

$$u_x(z) - u'(z) - u_x^{int}(z) + 1 - \frac{1}{\sum_1 \phi_1(z)} = 0$$ (A10)

where $u_x^{int}(z)$ is defined as:

$$u_x^{int}(z) = kT \sum_y \chi_{xy} \left(\frac{<\phi_y(z)>}{\sum_1 \phi_1(z)} - \phi_y^b \right)$$ (A11)

and u'(z) is equated as

$$u'(z) = \frac{\sum_x \left(u_x(z) - u_x^{int}(z) \right)}{\sum_x 1}$$ (A12)

The set of equations (A10) is reasonable linear in $\{u_x(z)\}$ and when solved it guarantees that $u_x(z) = u'(z) + u_x^{int}(z)$ and $\sum_1 \phi_1(z) = 1$. The iteration is started with an initial guess for $\{u_x(z)\}$. To find $G_x(z)$ the values for $u_x(z)$ are substituted into equation (1). The weighting factor

$G_1(z)$ can be obtained by using equation (A1). With $G_1(z)$ and relations (5), (6), and (7), $\phi_1(z)$ is found. The values for $v_{x1}(z)$ are obtained from equation (A9). The volume fractions $\phi_{x1}(z)$ are enumerated as $v_{x1}(z)\phi_1(z)$. In this way, all values necessary in equation (A10) are known. Now, for every segment x equation (A10) is tested, a new estimate for the set of potentials $u_x(z)$ is made and a new cycle started. The iterations are stopped when the residual error in equation (A10) is smaller than 10^{-7}.

Appendix B

The fraction and average length of tails, loops and trains is obtained in a similar way as described in ref (18). Only the most important equations are given here.

The end segment distribution function of free chains (chains with no segments in the first layer), $G_{x1}^f(z,s|\,1)$, can be obtained by the recurrence relation (Equation 12) and the condition that $G_x(1) = 0$ for all x. The end segment distribution function of adsorbed chains (chains with at least 1 segment at the surface), $G_{x1}^a(z,s|\,1)$, is equal to $G_{x1}(z,s|\,1)$ - $G_{x1}^f(z,s|\,1)$. Numerically accurate values of $G_{x1}^a(z,s|\,1)$ are obtained in a slightly different way.[18]

A loop ending at segment s will have segment s in layer 2 and segment s + 1 in layer 1. Both segments are attached to a part of a chain with at least one segment at the surface. The average number of loops per chain can be calculated as:

$$n_1^l = \frac{\lambda_1}{\sum_x \sum_z G_{x1}^a(z,r|\,1)} \sum_x \{v_x \sum_{s=1}^{r-1} G_{x1}^a(2,s|\,1)\, G_{x1}^a(1,s+1)|r)\} \qquad (B1)$$

The average number of trains per chain is obviously:

$$n_1^{tr} = n_1^l + 1 \qquad (B2)$$

The average number of tails per chain with length s is obtained from:

$$n_i^t(s) = \frac{2\lambda_1}{\sum_x \sum_z G_{xi}(z,r|1)} \sum_x v_x \, G_{xi}^f(z,s|1) G_{xi}^a(1,s+1|r) \tag{B3}$$

The average number of tails per chain, n_i^t, is simply found by summing equation (B3) over s. The fraction of segments of the adsorbed chains in trains, tails and loops is given by:

$$v_i^{tr} = \frac{\phi_i(1)}{\theta_i^a} \tag{B4}$$

$$v_i^t = \frac{1}{r_i} \sum_{s=1}^{r-1} s n_i^t(s) \tag{B5}$$

$$v_i^l = 1 - v_i^{tr} - v_i^t \tag{B6}$$

And the average lengths of trains, tails and loops are equal to:

$$l_i^{tr} = \frac{r_i v_i^{tr}}{n_i^{tr}} \tag{B7}$$

$$l_i^t = \frac{r_i v_i^t}{n_i^t} \tag{B8}$$

$$l_i^l = \frac{r_i v_i^l}{n_i^l} \tag{B9}$$

References

1) Tadros Th. F., and Vincent B., J. Phys. Chem. (1980), <u>84</u>, 1575
2) Kayes J.B., Rawlins D.A., Colloid and Polymer Sci. (1979), <u>257</u>, 622
3) Hadziioannou G., Patel S., Granick S., and Tirrell M., J. Am. Chem. Soc. (1986), <u>108</u>, 1869

4) Evers O.A., PhD Thesis, Wageningen Agricultural University (1989)

5) Munch M.R., and Gast A.P., Macromolecules (1988), 21, 1366

6) Marques C.M., Joanny J.F., and Leibler L., Macromolecules (1988),21, 1051

7) Van Lent B., and Scheutjens J.M.H.M. Macromolecules (1989), 22, 1931; chapter 2

8) Billmeyer F.W, "Textbook of Polymer Science", Sec. Ed. (1971), John Wiley & Son Inc, NY, 328-351

9) Wang Z., and Yan D., J. of Polym. Sci. Part B: Polym. Phys. (1986), 24, 2219, ibid. 2229, ibid. 2241., ibid. 2255

10) Galina H., Eur. Polym. J. (1986), 22, 665, ibid. 671

11) Buscall R. and Corner T., Colloids Surfaces (1986), 17, 39

12) Cosgrove T., Finch N., Vincent B., and Webster J., Colloids Surfaces, (1988), 31, 33

13) Diaz-Barrios D. and Howard G.J., Macromol. Chem. (1981), 182, 1081

14) Diaz-Barrios D. and Rengel A., J. Polym. Sci. Polym. Chem. Ed. (1984), 22, 519

15) Pennings J.F.M., PhD thesis, Eindhoven Technical University (1982)

16) Marques C.M., and Joanny J.F., submitted

17) Scheutjens J.M.H.M., and Fleer G.J., J. Phys. Chem. (1979), 83, 1619

18) Scheutjens J.M.H.M., and Fleer G.J., J. Phys. Chem. (1980), 84, 178

19) Björling M., Linse P., and Karlström G., submitted to J. Phys. Chem.

20) Cohen Stuart M.A., Scheutjens J.M.H.M., and Fleer G.J., J. Polym. Sci., Polym. Phys. Ed. (1980), 18, 559

21) Scheutjens J.M.H.M., Fleer G.J., and Cohen Stuart M.A., Colloids Surfaces (1986), 21, 285

22) Van der Beek G.P., and Cohen Stuart M.A., J. Physique (Les Ulis.,Fr.) (1988), 49, 1449

Chapter 4

Interaction between Hairy Surfaces and the Effect of Free Polymer

Abstract

In this paper, the interaction between surfaces coated with grafted polymer is studied. The influence of free, nonadsorbed polymer on the interaction is described in some detail. A self-consistent field theory, based on the model for homopolymer adsorption of Scheutjens and Fleer, is used to take into account all the possible conformations of terminally anchored and free polymer and to calculate the interaction between the two surfaces. For hard surfaces in the presence of free polymer, the attraction is only determined by the osmotic effect. In the case of hairy surfaces, the mixing of the grafted polymer layers gives an additional attractive contribution, because the hairs mix more easily than hairs and free polymer; this attraction is strongest at plate separations just below twice the hydrodynamic layer thickness. At small separations, the hairs become repulsive. The free energy of interaction shows a minimum as a function of the bulk volume fraction of free polymer. For infinitely large plates, the attraction is always stronger for higher chain lengths of free polymer. Increasing the mixing energy of grafted and free polymer (χ_{gf}) increases the attraction drastically, whereas their solvency (χ_{f0}, χ_{g0}) has a much less pronounced effect. If no free polymer is present, the interaction becomes attractive when the solvency of the grafted chains becomes worse than theta conditions.

Introduction

The stability of colloidal suspensions in the presence of nonadsorbing (free) polymer has been a subject of much interest. Theoretically, many authors have been concerned with the case of bare particles, so called hard spheres[1-9]. The destabilization of these systems

is explained in terms of an osmotic attraction caused by depletion of the free polymers in the vicinity of the surface. Only few experimental data are available for this kind of systems.[4]

Li-In-On et al.[10] were the first to report that sterically stabilized particles i.e. particles coated with a grafted polymer layer (also called soft spheres or hairy particles) can be destabilized by adding free polymer in relatively low concentrations, and are restabilized in concentrated polymer solutions. This restabilization has later been predicted for hard spheres[3,9] but has, as yet, only been observed experimentally for soft spheres. Studies on soft spheres[10-16] have revealed that the flocculation is weak and reversible. The critical destabilization and restabilization concentrations are generally found to decrease with increasing molecular weight of the free polymer. The influence of other parameters, such as grafted amount and solvent quality, are less clear.

Only few theories have been developed to describe the stability of soft spheres in the presence of free polymer. Vincent et al.[12] calculated the free energy of mixing polymer coils with the polymer sheaths on the two particles and that of the mutual mixing of the two sheaths. This model neglects the existence of the depletion region, which is the origin of the flocculation of hard spheres. According to the Monte Carlo Rotational Isomeric State model of Feigin and Napper[3], the restabilization of the hairy particles is caused by an energetic barrier. This is in contradiction with the experimental observation that the flocculation is reversible. Rao and Ruckenstein[17] studied two limiting cases: in the first the grafted layer is considered as an impenetrable barrier, and in the second the free polymer is allowed to penetrate the grafted layer completely. Vincent et al.[16] introduced a simple model in which they extend the theory for bare particles by Fleer et al.[9] to describe the flocculation of hairy particles.

The purpose of the present paper is to obtain more insight in the interaction between plates coated with a grafted layer in a polymer solution, without making a priori assumptions about the extent of interpenetration of grafted and free polymer. We start with a brief description of the model for hard spheres by Fleer et al.[9] and the extension to soft spheres by Vincent et al.[16] Then we introduce a

model for the interaction between soft plates, based upon the Self-Consistent Field (SCF) theory of Scheutjens and Fleer for adsorption of homopolymers.[18,19] Earlier, Cosgrove et al.[20] extended this theory to the case of grafted chains. The incorporation of extra components is straightforward.[21] The free energy of interaction is calculated using the so called "restricted equilibrium" argument.[22] When the particles approach, the free polymer and the solvent are allowed to leave the gap to equilibrate with the bulk solution, whereas the grafted polymer (the restricted component, although it is in complete equilibrium) can only adapt its configuration. Scheutjens and Fleer[22] have shown how to calculate the free energy of interaction in such systems. In the results section we study the influence of different parameters, such as the solvency parameters (χ_{f0}, χ_{g0}, χ_{gf}), the chain lengths, the concentration of free polymer, and the grafted amount. A qualitative comparison with the model of Vincent et al.[16] will be made.

Theory

The model for hard spheres by Fleer et al.[9]

Polymer molecules will lose conformational entropy when they come close to a solid surface. As a result, nonadsorbing (free) polymer has a lower concentration near the surface than in the bulk solu-
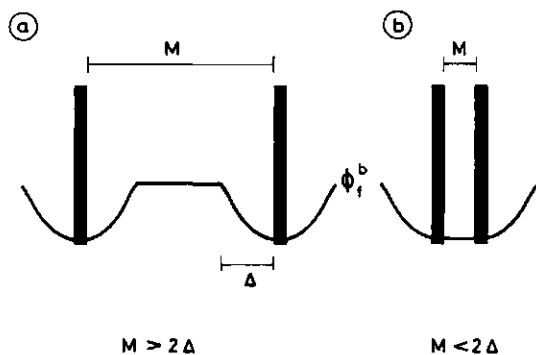
Figure 1.
Concentration profile of nonadsorbing polymer between two plates at (a) large and (b) small separation.

tion over a region of thickness Δ. The parameter Δ may be called the depletion layer thickness. When two plates in a solution with nonadsorbing polymer are at a separation $M > 2\Delta$, the polymer concentration halfway the plates is the same as in the bulk solution (Figure 1a). We denote the volume fraction of free polymer in the bulk solution as ϕ_f^b and that of the solvent as ϕ_0^b. At small separation, $M < 2\Delta$, (almost) all free polymer has left the gap (Figure 1b). Further reduction of the surface separation gives a change in interaction free energy $A^{int}(M)$ due to the transportation of solvent molecules from the pure solvent region (with chemical potential μ_0^*) between the surfaces to the bulk solution, where the solvent molecules have a chemical potential μ_0. Throughout this paper we use the subscript 0 for solvent. For flat plates of area A_s at separation $M < 2\Delta$, the transported volume of solvent is $A_s(2\Delta - M)$ as compared to $M = 2\Delta$, where the interaction starts. Consequently, $A^{int}(M)$ equals $A_s(2\Delta - M)(\mu_0 - \mu_0^*)/v_0$, where v_0 is the solvent molecular volume. For spheres with radius a the geometrical factor is different. At separation $M < 2\Delta$ we have:

$$A^{int}(M) = 2\pi a \frac{\mu_0 - \mu_0^*}{v_0}\left(\Delta - \frac{M}{2}\right)^2\left(1 + \frac{2\Delta}{3a} + \frac{M}{6a}\right) \qquad (M < 2\Delta)$$

$$\approx 2\pi a \frac{\mu_0 - \mu_0^*}{v_0}\left(\Delta - \frac{M}{2}\right)^2 \qquad (\Delta << a, M << a)$$

$$(1)$$

One could also say that the osmotic pressure difference $\Pi = (\mu_0^* - \mu_0)/v_0$ between the bulk solution and the gap forces the particles together. The chemical potential of the solvent can be calculated using Flory's equation[23]:

$$\frac{\mu_0 - \mu_0^*}{kT} = \ln\phi_0^b + 1 - \phi_0^b - \frac{\phi_f^b}{r_f} + \chi_{f0}(\phi_f^b)^2 \qquad (2)$$

where χ_{f0} is the Flory-Huggins interaction parameter between the free polymer and the solvent. The depletion thickness Δ can be obtained numerically from the lattice model for homopolymer adsorp-

tion of Scheutjens and Fleer[18] as $-\theta_f^{exc}/\phi_f^b$, where θ_f^{exc} is the (negative) excess adsorbed amount, expressed in number of segments per surface site. An analytical expression which closely fits the numerical results for Δ is presented in ref (9). The minimum A_{min}^{int} in the free energy of interaction is situated at M = 0, and is given by:

$$A_{min}^{int} = 2\pi a \frac{\mu_0 - \mu_0^*}{v_0} \Delta^2 \tag{3}$$
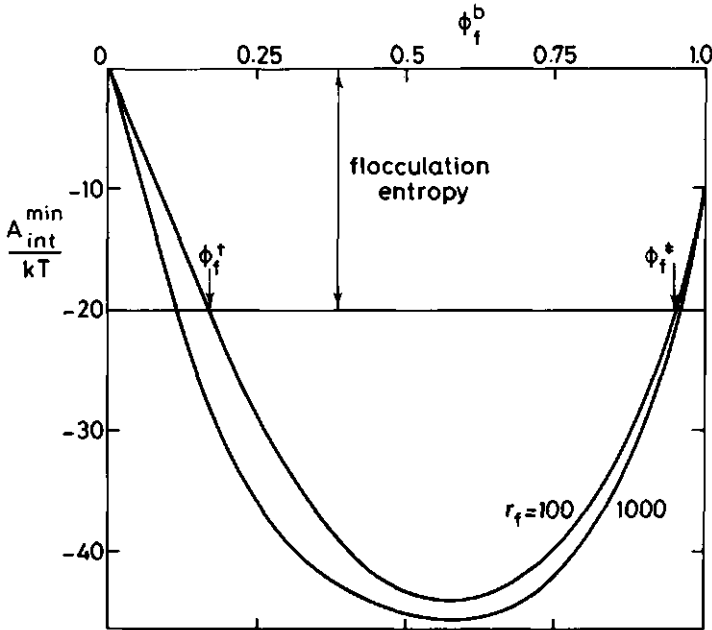
Figure 2. *Interaction free energy A_{min}^{int} between two hard spheres as a function of the volume fraction ϕ_f^b of free polymer in the bulk solution, according to ref 9, for r_f = 100 and r_f = 1000. The entropy loss per particle when a particle is transferred from the dispersion to the floc phase (for a particle concentration of 10^{-4}) is assumed to be 20k, corresponding to a free energy of transfer of 20kT. The critical flocculation concentration ϕ_f^t and the restabilization concentration ϕ_f^* are indicated. Particle diameter 100 nm, χ_{f0} = 0.5.*

With increasing ϕ_f^b, the osmotic pressure and, hence, $\mu_0^* - \mu_0$ increase, but Δ decreases because the osmotic pressure pushes the chains towards the surface. As a consequence of these two opposing effects, the attraction goes through a maximum at a certain volume fraction of polymer in the bulk solution. The polymer volume fraction $\phi_f^\dagger$ at which the particles will flocculate and the (higher) volume fraction $\phi_f^\ddagger$ at which they will restabilize depend on the entropy loss of the particles, which is in first approximation independent of ϕ_f^b. In Figure (2), A_{min}^{int} is plotted as a function of ϕ_f^b for two chain lengths. In this example, stable dispersions are obtained for ϕ_f^b lower than ≈ 0.2 and higher than ≈ 0.95; in between depletion flocculation occurs. For hard spheres the second critical volume fraction $\phi_f^\ddagger$ has never been observed experimentally.

The model for soft spheres by Vincent et al.[16]

Vincent et al.[16] extended the hard sphere model by Fleer et al. to describe the depletion flocculation of spheres coated with grafted polymer. The free polymer is assumed to enter the polymer sheath over a distance Δ^{ov} (Figure 3a). The penetration depth Δ^{ov} is found by equating the osmotic pressure in the overlap region to that in the bulk solution. For the volume fraction profiles of the anchored chains and the free polymer, predetermined shapes are taken. From the profile of the anchored chains the thickness Δ^g of the grafted layer is estimated. If there would be no grafted layer, the interaction would start at a plate separation $2\Delta^d$, where Δ^d is the depletion layer thickness for hard surfaces. In the presence of a hairy layer the polymer segments cannot come closer to the surface than $\Delta^g - \Delta^{ov}$, and the interaction starts at a separation $2(\Delta^g + \Delta^d - \Delta^{ov})$. For the evaluation of Δ^d a very simple approximation is used: $\Delta^d = 1.4 R_f^{gr} (1 - \phi_f^b)/(1 - \phi_f^*)$, where R_f^{gr} is the radius of gyration and ϕ_f^* the critical overlap concentration of the free chains. The factor $\Delta^d + \Delta^g - \Delta^{ov}$ could be called the effective depletion layer thickness Δ^{eff}. At plate separations smaller than $2\Delta^{eff}$, no free polymer is considered to be present between the spheres, see Figure (3b). The interaction free energy due to this depletion can be obtained from equation (1) by substituting Δ^{eff} for Δ:
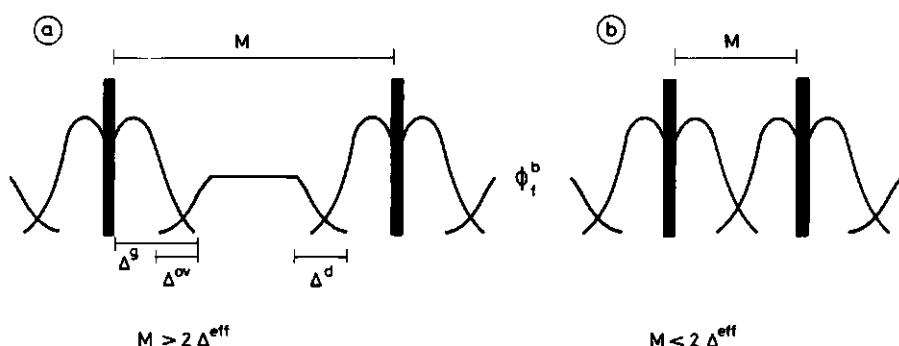
Figure 3. *Concentration profiles of grafted and free polymer between two plates for (a) large and (b) small plate separation.*

$$A^{dep}(M) \approx 2\pi a \frac{\mu_0 - \mu_0^*}{v_0}\left(\Delta^{eff} - \frac{M}{2}\right)^2 \quad \frac{M}{2} \leq \Delta^{eff} \tag{4}$$

To obtain the change in the total interaction free energy, Vincent et al.[16] add to this depletion contribution two other terms, i.e., the free energy of mixing the two polymer sheaths $(M < 2\Delta^g)$ and an elastic deformation term $(M < \Delta^g)$. As expected, $\phi_f^\dagger$ increases and $\phi_f^\ddagger$ decreases as compared to hard spheres.

The theory of Vincent et al.[16] is based upon a number of assumptions. The attraction is caused by an osmotic force. The profiles of the attached polymer and the free polymer have a given shape. Furthermore, the depletion interaction range Δ^{eff} is an assumption in itself. Any variation in the profiles while the particles approach is not taken into account. The grafted amount and the layer thickness can be varied independently in this model.

The self-consistent field theory[18,19]

The SCF theory of Scheutjens and Fleer is a lattice theory. The layers are numbered sequentially from one surface to the other, $z = 1,....,M$. Layers 1 and M are assumed to be next to the surface of a solid. Each lattice site has Z nearest neighbours, of which a fraction λ_0 are in the same, a fraction λ_{-1} in the previous, and a fraction λ_1 in

the next layer. For a hexagonal lattice $\lambda_0 = 0.5$ and $\lambda_{-1} = \lambda_1 = 0.25$. Molecules of type i, with chain length r_i, have a volume fraction $\phi_i(z)$ in layer z. In a system of grafted polymer in a solution of free polymer, the index i is either 0 (solvent), f (free polymer), or g (grafted chains).

The statistical weights of the conformations of the molecules are calculated using a step weighted walk in a potential field. This potential field is assumed to be perpendicular to the surface and is created by the concentration gradients of the molecules in the lattice. In turn, these concentration gradients are dependent on the potential (i.e., self-consistent) field. Each step (or segment of a molecule i) is weighted with the appropriate segment (Boltzmann) weighting factor $G_i(z)$, which is given by:

$$G_i(z) = e^{\dfrac{-u_i(z)}{kT}} \tag{5}$$

The factor $G_i(z)$ describes the preference for a segment i to be in layer z rather than in the bulk solution. Hence, in the bulk solution $G_i(z)$ is unity. A segment of molecule i in layer z feels a potential $u_i(z)$, with $u_i(\infty) \equiv 0$. The expression for $u_i(z)$ is:

$$u_i(z) = u'(z) + kT\sum_j \chi_{ij}(<\phi_j(z)> - \phi_j^b) + u_i^{ads}(z) \tag{6}$$

where u'(z) is a (segment type independent) hard core potential which is numerically adjusted such that the packing constraint $\sum_j \phi_j(z) = 1$ is obeyed. The second term in equation (6) accounts for the contact energies between a segment of type i in layer z with other segments in the system, in excess to the interaction it would have in the bulk solution. For simplicity, only nearest neighbour interactions are taken into account. The parameter χ_{ij} is the familiar Flory-Huggins parameter for the interaction between segments of molecule i and j. The contact volume fraction $<\phi_i(z)>$ is defined as:

$$<\phi_i(z)> = \lambda_{-1}\phi_i(z-1) + \lambda_0\phi_i(z) + \lambda_1\phi_i(z+1) \tag{7}$$

The interaction between segments and the surfaces is accounted for in equation (6) through $u_i^{ads}(z)$. In the present paper, $u_i^{ads}(z)$ will be taken zero for all i and all z.

The next step in the theory is to calculate the end segment distribution functions $G_i(z,s|1)$, the average weighting factor of all the conformations (walks) of an s-mer with segment s in layer z and starting (with segment 1) in an arbitrary layer. The following recurrence relation applies:

$$G_i(z,s|1) = G_i(z) < G_i(z,s-1|1)> \tag{8}$$

where

$$< G_i(z,s-1|1) > = \lambda_{-1}G_i(z-1,s-1|1) + \lambda_0 G_i(z,s-1|1)$$
$$+ \lambda_1 G_i(z+1,s-1|1) \tag{9}$$

This means that the end segment distribution function of an s-mer is related to the end segment distribution function of an (s-1)-mer. For a segment s, which is connected to an (s-1)-mer, it is only possible to be in layer z if this (s-1)-mer ends in one of the layers z-1, z, or z+1. The factors λ_{-1}, λ_0, and λ_1 are the fractions of steps to layer z from these possible positions for segment (s-1). The multiplication with $G_i(z)$ accounts for the weighting factor of segment s. Equation (9) is a recurrence relation which starts at segment 1, for which $G_i(z,1|1) = G_i(z)$. One can also start at the other end of the chain. Then all walks of r_i-s steps end at segment s and the average weighting factor is $G_i(z,s|r)$. For a symmetrical chain, e.g., a homopolymer, $G_i(z,s|1) = G_i(z,r-s+1|r)$. In order to find the volume fraction $\phi_i(z)$, the walks starting at each end of the chain and ending with segment s (s = 1,...,r_i) in layer z are to be combined:

$$\phi_i(z) = C_i \sum_{s=1}^{r_i} \frac{G_i(z,s|1)G_i(z,s|r)}{G_i(z)} \tag{10}$$

The factor $G_i(z)$ in the denominator corrects for double counting ($G_i(z)$ is included in both end segment distribution functions), and C_i

is a normalization constant. In the bulk solution all G_i's are unity, and therefore:

$$C_i = \frac{\phi_i^b}{r_i} \qquad (11)$$

where ϕ_i^b is the volume fraction of molecules i in the bulk solution. Another expression for C_i can be derived if the amount of segments belonging to molecules i between the two plates, $\theta_i = \sum_{z=1}^{M} \phi_i(z)$, is given. Each segment number contributes to θ_i by an amount of θ_i/r_i. If only segment r_i is considered, it can easily be verified that:

$$C_i = \frac{\theta_i}{r_i G_i(r|1)} \qquad (12)$$

where $G_i(r|1)$ is the chain weighting factor, defined as $\sum_{z=1}^{M} G_i(z,r|1)$. With equations (5), (6), (10), and (11) or (12), together with the M boundary conditions $\sum_i \phi_i(z) = 1$, a numerical solution can be obtained.

Terminally attached chains[20]

Two grafted components "g" can be distinguished, one is grafted in layer 1 and the other in layer M. For terminally attached chains both chain ends are treated differently. $G_g(z,s|r)$ is obtained in the same way as in the previous section, because the last segment may, in principle, be anywhere in the system. The first segment, however, is restricted to either layer 1 or M. Therefore:

$$G_g(z,1|1) = \begin{cases} G_g(1) & \text{if } z = 1 \text{ and g is grafted in layer 1} \\ G_g(M) & \text{if } z = M \text{ and g is grafted in layer M} \\ 0 & \text{otherwise} \end{cases} \qquad (13)$$

For chains grafted in layer 1, the second segment can only be in layers 1 or 2, the third segment in layers 1 to 3, and so on. In this case $G_g(z,s|1) \neq G_g(z,r-s+1|r)$, in contrast with symmetrical chains. The computation of the volume fraction profile can still be achieved using

equation (10). The grafted amount is constant, so equation (12) is used for the calculation of the normalization constant C_g. The grafting density σ_g (in layer 1 and layer M), i.e., the number of molecules per surface site, is equal to θ_g/r_g. Note that θ_g is defined per plate, whereas for the mobile components θ_i is the total number of mono-layers between the two plates.
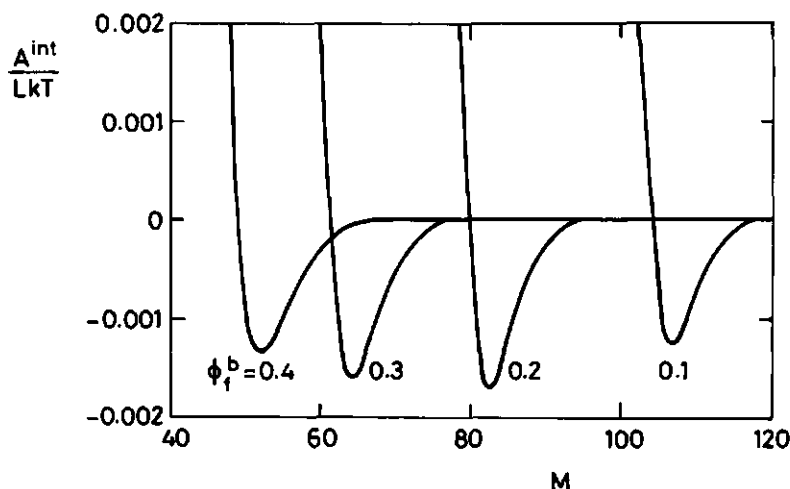
The free energy of interaction

The derivation of the free energy A(M) for a system of M layers be-tween two surfaces with grafted polymer g is very similar to that de-scribed in ref 18 and 21, see appendix.

$$\frac{A(M)}{LkT} = \sum_i \sum_z \phi_i(z) \left\{ \frac{1}{r_i} \ln \frac{\theta_i}{G_i(r|1)} + \ln G_i(z) + \frac{1}{2} \sum_j \chi_{ij} < \phi_j(z) > \right\} + c(\sigma_g)$$

(14)

The summation over i includes both the mobile and the grafted com-ponents. The term $c(\sigma_g)$ is only a function of the amount of grafted chains and therefore independent of the plate separation M. When the distance between the two plates is reduced, the free polymer f and the solvent 0 are allowed to leave the gap. These two compo-nents are considered to be in equilibrium with the bulk solution. Thus the excess free energy $A^{exc}(M)$ becomes:

$$\frac{A^{exc}(M)}{L} = \frac{A(M)}{L} - (\mu_0 - \mu_0^*)\theta_0 - (\mu_f - \mu_f^*)\frac{\theta_f}{r_f}$$

(15)

Equation (15) applies to the system under consideration, i.e., plates coated with a grafted layer in a solution of nonadsorbing polymer. For a system with more components, for each extra component i in equi-librium with the bulk solution a term $-(\mu_i - \mu_i^*)\theta_i/r_i$ should be in-cluded in equation (15). The chemical potential of free polymer in a monomeric solvent with respect to the pure amorphous phase (denoted by *) is equal to[23]:

Figure 4. *The free energy of interaction per surface site as a function of the separation between two plates covered with grafted chains, in four different concentrations ϕ_f^b of free polymer. Chain lengths r_f = 400, r_g = 200; grafted amount per plate θ_g = 10; interaction parameters $\chi_{f0} = \chi_{g0} = \chi_{gf}$ = 0.*

$$\frac{\mu_f - \mu_f^*}{kT} = \ln\phi_f^b + (1 - r_f)(1 - \phi_f^b) + r_f\chi_{f0}(1 - \phi_f^b)^2 \qquad (16)$$

The expression for the chemical potential of the solvent is given in equation (2). The quantity of interest is $A^{int}(M)$, the free energy of interaction, which equals the excess free energy at plate separation M with respect to that at infinite plate separation:

$$A^{int}(M) = A^{exc}(M) - A^{exc}(\infty) \qquad (17)$$

Results and Discussion

In this section we analyse the effects of several parameters on the interaction of hairy plates in a polymer solution. For all calculations a hexagonal lattice has been used, i.e., λ_0 = 0.5 and $\lambda_{-1} = \lambda_1$ = 0.25.

Throughout this paper, the properties of the molecules grafted in layer 1 and M (chain length, grafted amount, solvency) will be identical. We use the subscript "g" for grafted polymer, "f" for nonadsorbing free polymer and "0" for solvent. None of the molecules will be considered to have an excess interaction with the surface: $u_i^{ads}(z) = 0$ for all i and z.

In Figure (4), the interaction free energy $A^{int}(M)$ as a function of the plate separation M is shown for four volume fractions ϕ_f^b of the free polymer in the bulk solution. In this case $r_g = 200$, $\theta_g = 10$ monolayers per plate, $r_f = 400$, and $\chi_{g0} = \chi_{f0} = \chi_{gf} = 0$. A clear minimum and hardly any maximum (in contrast with results obtained by Feigin and Napper[9]) is observed for each of the bulk volume fractions of free polymer. The trends in Figure (4) can be understood by considering the segment concentration profiles, see Figure (5). This figure shows, for the case $\phi_f^b = 0.2$, how the profiles between the plates change when the plate separation is reduced. In Figure (5a), at
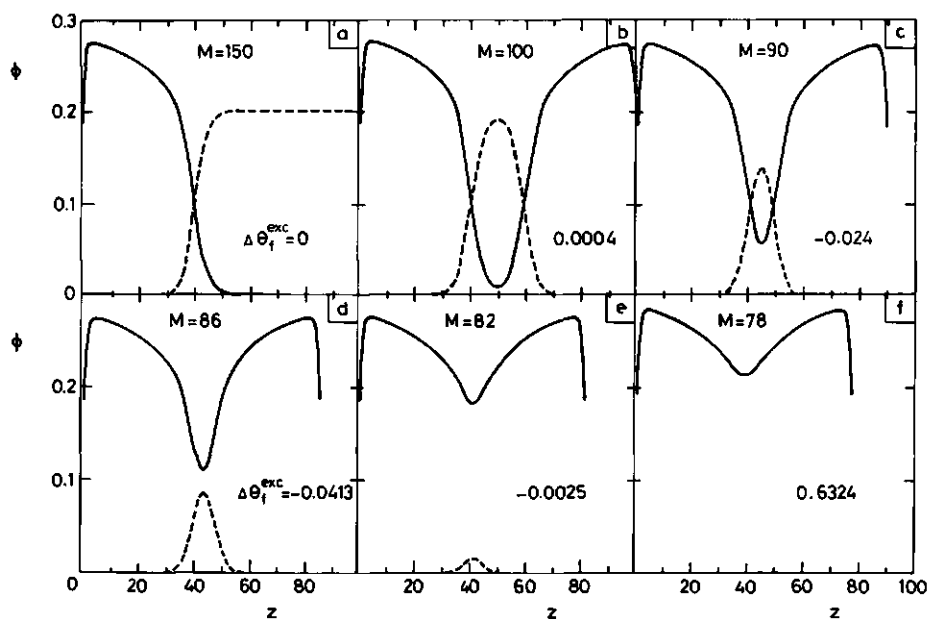
Figure 5. *Profiles of the grafted (solid curves) and free polymer (dashed curves) at six different plate separations M for the case $\phi_f^b = 0.2$ of Figure (4). The value of $\Delta\theta_f^{exc}(M) = \theta_f^{exc}(M) - \theta_f^{exc}(\infty)$ is indicated in the diagrams.*

plate separation M = 150, a profile (of which only the first 100 layers are shown) is obtained at which the particles have essentially no interaction. There is an overlap region of about 15 layers between free and attached molecules. Figure (5b) shows the situation where the separation M equals 100 layers. The maximum volume fraction of the free polymer has decreased slightly and the grafted polymers overlap to a small extent. The interaction is still very weak. At M = 90 (Figure 5c), some attraction sets in. As M decreases, the amount of free polymer between the plates diminishes, see for example M=86 (Figure 5d) and M = 82 (Figure 5e). The free energy of interaction is minimal at M = 82. Almost all the free polymer has left the gap. The overlap region between the anchored layers is extensive. Upon a slight reduction of the plate separation, to M = 78 (Figure 5f), essentially all the free chains have left the gap and the interaction has become repulsive. Note that in most cases the maximum in the profiles of the anchored chains remains the same. Only in Figure (5f) the maximum in the profile close to the surface has increased slightly.

Vincent et al.[16] interpret the interaction only in terms of osmotic forces. Due to the depletion of free polymer in the gap the osmotic pressure is lower than in the bulk solution, leading to attraction. Upon further reduction of M, the grafted polymer layers start to overlap considerably, which causes the strong repulsive part in the interaction curve.

However, the osmotic pressure is not the only effect which determines the depletion interaction between soft surfaces. To illustrate this, we rewrite equations (14) and (15) for an athermal mixture (all χ's zero) of free polymer and solvent between plates without and with hairs. In the first case, all components (f and 0) are mobile. We may now replace $\theta_i/G_i(r|1)$ by ϕ_i^b, according to equations (11) and (12), and express ln $G_i(z)$ in the solvent volume fraction profile: for $\chi = 0$, ln $G_i(z) = -u'(z)/kT = $ ln $G_0(z) = $ ln $\phi_0(z)/\phi_0^b$. After some rearrangement we obtain from equation (15), after substitution of μ_0 and μ_f:

$$\frac{A^{exc}(M)}{LkT} = \frac{A_{f0}^{exc}(M)}{LkT} = \sum_z \left\{ \ln \frac{\phi_0(z)}{\phi_0^b} - (\phi_0(z) - \phi_0^b) - \frac{1}{r_f}(\phi_f(z) - \phi_f^b) \right\}$$

(18a)

$$= -\sum_z (\Pi(z) - \Pi^b) v_0 /kT \qquad (18b)$$

where $\Pi^b = -(\mu_0 - \mu_0^*)/v_0$ is the osmotic pressure of the bulk solution with respect to pure solvent and $\Pi(z)$ is the osmotic pressure of a solution of volume fraction $\phi_f(z) = 1 - \phi_0(z)$. Equation (18) is valid for hard surfaces, and it is clear that in this case the free energy of interaction can be written entirely in terms of $\Pi(z) - \Pi^b$. This applies also to the more general case $\chi \neq 0$ in full equilibrium.[24]

For hairy surfaces, additional terms enter A^{exc} due to the grafted component, which is in restricted equilibrium. A similar procedure leads to:

$$\frac{A^{exc}(M)}{LkT} = \frac{A_{f0}^{exc}(M)}{LkT} + \frac{2\theta_g}{r_g} \ln \frac{\theta_g}{G_g^M(r|1)} + c(\sigma_g) - 2 r_g \sigma_g (\phi_0^b + \phi_f^b /r_f)$$

$$(19)$$

where $A_{f0}^{exc}(M)$ is given by equation (18) (although its numerical value is different from that for hard plates because the profiles are affected by the presence of the hairs), and $G_g^M(r|1)$ is the chain weighting factor at separation M, see below equation (12). The last terms in equation (19) are constants that do not depend on M and that, consequently, cancel in A^{int}. Now we may split $A^{int}(M)$ into two terms:

$$A^{int}(M) = A_{f0}^{int}(M) + A_g^{int}(M) \qquad (20)$$

where $A_{f0}^{int}(M) = A_{f0}^{exc}(M) - A_{f0}^{exc}(\infty)$, and $A_g^{int}(M)$ is given by:

$$A_g^{int}(M) = \frac{2\theta_g}{r_g} \ln \left(\frac{G_g^\infty(r|1)}{G_g^M(r|1)} \right) \qquad (21)$$

The term $A_{f0}^{int}(M)$ may be considered as the osmotic term due to the free polymer, whereas $A_g^{int}(M)$ is the (purely entropic) contribution due to the hairs.
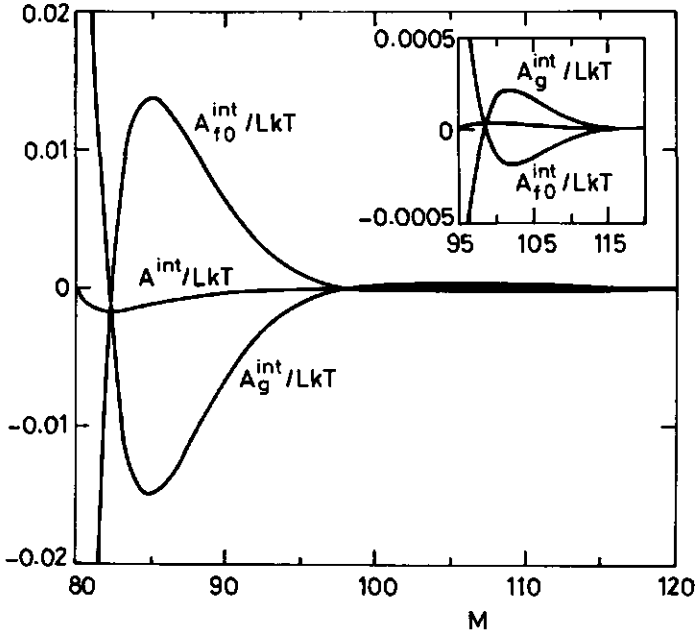
Figure 6. *The free energy of interaction and its contributions $A_g^{int}(M)$ due to the attached chains and $A_{f0}^{int}(M)$ due to free polymer and solvent, as a function of the plate separation M, for the system of Figure (5).*

Figure (6) shows these two contributions and their sum $A^{int}(M)$ for the system of Figure (5). The osmotic term $A_{f0}^{int}(M)$ has a small minimum at M = 102 (see inset), passes a maximum at M = 85, and decreases steeply at shorter separations. The contribution $A_g^{int}(M)$ displays the opposite trends, and even overcompensates $A_{f0}^{int}(M)$; the net effect is a minimum in $A^{int}(M)$ at M=82 and a steep repulsion at shorter distances, see also Figure (4). The behaviour of the two contributions to $A^{int}(M)$ is rather unexpected, especially the repulsive part of the osmotic term and the attraction due to the hairs. We interpret these trends as follows.

In the simple model for hard surfaces, discussed above, $A^{int}(M) \approx \Pi^b (M - 2\Delta)$ for $M < 2\Delta$. This can be rewritten as $A^{int}(M) \approx -\Pi^b / \phi_f^b [\theta_f^{exc}(M) - \theta_f^{exc}(\infty)]$ because $\theta_f^{exc}(M) = -M\phi_f^b$ (if $M < 2\Delta$) and $\theta_f^{exc}(\infty) = -2\Delta\phi_f^b$. In other words, in this case $A^{int}(M)$ is determined solely by the change in $\theta_f^{exc}(M)$. Let us assume that this, as a first approxima-

tion, also applies to the osmotic term $A_{f0}^{int}(M)$ for soft plates. The values of $_\Delta\theta_f^{exc}(M) = \theta_f^{exc}(M) - \theta_f^{exc}(\infty)$ are indicated in the diagrams of Figure (5). It turns out that the trends are correctly predicted: at M=102 where there is a shallow minimum in $A_{f0}^{int}(M)$, $_\Delta\theta_f^{exc}(M)$ has a small positive value, and when $A_{f0}^{int}(M)$ is maximal $_\Delta\theta_f^{exc}(M)$ has its largest negative value. The free energy of interaction passes through zero when $\theta_f^{exc}(M) \approx \theta_f^{exc}(\infty)$, and decreases linearly with decreasing M when all polymer has left the gap so that $\theta_f^{exc}(M)$ is linear in M.

One may wonder why the depletion around M = 85 is higher than at infinite separation. The same effect is found for hard surfaces[7], but in this case the free energy effect is quite small. This extra increase in the case of soft surfaces is probably due to the fact that the mutual overlap of two grafted layers is entropically more favourable than the overlap of (two) grafted layers with free polymer, because a more homogeneous grafted layer is formed. The negative value of $A_g^{int}(M)$ in this region points in the same direction. A similar overlap effect was calculated by Vincent et al.[12]

At distances below M = 82 the depletion interaction $A_{f0}^{int}(M)$ becomes rather strong. On its own this would lead to attraction. However, at that point the hairs overlap to such extent that the overall effect of $A^{int}(M)$ is repulsive.

We are led to the conclusion that the depletion interaction between soft surfaces is more complicated than between hard surfaces because not only the osmotic force, but also the interaction between the hairs play a role. The latter may be more important than the first, even at the onset of depletion interaction, leading to an attraction in the region where the osmotic term is repulsive and to repulsion where the osmotic term is attractive. One should therefore be very cautious when applying models[16] that assume that the attraction is only caused by the osmotic term, while disregarding the positive entropic effects when the grafted layers begin to overlap.

Returning now to Figure (4), we consider the position of the minimum in $A^{int}(M)$ with varying ϕ_f^b. Upon increasing the bulk concentration, the separation at which the interaction becomes attractive shifts to a lower M (see Figure 4). This point turns out to be about twice the hydrodynamic layer thickness of the grafted chains. This

can be concluded from Figure (7), where the hydrodynamic layer thickness δ_h of the grafted layer, calculated with the method proposed by Scheutjens et al.[25], is given as a function of the bulk concentration of free polymer. All the other parameters are the same as in Figure (4). As ϕ_f^b rises, the osmotic pressure of the solution increases which, in turn, decreases the hydrodynamic layer thickness. The free polymer compresses the hairs. The hydrodynamic layer thickness hardly changes with varying chain length of the free polymer (not shown), because the osmotic pressure is almost independent of r_f, see equation (2): the term ϕ_f^b/r_f is relatively small.
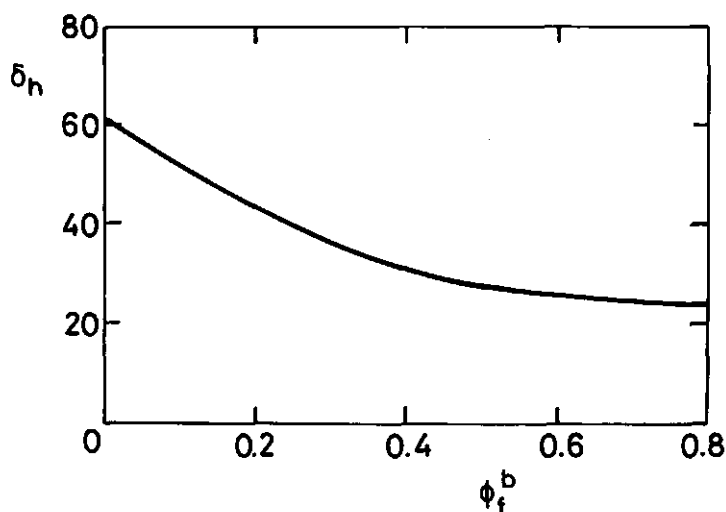
Figure 7.   *Hydrodynamic layer thickness δ_h of the grafted polymer as a function of free polymer concentration ϕ_f^b. The system is the same as in Figure (4).*

For hard spheres, the interaction free energy is minimal at M = 0, see equation (3). From Figure (4) it follows that the minimum A_{min}^{int} in the interaction curve for soft surfaces is situated at a finite separation, somewhat below M = $2\delta_h$. The depth of the minimum depends on ϕ_f^b (see Figure 4) and on the chain length of free polymer. Figure (8) shows A_{min}^{int} as a function of the volume fraction of free polymer, for three different chain lengths, viz. r_f = 200, 400, and 600. The other parameters are the same as in Figure (4). As explained in the

theory section, upon increasing the polymer concentration, the osmotic pressure and, hence, the attraction, increase initially. However, at high ϕ_f^b the depletion thickness decreases and the attraction becomes less again. These two opposing effects cause the minima in Figure (8). This minimum as a function of ϕ_f^b cannot be observed for hard plates. However, for hard spheres, where A_{min}^{int} is proportional to Δ^2 (equation 3), a minimum is found, see Figure (2).

For an estimation of the critical flocculation (ϕ_f^+) and restabilization (ϕ_f^+) concentrations (see Figure 2), one would have to know the entropy loss of the particles upon flocculation. This entropy loss can be considered to be almost independent of ϕ_f^b and must be balanced by A_{min}^{int}. We have made no attempt to calculate the particle entropy effect, because the model so far is only valid for plates. Moreover, no good model is available to describe the entropy of hairy particles. The primary aim of this study is to predict some general trends in the interaction of soft surfaces.
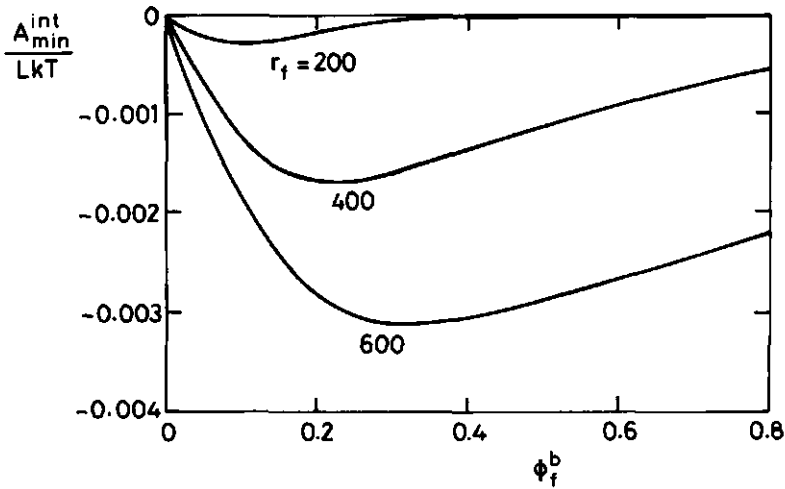

Figure 8. *The minimum in the interaction curves of Figure (4) as a function of ϕ_f^b for three chain lengths r_f of free polymer.*

Upon increasing the length of the free polymer, A_{min}^{int} decreases rapidly due to a larger depletion region, see Figure (8). This leads to

a lower value of $\phi_f^\dagger$. Note that also the restabilization concentration will be higher. However, this increase of the restabilization concentration with chain length of free polymer is in contrast with some experimental results.[10,11] Possibly, a curvature effect could play a role here.

In Figure (9), the influence of the surface coverage $\sigma_g = \theta_g/r_g$ on the depth of the interaction minimum A_{min}^{int} is shown for two different chain lengths of the grafted polymer, $r_g = 200$ and 400. The free polymers have a chain length of $r_f = 400$ and a bulk volume fraction of $\phi_f^b = 0.15$. As before, all Flory-Huggins interaction parameters χ_{ij} are zero. For $\sigma_g = 0$, the interaction is equal to the case of bare plates. When some polymer is grafted, the surfaces become "softer" and the attraction is much weaker. At a given (rather low) surface coverage the curves pass through a maximum. When more molecules are attached, the plates become "harder" again and the minimum deeper. For longer grafted molecules, the attraction is always less than for shorter ones, because the plates are slightly softer (except in the extremes $\theta_g = 0$ and $\theta_g = r_g$, which correspond to hard plates).
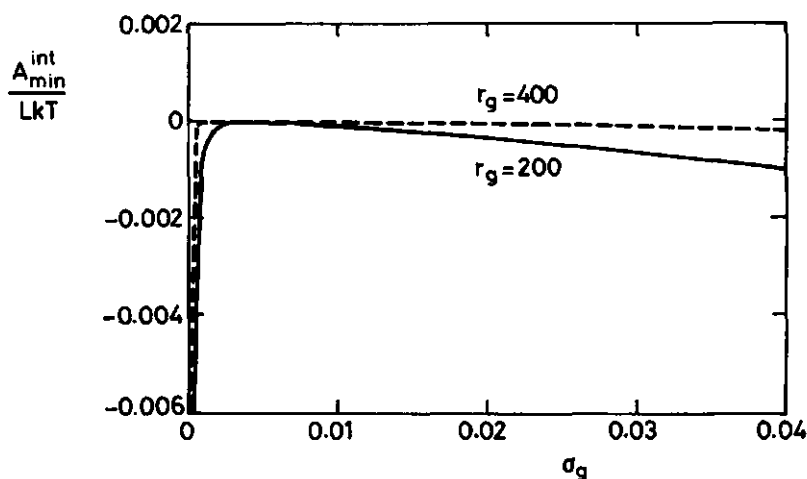
Figure 9. *The effect of surface coverage $\sigma_g = \theta_g/r_g$ on the interaction minimum. Parameters: $r_f = 400$, $\phi_f^b = 0.15$, $\chi_{f0} = \chi_{g0} = \chi_{gf} = 0$.*
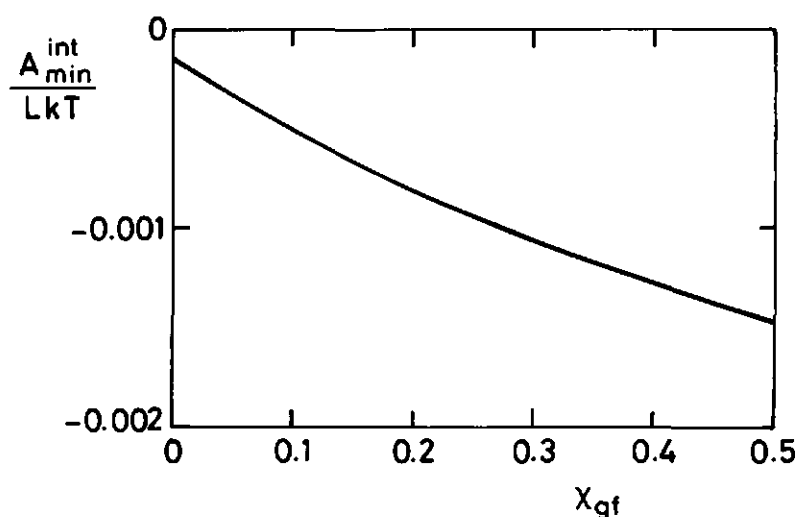
Figure 10. *The influence of the interaction parameter χ_{gf} between segments of grafted and free polymer on the interaction minimum. Parameters: $r_f = 400$, $\phi_f^b = 0.10$, $r_g = 200$, $\theta_g = 10$, $\chi_{f0} = \chi_{g0} = 0$.*
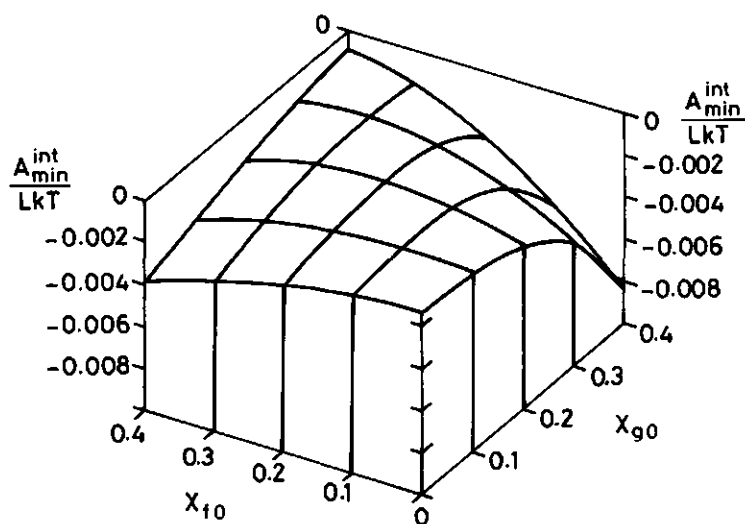
Figure 11. *The interaction minimum A_{min}^{int} as a function of the solvent quality χ_{f0} of free polymer and χ_{g0} of grafted chains. Parameters: $r_f = 400$, $\phi_f^b = 0.10$, $r_g = 200$, $\theta_g = 10$, and $\chi_{gf} = 0$.*

So far, only athermal mixtures have been considered ($\chi_{ij} = 0$). The effect of the compatibility of the two polymers is illustrated in Figure (10), where A_{min}^{int} is plotted as a function of χ_{gf}. When the miscibility decreases (i.e., χ_{gf} increases), the interpenetration of free polymer and grafted layer diminishes. The effective depletion layer thickness becomes larger and the attraction much stronger. Increasing χ_{gf} has the effect of making the surfaces "harder".

The influence of the two other solvency parameters, χ_{g0} and χ_{f0}, is demonstrated in Figure (11). The interaction minimum A_{min}^{int} is plotted as a function of these two parameters for $\chi_{gf} = 0$. When the solvency for hairs and free polymer is the same ($\chi_{f0} = \chi_{g0}$), the inter-action is less attractive in a poorer solvent (higher χ). A difference between χ_{g0} and χ_{f0} increases the depth of the interaction minimum. To explain these trends, volume fraction profiles have been drawn in Figure (12) for four different cases. Figure (12a) gives the athermal situation. In Figure (12b), χ_{f0} has been changed from 0 to 0.4, while $\chi_{g0} = 0$. The attraction has become stronger. Upon increasing χ_{f0} the osmotic pressure Π is reduced, which would give a less deep mini-mum. However, because Π decreases, the overlap region with grafted polymer becomes smaller and as a result the effective depletion layer thickness will increase and cause a deeper minimum. Obviously, this latter effect prevails. Going from Figure (12a) to (12c), χ_{g0} changes from 0 to 0.4, while $\chi_{f0} = 0$. The profile of the grafted chains becomes steeper, the surfaces harder and A_{min}^{int} more negative. If now χ_{f0} is increased from 0 to 0.4 (from Figure (12c) to (12d)) a weaker inter-action is observed. In this case the grafted layer is so hard that the penetration depth does not change much. The reduction of Π is the most important factor. The last variation to consider is going from Figure (12b) to (12d). In Figure (12d) both polymers have a relatively low solvency, $\chi_{g0} = \chi_{f0} = 0.4$. The polymers tend to mix better with each other than in Figure (12b), where $\chi_{g0} = 0$. This results in a smaller depletion thickness.

Figure (11) shows that changing the solvency conditions experi-mentally may give results which will be difficult to interpret. A change in one interaction parameter will, as a rule, imply variations in at least one of the other two. Moreover, upon varying the solvency conditions, adsorption energy effects (u^{ads}) may be introduced as

well. Comparing Figures (10) and (11), it can be noted that, with changing solvency conditions, the variation in χ_{gf} will often be the dominant factor. When the grafted and free polymers are of the same type ($\chi_{gf} = 0$), the interaction with the solvent ($\chi_{f0} \approx \chi_{g0}$) may play a role.
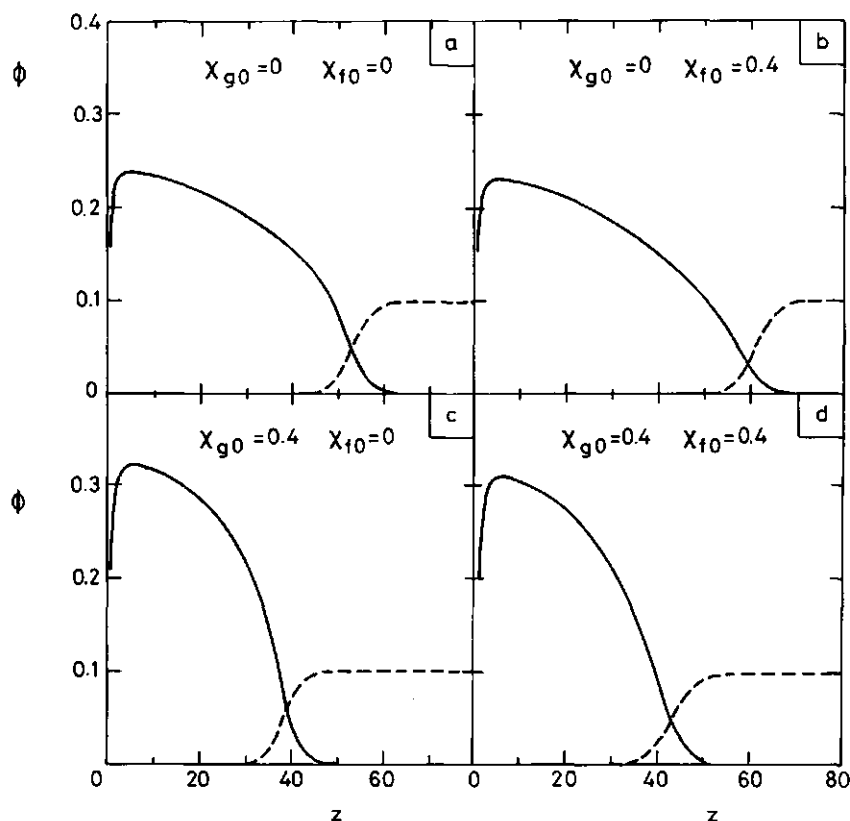
Figure 12. *The profiles of grafted (solid curves) and free (dashed curves) polymer for four different combinations of the solvent quality χ_{g0} and χ_{f0} (indicated). Other parameters: $r_f = 400$, $\phi_f^b = 0.10$, $r_g = 200$, $\theta_g = 10$, $\chi_{gf} = 0$.*

A common way to destabilize hairy particles, without adding free polymer, is to change the solvency of the grafted chains, χ_{g0}. In this case we consider the effect of the solvency on steric stabilization.[26] In Figure (13), interaction curves are shown for hairy surfaces ($\theta_g =$

10, $r_g = 200$) in a solvent, for different χ_{g0} values. Varying χ_{g0} from just below 0.5 to just above 0.5 results in a sudden change from curves without to curves with a minimum. The phase behaviour of grafted chains is similar to that of infinitely long chains in solution, because the translational entropy is essentially zero. Therefore, the minimum exists above $\chi_{g0} = 0.5$. Obviously, the entropy loss of the particles should be known to find at which χ_{g0} the particles start to flocculate. Experiments have shown[27] that hairy particles start to flocculate near the theta temperature of the chains. According to our calculations particles would flocculate just above $\chi = 0.5$, in good agreement with those measurements.
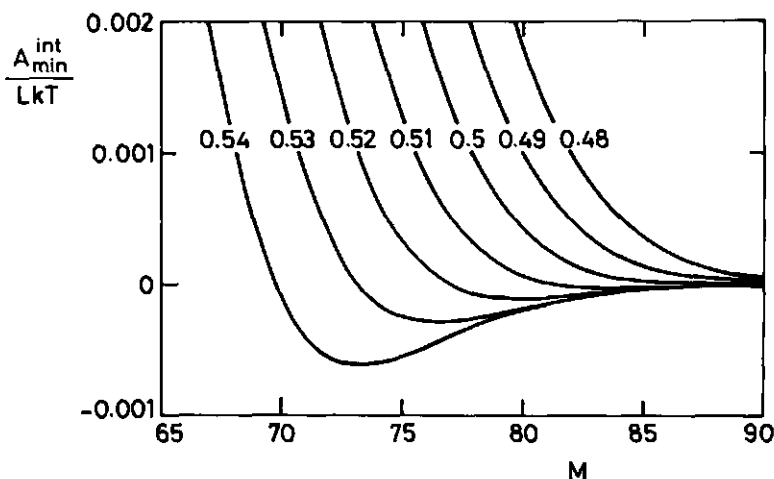
Figure 13. *The free energy of interaction between hairy plates in a solvent as a function of the plate separation, for seven different values of χ_{g0}. There is no free polymer in the system. $r_g = 200$, $\theta_g = 10$.*

Conclusions

For hard plates in the presence of nonadsorbing polymer the attraction between the surfaces is determined by osmotic forces. When the plates are covered with a grafted polymer layer, the interaction is not only determined by the osmotic pressure, but also by the confor-

mational changes of the grafted polymer. The minimum in the interaction curves occurs at a plate separation slightly below twice the hydrodynamic layer thickness of the grafted layers. For a very low surface coverage (less than 1%) the attraction is minimal. For both higher and lower surface coverages the attraction becomes stronger. The attraction is maximal at full surface coverage (dense polymer layer) and when there is no grafted polymer on the surfaces (bare hard plates). Increasing the length of the grafted polymers, while keeping the surface coverage constant, decreases the attraction. On the other hand, increasing the length of the free polymer increases the attraction between the plates. The energy of mixing of the grafted layer and the free polymer has a strong influence on the interaction. When the mixing effect changes from $\chi_{gf} = 0$ to 0.5, the attraction between the plates becomes much stronger. The effect of the solvency conditions of grafted and free polymer is smaller. Surfaces coated with a grafted polymer layer, in the absence of free polymer, can also become attractive when the a solvent is worse than a theta solvent for the grafted polymer chains. The interaction curves can be fitted very accurately by a third order polynomial.

Appendix
Derivation of the free energy

The free energy $A(\{n_i^c\}, M, L, T)$ of a mixture of $\{n_i\}$ molecules in a given set of conformations $\{n_i^c\}$ in a lattice of M parallel layers of L sites each can be calculated by

$$A(\{n_i^c\}, M, L, T) = -kT \ln Q(\{n_i^c\}, M, L, T) \qquad (A1)$$

where Q is the canonical partition function. A conformation is defined as the sequence of layers in which the successive segments of a chain find themselves. In a particular conformation c, segment s of a chain of type i can be placed after segment s-1 in $\lambda_i^c(s|s-1)Z$ ways, where Z is the coordination number of the lattice and $\lambda_i^c(s|s-1) = \lambda_0, \lambda_{-1}$, or λ_1, as prescribed by the conformation. The total number of ways of placing all the $r_i - 1$ bonds of conformation c into the lattice is equal

to $\lambda_i^c Z^{r_i-1}$, where λ_i^c is defined as $\prod_{s=2}^{r} \lambda_i^c(s \mid s-1)$. The canonical partition function Q is equal to:

$$Q = Q^* \frac{\Omega}{\Omega^*} \exp\left(-(U - U^*)/kT\right) \qquad (A2)$$

In equation (A2), Ω is the number of ways to arrange all the molecules $\{n_i\}$ in their specified set of conformations $\{n_i^c\}$ in the lattice and U is the energy of the system. The superscript * denotes the reference state. The difference with the derivation of the equation for the canonical partition function of a multi-component system by Evers et al.[21] is that in this case one type of molecule is grafted. Therefore, we have to modify the derivation of Q as given in ref (18).

There may be different types g of grafted molecules, which have a grafting density $\sigma_g(z)$ in layer z. The grafting density is zero in all layers except in layers 1 and M. The number of grafted molecules of type g is n_g. The total density of grafted molecules in layer z, $\sigma(z)$, is equal to $\sum_g \sigma_g(z)$. The first of the n_g^c conformations c of a grafted chain of type g can be assigned to n_g different chains. If we would neglect the fact that a site can be occupied by a previously placed segment, the number of ways of arranging the first grafted chain of r_g segments in conformation c in the empty lattice, $\omega_g(1)$, would be equal to $\lambda_g^c Z^{r_g-1}$. The correction for multiple site occupancy is, in a mean field approximation, carried out as follows. Let us define $v(z)$ as the number of occupied lattice sites. If the first conformation has three segments in layer z ($r_1^c(z) = 3$) we have to correct $\lambda_g^c Z^{r_g-1}$ with a factor $(1-1/L)(1-2/L)$, if z is not 1 or M. In the first layer a fraction $\sigma(1)$ of the sites are unavailable for the nongrafted segments. If the first conformation would have three segments in layer 1 (of which one is the grafted segment) we include a factor $(1-\sigma(1))(1-\sigma(1)-1/L)$. The equation for $\omega_g(1)$ is therefore given by:

$$\omega_g(1) = n_g \lambda_g^c Z^{r_g-1} \prod_{z=2}^{M-1} \prod_{v(z)=0}^{r_g^c(z)-1} \left(1 - \frac{v(z)}{L}\right) \prod_{z=1,M} \prod_{v(z)=0}^{r_g^c(z)-2} \left(1 - \sigma(z) - \frac{v(z)}{L}\right)$$

$$(A3)$$

Here, $r_g^c(z)$ is defined as the number of segments of conformation c in layer z. The next conformation can be assigned to $n_g - 1$ different chains. The number of possibilities to arrange $\{n_g\}$ chains is given by:

$$\omega(\{n_g\}) = \prod_g \left[n_g! \prod_c \left(\lambda_g^c \left(\frac{Z}{L} \right)^{r_g-1} \right)^{n_g^c} \right] \prod_{z=1}^{M} \prod_{v(z)=L\sigma(z)}^{\sum_g \sum_c n_g^c r_g^c(z)-1} (L - v(z)) \tag{A4}$$

The first conformation of a nongrafted component can start at $L - \sum_g \sum_c n_g r_g^c(z)$ different positions. Placing the other components one by one onto the lattice and accounting for the indistinguishability of chains with the same conformation gives for Ω:

$$\Omega = \prod_g n_g! \prod_z [L(1 - \sigma(z))]! \prod_i \prod_c \left[\left(\lambda_i^c \left(\frac{Z}{L} \right)^{r_i-1} \right)^{n_i^c} \frac{1}{n_i^c!} \right] \tag{A5}$$

This result is independent of the order in which the molecules are placed. Equation (A5) is a generalization of previous expressions to systems with grafted components. After substitution of $n_g = \sigma(z) = 0$, it reduces to earlier results.[18,21]

For the reference state the pure liquid phase is taken for all the components, including the grafted ones. Flory[23] has derived Ω_i^* as:

$$\Omega_i^* = \frac{(r_i n_i)!}{n_i!} \left(\frac{Z}{r_i n_i} \right)^{n_i(r_i-1)} \tag{A6}$$

Where Ω_i^* is the number of ways to arrange n_i molecules i over $r_i n_i$ lattice sites. Using Stirlings approximation $\ln N! = N \ln N - N$ and equations (A5) and (A6) gives:

$$\ln \frac{\Omega}{\Omega^*} = \sum_i \sum_c n_i^c \ln \left(\frac{L\lambda_i^c}{r_i n_i^c} \right) + \sum_z \left\{ L(1 - \sigma(z)) \ln(1 - \sigma(z)) + \sum_g L\sigma_g(z) \ln \sigma_g(z) \right\} \tag{A7}$$

The first term includes all components (both grafted and mobile), the second term constitutes a negative correction because the grafted components have less (translational) entropy. The interaction energy U with respect to the reference state is, in the Flory-Huggins approximation, equal to:

$$\frac{U - U^*}{LkT} = \frac{1}{2}\sum_z\sum_i\sum_j \chi_{ij}\phi_i(z) < \phi_j(z) > \tag{A8}$$

The equilibrium condition is found by maximizing $\ln \Xi = \ln Q + \sum_i n_i\mu_i/kT$ under the packing constraint for each layer and the boundary condition of constant $\{n_g\}$. The Lagrange function f which has to be maximized is:

$$f = \ln Q + \sum_{i \neq g}\frac{n_i\mu_i}{kT} + \sum_z\alpha(z)\left\{\sum_i\sum_c(n_i^c r_i^c(z)) - L\right\} + \sum_g\beta_g\left\{\sum_c n_g^c - n_g\right\}$$

$$\tag{A9}$$

The factors $\alpha(z)$ and β_g are Lagrange multipliers which account for the boundary conditions $\sum_i\phi_i(z) = 1$ and $\sum_c n_g^c = n_g$. Substituting equations (A2), (A7), and (A8) into equation (A9) and differentiating f with respect to n_g^c, the number of grafted chains g in a specific conformation c is found as:

$$\frac{n_g^c}{L} = C_g \lambda_g^c \prod_z(G_g(z))^{r_g^c(z)} \tag{A10}$$

The value for the normalization constant $C_g = \exp(\beta_g - 1)/r_g$ can be deduced from equation (A10) by summation of n_g^c/L over all conformations: $\sum_c n_g^c r_g/L = \theta_g = C_g r_g G_g(r \mid 1)$, or

$$C_g = \frac{\theta_g}{r_g G_g(r \mid 1)} \tag{A11}$$

For nongrafted chains a similar result is obtained[21]:

$$\frac{n_i^c}{L} = \frac{\theta_i \lambda_i^c}{r_i G_i(r|1)} \prod_z \left(G_i(z)\right)^{r_i^c(z)} \tag{A12}$$

The factor $\theta_i/(G_i(r|1))$ may be replaced by ϕ_i^b, the volume fraction of molecules in the bulk solution (see equations 11 and 12). Combination of equations (A1), (A2), (A7), (A8), (A10), (A11), and (A12) gives:

$$\frac{A(M)}{LkT} = \sum_i \sum_z \phi_i(z) \left\{ \frac{1}{r_i} \ln \frac{\theta_i}{G_i(r|1)} + \ln G_i(z) + \frac{1}{2} \sum_j \chi_{ij} < \phi_j(z) > \right\}$$

$$- \sum_z \left\{ (1 - \sigma(z)) \ln(1 - \sigma(z)) + \sum_g \sigma_g(z) \ln \sigma_g(z) \right\} \tag{A13}$$

References

1) Asakura S., and Oosawa F., J. Chem. Phys. (1954), 22, 1255

2) Asakura S., and Oosawa F., J. Polym. Sci. (1958), 33, 183

3) Feigin R.I, Napper D.H, J. Colloid Interface. Sci.(1980), 75, 525

4) De Hek H., and Vrij A., J. Colloid Interface Sci. (1981), 84, 409

5) Joanny J.F., Leibler L., and de Gennes P.G., J. Polym. Sci. Polym. Phys. (1979), 17, 1073

6) Sperry P.R., J. Colloid Interface Sci. (1982), 87, 375

7) Scheutjens J. M. H. M. , and Fleer G. J. , Adv. Colloid Interface Sci. (1982), 16, 361; Erratum: ibid. (1983), 18, 309

8) Gast A.P., Hall C.K., and Russel W.B., J. Colloid Interface Sci. (1983), 96, 251

9) Fleer G.J., Scheutjens J.M.H.M., and Vincent B., ACS Symp.Ser. (1984), 240, 245

10) Li-In-On F.K.R, Vincent B., and Waite F.A., ACS Symp. Ser. (1975), 9, 165

11) Cowel C, Li-In-On F.K.R., and Vincent B. , J. Chem. Soc. Faraday Trans. 1 (1978), 74, 337

12) Vincent B., Luckham P.F., and Waite F.A., J. Colloid Interface Sci. (1980), 73, 508

13) Clarke J., and Vincent B., J. Chem. Soc. Faraday Trans. 1 (1981), <u>77</u>, 1831

14) Clarke J., and Vincent B. , J. Colloid Interface Sci. (1981), <u>82</u>, 208

15) Vincent B., Clarke J., and Barnett K.G., Colloids and Surfaces (1986), <u>17</u>, 51

16) Vincent B., Edwards J., Emmet S., and Jones A., Colloids and Surfaces (1986), <u>18</u>, 261

17) Rao I.V., and Ruckenstein E., J. Colloid Interface Sci. (1985), <u>108</u>, 389

18) Scheutjens J.M.H.M., and Fleer G.J., J. Phys. Chem. (1979), <u>83</u>, 1619

19) Scheutjens J.M.H.M., and Fleer G.J., J. Phys. Chem. (1980), <u>84</u>, 178

20) Cosgrove T., Heath T., Lent van B., Leermakers F.A.M., and Scheutjens J.M.H.M., Macromolecules(1987), <u>20</u>, 1692

21) Evers O.A., PhD Thesis, Wageningen Agricultural University(1989); Macromolecules, submitted.

22) Scheutjens J.M.H.M., and Fleer G.J. , Macromolecules(1985), <u>18</u>, 1882

23) Flory P.J., Principles of Polymer Chemistry (1953), Cornell University Press, Ithaca, NY

24) Fleer G.J. and Scheutjens J.M.H.M., Croata Chemica Acta(1987), <u>60</u>, 477

25) Scheutjens J.M.H.M., Fleer G.J., Cohen Stuart M.A., Colloids and Surfaces (1986), <u>21</u>, 285

26) Milner S.T., Witten T.A., and Cates M.E., Macromolecules(1988), <u>21</u>, 2610

27) Napper D.H., J. Colloid Interface Sci (1977), <u>58</u>, 390

Summary

The aim of this study was to investigate the influence of the molecular structure on the interfacial behaviour of polymers. Theoretical models were developed for three different systems. All these models are based on the self-consistent field theory of Scheutjens and Fleer for the adsorption of homopolymers.

This self-consistent field theory is a lattice model. All possible polymer conformations on the lattice are taken into account. The potential of a conformation is sum of the local potentials of the segments of the molecule. In each layer a mean field approximation is used to calculate the mixing energy. The volume fraction profile is determined by the segmental potentials and vice versa. A numerical method is used to solve the obtained set of equations.

In chapter 2 the influence of association of block copolymers on adsorption is considered. In order to model spherical aggregates (micelles), the planar lattice, as used for modelling planar aggregates (membranes) and adsorption on flat surfaces, is replaced by a spherical lattice. The equilibrium solution concentration in a micellar solution is determined by a small system thermodynamics argument. The adsorption of diblock copolymers with long lyophobic and short lyophilic blocks shows strongly cooperative effects. A single molecular layer is present if the lyophobic block adsorbs. The adsorption isotherm shows an S-shape at the onset of adsorption. A strong increase of the adsorbed amount occurs near the cmc and above the cmc the adsorbed amount is almost constant. A bilayer at the surface can be formed if the lyophilic block adsorbs. Adsorption of the lyophilic blocks would expose the insoluble blocks to the solvent. Therefore, a second layer of molecules adsorbs with their lyophobic block towards the molecules attached to the surface. The influence of the interaction energies and the block sizes on these trends is described. The results obtained show good qualitative agreement with experimental results on surfactant adsorption.

The adsorption of random copolymers from solution is described in chapter 3. Experimentally, random copolymers are usually very polydisperse, both in chain length and in primary structure. Random

copolymers which are only polydisperse in primary structure are considered here. They can be prepared experimentally by random chemical modification of monomer units of monodisperse homopolymers. The sequence distribution of random copolymers is determined by the fractions of the segment types in the polymer and the correlation factors between them. For random copolymers consisting of two different segment types, a blockiness parameter B is defined. The extremes of this parameter are -1 and 1, where the lower limit depends on the fractions of the different segment types. A value of B = -1 represents an alternating copolymer, whereas B = 1 stands for a mixture of two homopolymers. The complete statistical sequence distribution is implemented into the theory. In the results section random copolymers with two different segment types are studied. Chains with a higher than average content of adsorbing segments are preferentially adsorbed from the bulk solution. Only in the first few layers near the surface this preferential effect plays a role. In the remainder of the profile the segment types are more randomly mixed. The adsorption behaviour of these random copolymers is remarkably different from the adsorption of diblock copolymers. In the latter case, the chains have their adsorbing segments mainly in the layers near the surface, whereas further away from the surface long dangling tails of nonadsorbing segments are found. Random copolymers cannot spacially separate their segments so easily. Much higher adsorbed amounts are found for diblock copolymers than for random copolymers with the same fraction of adsorbing segments. The adsorption of random copolymers is less than that of homopolymer of equal length and consisting of the same type of adsorbing segments. Only for very high adsorption energies the adsorbed amounts are essentially the same. An increase in the blockiness parameter of the chains gives an higher adsorbed amount, but it is always below the adsorbed amount of the homopolymer. Analytical expressions have been derived which relate the interaction parameters of purely random copolymer and homopolymer.

In chapter 4 the interactions between surfaces coated with grafted polymer (also called hairy plates or soft surfaces) in the presence of nonadsorbing polymer is studied. The interaction free energy between the surfaces is obtained from the partition function, which is

rederived for this more general case. For hard plates the interaction is fully determined by the osmotic pressure of the bulk solution and the depletion layer thickness. However, it turns out that in the case of soft surfaces the hairs have an attractive contribution to the free energy of interaction at a plate separation just below twice the hydrodynamic layer thickness of the grafted layer. The hairs mix mutually more easily than with free polymer. At a larger overlap of hairs the interaction becomes repulsive. In contrast with bare planar surfaces, the free energy of interaction between hairy surfaces shows a minimum as a function of the concentration of free polymer in the bulk solution. At a certain (very low) surface coverage the attraction is minimal. For even lower and for larger grafting densities the plates become more attractive. Increasing the repulsion between the hairs and free polymer makes the attraction stronger. The solvencies of grafted and free polymer have a less pronounced effect. Without free polymer, the interaction between the hairy surfaces becomes attractive if the solvency becomes worse than theta conditions.

It can be concluded that the self-consistent field theory has been successfully extended to three rather complex but technologically relevant systems. In this way a better understanding of the behaviour of polymers near interfaces has been obtained.

Moleculaire Structuur en Grensvlakchemisch Gedrag van Polymeren

Samenvatting

Het doel van het in dit proefschrift beschreven onderzoek was de invloed van de moleculaire structuur op het gedrag van polymeren aan grensvlakken te bestuderen. Hiervoor werden modellen ontwikkeld voor drie verschillende systemen. Deze modellen zijn gebaseerd op de theorie van Scheutjens en Fleer voor de adsorptie van homopolymeren aan een vast/vloeistof-grensvlak.

Polymeren aan grensvlakken spelen een belangrijke rol in veel processen. Zo vinden ze hun toepassing in verven, lijmen, coatings voor magnetische disks en tapes, in de waterzuivering en in de pharmacie.

Polymeren zijn lange moleculen die uit verschillende segmenten zijn opgebouwd. Het aantal segmenten kan zeer groot zijn, soms zelfs meer dan 10000. Ze kunnen op verschillende manieren zijn opgebouwd. De meest simpele structuur is die van een homopolymeer. In dat geval zijn alle segmenten identiek. In dit proefschrift komt men nog drie andere structuren tegen: blokcopolymeren, statistische copolymeren en eindstandig verankerde polymeren. Copolymeren bestaan uit verschillende soorten segmenten. Indien de segmenten van hetzelfde soort in aangesloten rijen aan elkaar vastzitten, spreken we van blokcopolymeren. De meest eenvoudige versie daarvan is een diblokcopolymeer, bestaande uit twee blokken, ieder opgebouwd uit één segmentsoort. Bij de statistische copolymeren heeft ieder segment in de keten een bepaalde statistische kans om van een bepaalde soort te zijn. Een eindstandig verankerd polymeer is een polymeer (meestal, maar niet noodzakelijk, een homopolymeer) waarvan één van de segmenten aan het uiteinde van de keten chemisch gebonden is aan een vast oppervlak.

Polymeermoleculen in een oplosmiddel veranderen voortdurend van vorm. Gemiddeld gezien zullen de ketens van een homopolymeer een bolvormige kluwenvorm aannemen. Statistische copolymeren zullen dat over het algemeen ook doen. Bij blokcopolymeren kan dit

anders zijn. Als bij een diblokcopolymeer één blok(het zogenaamd ly-
ofiele blok) wel en het het andere (lyofobe) blok niet graag omringd
wordt door oplosmiddel, staat het molecuul voor een dilemma. De
moleculen hebben daar een oplossing voor gevonden door bij elkaar
te gaan zitten. Ze vormen aggregaten van moleculen, waarin de on-
oplosbare delen aan de binnenkant zitten en de oplosbare delen aan
de buitenkant. Deze aggregaten kunnen verscheidene vormen aan-
nemen. Ze zijn bijvoorbeeld bolvormig (micellen), staafvormig of vlak
(membranen). De aggregatie vindt pas boven een bepaalde concen-
tratie plaats, de zogenaamde critische micelvormingsconcentratie
(cmc).

Brengt men een oplossing van een polymeer in contact met een
vaste stof dan kunnen de polymeren zich vasthechten aan het op-
pervlak van deze vaste stof. We spreken dan van adsorptie. Een seg-
ment aan de wand moet echter wel voldoende adsorptie-energie
winnen. Het aantal rangschikkingen of conformaties van een poly-
meerketen in de buurt van de wand is namelijk kleiner dan in oplos-
sing. Polymeren willen dus alleen bij een wand zitten indien ze een
voordelige interactie met die wand hebben. Als de adsorptie-energie
te laag is, wordt de concentratie dicht bij de wand lager dan in
oplossing en hebben we te maken met depletie.

Polymeren kunnen de stabiliteit van kolloïdale oplossingen sterk
beïnvloeden (kolloïden zijn deeltjes met een grootte van zo'n 10 tot
1000 nanometer doorsnede). Een dikke geadsorbeerde laag kan er-
voor zorgen dat de deeltjes niet bij elkaar kunnen komen, terwijl in
het geval van depletie kolloïden juist naar elkaar toe kunnen worden
gedreven. Dit laatste heeft tot gevolg dat de kolloïdale deeltjes uit-
vlokken. De aggregaten worden te groot om in oplossing te blijven en
scheiden zich af; de kolloïdale oplossing wordt instabiel.

Ruim tien jaar geleden is door Scheutjens en Fleer een theorie
ontwikkeld die het adsorptiegedrag van homopolymeren goed bleek
te kunnen beschrijven. Het principe van deze theorie berust op een-
voudige Boltzmann-statistiek. De ruimte wordt in discrete lagen par-
allel aan de wand opgedeeld. De segmenten van het polymeer worden
aangetrokken door de wand. In de laag grenzend aan de wand winnen
zij adsorptie-energie t.o.v. de andere lagen. Hierdoor zullen er meer-
dere segmenten aan de wand gaan zitten. Deze segmenten "trekken"

de rest van de keten mee. Er ontstaat een concentratiegradiënt, n.l. een hoge segmentconcentratie tegen de wand, aflopend naar een constante concentratie in de bulk. In iedere laag kan aan een segment een potentiaal worden toegekend, die bepaald wordt door de adsorptie-energie (alleen in de eerste laag), de concentratie aan andere segmenten en oplosmiddel in die laag, en de wisselwerkingsenergie tussen de verschillende componenten in het systeem. (Dit is een beetje vergelijkbaar met het zwaartekrachtsveld, waar de potentiaal bepaald wordt door de massa van de deeltjes, de hoogte en de gravitatieversnelling. Een verschilpunt is dat bij de zwaartekracht het veld niet afhankelijk is van de lokale concentraties.) Nu is het probleem met polymeren dat de segmenten aan elkaar vast zitten. Voor een bepaalde conformatie vind je de potentiaal van het polymeermolecuul door de potentiaal van zijn segmenten bijelkaar op te tellen. Stel we hebben een trimeertje met segment 1 in laag 1 en segmenten 2 en 3 in laag 2, dan is de potentiaal van deze conformatie gelijk aan de potentiaal van een segment in laag 1 vermeerderd met tweemaal de potentiaal van een segment in laag 2. Nadat de weegfactoren van alle conformaties zijn bepaald, kan men de concentratie in iedere laag berekenen. Nu is het een bijna ondoenlijke zaak alle conformaties van een polymeer met een groot aantal segmenten afzonderlijk te genereren. Het is echter mogelijk via een slimme matrixmethode de concentraties direct uit de segmentpotentialen te berekenen. Een computer is daarbij een onmisbaar hulpmiddel. De computer is echter niet alleen nodig voor het berekenen van de concentraties. De concentraties worden weliswaar bepaald door het potentiaalveld, maar dat hangt op zijn beurt weer af van het concentratieprofiel. Met behulp van een numerieke iteratiemethode valt dit probleem, het vinden van het zelfconsistente veld, wel op te lossen.

Deze theorie bleek het adsorptiegedrag van homopolymeren goed te kunnen beschrijven. Nu worden in de praktijk meestal ingewikkelde polymeren gebruikt. Vandaar dat in dit onderzoek dit model is uitgebreid naar complexere systemen.

In hoofdstuk 2 wordt het adsorptiegedrag van aggregerende blokcopolymeren bestudeerd. Om de structuur en vormingscondities van micellen te berekenen wordt het vlakke rooster, dat wordt gebruikt voor de berekening van adsorptie en membraanvorming, vervangen

door een bolvormig rooster. De micelvormingsconcentratie, de cmc, wordt berekend met behulp van de thermodynamica van kleine systemen. Bij de associatie van blokcopolymeren kan het oppervlak als een soort condensatiekern optreden. Indien men de concentratie verhoogt, vindt men vlakbij de cmc opeens een flinke stijging in de adsorptie. Een hele dikke polymeerlaag kan dan worden gevormd. Als het lyofobe blok adsorbeert ontstaat een moleculaire laag, terwijl als het lyofiele blok van een molecuul adsorbeert een bilaag aan het oppervlak kan worden aangetroffen. Als het lyofiele blok adsorbeert, zou het lyofobe blok aan de oplossing blootgesteld worden. Een tweede laag polymeer gaat dan aan het grensvlak zitten, met de lyofobe blokken gericht naar de uitstekende lyofobe delen van de polymeren die aan het oppervlak vastzitten en de lyofiele blokken naar de oplossing. De invloed van de bloklengte en van de interacties tussen de verschillende segmenten onderling en met het oppervlak zijn systematisch onderzocht.

In hoofdstuk 3 wordt het adsorptiegedrag van statistische copolymeren bekeken. In de praktijk kunnen statistische copolymeren een grote variatie hebben, zowel in ketenlengte als in samenstelling. Er wordt hier alleen gekeken naar statistische copolymeren van uniforme lengte. De verdeling van de segmentsoorten over de keten wordt bepaald door de gemiddelde fractie van elk segment in het polymeer en door correlaties in de volgorde van de verschillende segmenttypen. Voor statistische copolymeren bestaande uit twee soorten segmenten is een blokparameter gedefinieerd die als uiterste grenzen -1 en 1 heeft. De waarde van de ondergrens is afhankelijk van de onderlinge verhouding van de segmentsoorten. Indien de blokparameter gelijk is aan -1 hebben we te maken met een alternerend copolymeer: naast een segment van het ene soort zit altijd een segment van het andere soort. Als de blokparameter 1 is hebben we te maken met een mengsel van twee homopolymeren. Het ene soort segment kan dan namelijk niet naast het andere zitten. De blokparameter geeft aan, zoals de naam al zegt, hoe blokvormig de polymeren zijn opgebouwd. Resultaten worden gegeven voor statistische copolymeren bestaande uit twee soorten segmenten. Ketens die rijker zijn aan adsorberende segmenten worden preferent geadsorbeerd. Alleen in de eerste paar roosterlagen grenzend aan wand kan men dit zien.

In de rest van het profiel is is de mengverhouding van de segmenten practisch gelijk aan die in de bulkoplossing. Het adsorptiegedrag van deze statistische copolymeren is beduidend anders dan die gevonden voor diblokcopolymeren. Diblokcopolymeren zitten meestal met het adsorberend blok vlak tegen de wand en steken met het niet adsorberend blok in de oplossing. Statistische copolymeren kunnen hun segmentsoorten niet zo gemakkelijk ontmengen. Voor diblokcopolymeren worden veel hogere geadsorbeerde hoeveelheden berekend. Statistische copolymeren hebben ook een lagere adsorptie dan het homopolymeer van gelijke lengte dat volledig uit adsorberende segmenten bestaat. Alleen voor hele hoge adsorptie-energieën is de adsorptie vrijwel gelijk. Een grotere waarde voor de blokparameter leidt tot een hogere adsorptie, maar brengt die niet boven de geadsorbeerde hoeveelheid van het homopolymeer uit.

In het laatste hoofdstuk wordt de interactie berekend tussen twee vlakke platen, bedekt met verankerd polymeer ("haren"), in de aanwezigheid van niet adsorberend polymeer. In het geval van onbedekte platen wordt de interaktie geheel bepaald door de osmotische druk en de dikte van de depletielaag. Als we de polymeermoleculen simpelweg voorstellen als harde bollen, dan moeten deze tussen de platen verdwijnen als de afstand tussen de platen kleiner wordt dan de diameter van de bollen. Men heeft dan een systeem met puur oplosmiddel tussen de platen en een polymeeroplossing met een hogere osmotische druk daarbuiten. Deze osmotische druk duwt de platen naar elkaar toe. Als we de platen bedekken met verankerd polymeer blijkt het depletie-effect minder te worden, doordat het vrije polymeer met het verankerde polymeer kan mengen. De effectieve depletielaag wordt dunner. Het blijkt echter dat het mengen van de twee verankerde polymeerlagen bij een plaatafstand van iets minder dan twee maal de hydrodynamische laagdikte (een maat voor de dikte van de polymeerlaag) een extra attractie geeft. Het mengen van de haren onderling is entropisch gunstiger dan het mengen van de haren met vrij polymeer. Op korte plaatafstand stoten de haren elkaar af. De invloed van verschillende parameters op de wisselwerking tussen harige platen wordt uitgebreid beschreven.

Resumerend kunnen we concluderen dat de zelfconsistente veld theorie succesvol is uitgebreid naar drie complexe, maar voor de praktijk zeer relevante systemen. Dit heeft geleid tot een beter begrip van het gedrag van polymeren aan grensvlakken.

Curriculum Vitae

Boudewijn van Lent werd geboren op 16 mei 1962 in Amstelveen. In juni 1980 behaalde hij het Atheneum-b-diploma aan het Fioretti college te Lisse. In september van datzelfde jaar begon hij aan de studie Moleculaire Wetenschappen aan de de Landbouwhogeschool te Wageningen. Binnen de studie volgde hij de fysisch-chemische oriëntatie. In januari 1986 studeerde hij cum laude af. Het doctoraalpakket bestond uit een hoofdvak kolloïdchemie en de bijvakken natuurkunde en wiskunde. In 1985 is hij een half jaar op stage geweest naar "The School of Chemistry of Bristol University (U.K.)". Van februari 1986 tot augustus 1989 werkte hij als wetenschappelijk-assistent bij de vakgroep Fysische en Kolloïdchemie van de Landbouwuniversiteit te Waginingen. Vanaf 1 december 1989 is hij in dienst bij Bayer AG in Leverkusen, West-Duitsland.

Nawoord

Ik heb op de vakgroep Fysische en Kolloïdchemie een ontzettend leuke en leerzame tijd gehad. Een aantal mensen hebben een ruime bijdrage geleverd aan het tot stand komen van dit boekje.

JAN SCHEUTJENS is een grote stimulator voor mijn onderzoek geweest. Hij heeft mij altijd met een behulpzaam kritisch oog terzijde gestaan. Vele ideeën van hem zijn verwerkt in dit proefschrift.

Gerard Fleer is een bron van enthousiasme voor het wel en wee van de polymeergroep. Dit uit zich niet alleen in de inhoudelijke begeleiding van de projecten, maar ook in het tot stand brengen van goede verhoudingen tussen de mensen onderling.

Met Frans Leermakers, Peter Barneveld en Marcel Böhmer heb ik op een plezierige manier kunnen discussiëren over een groot aantal wetenschappelijke problemen. Maar ook buiten de muren van het scheikundegebouw was het met hen goed toeven.

De begeleiding van Rafel Israels en Katinka van der Linden tijdens hun doctoraalvak heb ik met veel plezier gedaan. Een gedeelte van Rafels werk is opgenomen in hoofdstuk 4. Helaas was er geen tijd meer om Katinka's werk in dit proefschrift op te nemen.

Zonder de tekencapaciteiten van Gerrit Buurman had dit boekje er een stuk minder mooi uitgezien.

Tot slot wil ik alle medewerkers van de vakgroep bedanken voor de prettige tijd.

Auf Wiedersehen,

Boudewijn